NASA CR - 137515
Available to the public
VIZEX CR - 74 - 1

A THEORETICAL STUDY OF THE APPLICATION OF JET FLAP CIRCULATION CONTROL FOR REDUCTION OF ROTOR VIBRATORY FORCES

by

Raymond A. Piziali

Andrew R. Trenka

May 1974

Prepared Under Contract No. NAS2-7307

For

Ames Directorate-U.S. Army Air Mobility Research and Development Laboratory
and
National Aeronautics and Space Administration
Ames Research Center
Moffett Field, California 94035

FORWARD

This report presents the results of a study to investigate the theoretical potential of a jet-flap control system for reducing the vertical and horizontal transmitted helicopter rotor blade root shears. A computer simulation was used to examine the reduction of each harmonic of the transmitted shears as a function of the jet parameters, the rotor operating conditions, and rotor configuration.

The research program was conducted by Vizex, Inc.under the sponsorship of the Ames Directorate-U.S. Army Air Mobility Research and Development Laboratory The contract no. was NAS2-7307. The effort commenced on Nobember 29, 1972 and was completed in May, 1974.

The Technical Monitor was Dr. Robert Ormiston of USAAMRDL. The technical guidance provided by Dr. Ormiston, was augmented by Mr. John McCloud of National Aeronautics and Space Administration. Their direction, helpful technical comments,and discussions were of considerable value to the conduct of this effort.

CONTENTS

LIST OF FIGURES

FIGURES (continued)

FIGURES IN APPENDIXES

LIST OF TABLES

SUMMARY

Presented herein are the results of a study to investigate the theoretical potential of a jet-flap control system for reducing the vertical and horizontal non-cancelling helicopter rotor blade root shears. A computer simulation describing the jet-flap control rotor system was developed to examine the reduction of each harmonic of the transmitted shears as a function of various rotor and jet parameters, rotor operating conditions and rotor configurations. The computer simulation of the air-loads included the influences of nonuniform inflow and blade elastic motions. (No hub motions were allowed.) The rotor trim and total rotor power (including jet compressor power) were also determined.

It was found that all harmonics of the transmitted horizontal and vertical shears could be suppressed simultaneously using a single jet control. The jet angle control schedule was found to be within practical limits with respect to amplitude. In no case did the total jet deflection angle required to suppress shears and maintain jet-off trim condition of the rotor exceed 60°. Of this maximum jet deflection angle of 60°, no more than 28° was required for suppression of the shears. The balance of the jet angle deflection was required to maintain the jet-off trim conditions of forces and moments.

The blade response plays an important roll in the mechanism of shear suppression. In particular, for the rotor studied, torsion was an essential and beneficial element in interacting with the jet-flap control to achieve shear suppression. The interaction was analogous to that of a trim tab in a conventional airfoil-mechanical flap system. The results indicate that the jet-flap could be employed to control the torsional response of the blade and thereby achieve shear suppression.

The results obtained concerning the additional power required for the jet-flap control rotor system were somewhat obscurred by the requirement of the study that the trim (forces and moments) of the rotor be maintained to identical values for both the jet-on and jet-off operation. In all cases, the power required by the jet-flap control to maintain trim appeared to be the dominant contributor to the total additional power required (rotor shaft power plus compressor power) to maintain trim and suppress all transmitted horizontal and vertical shears.

1.0 INTRODUCTION

Helicopter rotor vibration reduction is a desirable and elusive goal that has been pursued in many ways and for an appreciable length of time. Effort expended has been large because the potential benefits are large in terms of vehicle performance, pilot/payload performance, and machine life (cost). It was the purpose of the study reported on here to continue one of the more promising lines of attack - active control of oscillating aerodynamic forces to reduce net shaking shear loads transmitted to the fuselage. The particular mechanism for exercising this control was chosen to be the jet flap. It is important to recognize that the transmitted shear problem belongs to the general class of rotor aeroelastic phenomena and that the accurate computation of the forcing functions and blade response depends strongly on the accurate computation of the induced velocity distribution (nonuniform inflow).

The application of the jet-flap principle to helicopter rotors was first discussed over fifteen years ago (References 1 and 2), and interest has continued to the present (References 3 to 5, 19, 20, 31 and 32). Also of interest today are the circulation-controlled rotors first investigated both experimentally and theoretically in England by the National Gas Turbine Establishment (NGTE) (References 6 and 7). As considered by the NGTE, a circulation-controlled rotor consists of sections such as circular cylinders and thick ellipses with blowing from multiple slots in the vicinity of, but not at, the trailing edge. The objective is to obtain lift by controlling the circulation about these sections through control of the location of the stagnation points. In contrast, the jet flap is applied to sections that are more typically conventional airfoil shapes and lead to pressure distributions which can differ from that of conventional airfoils primarily in that the rear stagnation point is fixed at the jet location rather than at the trailing edge. In some current applications, e.g., (References 8 and 9), the distinction between circulation control and the jet flap is not always clear cut.

The jet flap remains attractive for rotor applications because of its potential, not only for integrating rotor propulsion and lift requirements efficiently, but also as a control device for achieving higher harmonic control (Reference 2 and 3). Such control can be used to improve rotor performance, especially at high advance ratios (References 10 to 12), and can also be applied to reduce vibration. Vibration reduction may be accomplished by eliminating, or reducing, the higher harmonic root shears that are transmitted to the rotor hub from the blades. The studies of References 13 and 14 have indicated that a redistribution of aerodynamic blade loads both spanwise and azimuthally can reduce the transmitted shears. This redistribution may be achieved via several approaches. One of the approaches is to use the rigid body

blade pitch control. The theoretical feasibility of this approach was demonstrated in References 13 and 14. Lemnios and Smith (Reference 33) analytically evaluated the use of a "controllable twist" rotor to achieve the desired loads control.

McCloud and Evans in Reference 3 noted the possible benefits of reducing hub shears by higher harmonic control of the jet flap. Various devices have been investigated to achieve the desired control of the jet (References 9, 31 and 32). The Honeywell system of Reference 31 employs a closed loop fluidic system to obtain the jet control while an open loop mechanical system is used by Giravions Dorand. Higher harmonic control by pulsing the jet supply pressure is being developed by the Navy (See Reference 9). These systems represent some of the approaches currently being studied to achieve higher harmonic control of the jet.

Some potential advantages of the jet flap higher harmonic control over the "mechanical" control systems are the possibility of a much simpler control system at the hub, the higher frequency response which may be achievable with the jet control, and the lower control loads possible due to the absence of significant inertia loads in the control system.

Thus because the jet flap offers a promising means of achieving this control, the study reported inerein was undertaken to aid in the assessment of the potential.

The objective of this effort was to investigate the theoretical potential of a jet-flap control system for reducing the vertical and horizontal transmitted helicopter rotor blade root shears. A computer simulation describing a jet-flap control rotor system was used to examine the reduction of each harmonic of the transmitted shears as a function of the jet parameters, the rotor operating conditions, and rotor configuration.

The rotor systems studied were assumed to be shaft powered rotor's, i.e. the jet was to be used primarily to control shears and not to power the rotor. Conventional collective and cyclic pitch was employed to provide rotor control in both the jet-off and jet-on flight conditions. In addition to the conventional pitch controls, one jet flap control at the first harmonic was provided to allow maintainence of both force and moment trim conditions. That is the forces and moments obtained for the rotor in a given flight condition, jet-off were maintained when the jet was turned on. The additional jet-flap control was required because the rotor trim (primarily rolling and pitching moments) was upset by the jet effects.

Described in the subsequent sections are the rotor systems analyzed, the mathematical and computational models employed for the analysis and some of the pertinent results and conclusions.

LIST OF SYMBOLS

A_n	Glauert coefficients, m/s
b	blade semichord, m
C_{D_p}	profile drag coefficient
$C_L, C_{L\alpha_0}, C_{L\hat{t}}$	section lift coefficient and lift-curve slope for α & $\hat{t}$ jet-off
$\mathcal{C}_j$	generalized coordinate for $j^{\underline{m}}$ control mode
C	matrix of aerodynamic mass, spring and damping coefficients
C_J	local jet momentum coefficient, $C_{J_{T_0}}\left(f_{c_J}/(\bar{r}+\mu\sin\psi)^2\right)$
$\bar{C}_{L\alpha}, \bar{C}_{L\hat{t}}, \bar{C}_{L\tau}$	section lift-curve slope for $\alpha, \hat{t}$ & τ, jet-on
$C_{M\alpha_0}, C_{M\hat{t}_0}$	section moment-curve slope for α & $\hat{t}$, jet-off
$\bar{C}_{M\alpha}, \bar{C}_{M\hat{t}}, \bar{C}_{M\tau}$	section moment-curve slope for $\alpha, \hat{t}$ & τ, jet-on
$C_{J_{T_0}}$	tip jet momentum coefficient based on rotor tip speed, $= \left(\frac{d\dot{m}_J}{dr}\right)V_J \Big/ b\rho(R\Omega)^2$
$\mathfrak{D}$	blade section drag per unit span, N/m
$\mathfrak{D}_{cJ}$	blade section jet dependent drag per unit span, N/m
D	matrix of mass, spring and damping coefficients
$\frac{d\dot{m}_J}{dr}$	jet mass flow rate per unit span, kg/s/m
e_0	distance of blade pitch axis forward of midchord, m
e	distance of blade elastic axis forward of midchord, m

E	matrix approximating $[C]$
$f_{q_i}(r)$	normalized deflection in the q^{TH} mode
f_{c_j}	nondimensional spanwise distribution of jet mass flow rate, unity at blade tip.
$\hat{F}$	matrix representing the matrix sum $[D+C]$
F_{TAIL}	tail rotor side force, N
$F_{x_{ROTOR}}$	rotor x-force in shaft plane, N
$F_{y_{ROTOR}}$	rotor y-force in shaft plane, N
$F_{z_{ROTOR}}$	rotor z-force in shaft plane, N
f_{τ_j}	nondimensional spanwise mode shapes for τ_j , $j=1,2$
F	$[D + E]$
$\overline{GF}$	$[\vec{Y}_o - C\vec{X}_i]$
h	blade section plunging velocity relative to fixed axes, m/s
h_i	generalized coordinate for i^{TH} vertical deflection mode, m
H_i	generalized coordinate for i^{TH} inplane deflection mode, m
$h_{J_{TIP}}$	jet slot height at blade tip, m
I_K	quasi-steady part of Γ_K , m^2/s
k_o	jet velocity/maximum relative air velocity at tip
ℓ_{TAIL}	distance from shaft axis to tail rotor center
$\mathcal{L}_M$	blade section stalled lift per unit span, N/m
$\mathcal{L}$	blade section lift per unit span, N/m
m	blade mass per unit span, kg/m

m_{LM}	blade section stalled pitching moment about midchord per unit span, m•N/m
m	blade section pitching moment about midchord per unit span, m•N/m
M_T	rotor tip mach number
M_N	local mach number
$\dot{M}_{J_T}$	total jet mass flow rate required for all blades, kg/s
N	number of rotor blades
NA	number of azimuth positions used in the computation
NR	number of blade radial segments used in the computation
NRA	total number of collocation points in rotor disc; NA•NR
p_{ATM}	freestream static pressure at infinity, N/m^2
P_T	total power required, rotor + compressor, W
PM_{ROTOR}	rotor pitching moment, m•N
P_R	power required by rotor, W
$\bar{p}_o$	compressor output pressure, N/m^2
P_c	compressor power required, W
q_i	generalized coordinate for i^{TH} vertical deflection, inplane deflection, torsional or control mode
RM_{ROTOR}	rotor rolling moment, m•N
R	total blade radius, m
r	radius to a blade section, m
$\bar{r}$	radius to a blade section, nondimensional (r/R)

r_J	inboard most radial position of jet, m
$\bar{R}$	gas constant
S_n	coefficients giving induced velocities due to mesh of vortex filaments in wake
$\bar{t}$	maximum chord displacement for parabolic camber, m
$\hat{t}_e$	equivalent parabolic camber, $b\dot{\alpha}_2/4V_1$
$\hat{t}_o$	geometric parabolic camber, $\bar{t}/2b$
T_{ROTOR}	rotor torque, m·N
t	time, s
τ	total jet angle, rad
τ_{nj}^c, τ_{nj}^s	cosine, sine components of the j^{TH} jet control mode at the n^{TH} rotor harmonic, rad
T_R	jet thrust recovery factor
T_{ATM}	freestream ambient temperature, K
v_k	velocity relative to the surface of the airfoil due to plunging motion at the k^{TH} collocation position, m/s
V_f	rotor translational (forward) velocity, m/s
V_1	component of total velocity of blade section perpendicular to the shaft and to the blade axes, m/s
V_J	jet velocity, m/s
w_k	normal induced velocity distribution at the k^{TH} collocation position, m/s
x	chordwise coordinate; distance aft of midchord, m
$\bar{x}_1$	distance of the CG aft of EA, m
$\hat{x}_o$	vector of unconstrained variables

$\vec{Y}_o$	vector of driving forces (forcing functions)
$\bar{\alpha}$	$= (1.25)\alpha_M$
α_i	induced angle, arc tan (V_2/V_1), rad
α_e	effective angle of attack of blade section relative to V_1 , rad
α_g	geometric angle of attack of blade section relative to V_1 , rad
$\dot{\alpha}_g$	time rate of change of geometric angle of attack, rad/s
α_M	stall angle for airfoil section $\lvert\alpha_M\rvert \leq \pi/2$, rad
$\bar{\alpha}_M$	stall angle for airfoil section $\pi/2 < \lvert\alpha_M\rvert \leq \pi$, rad
α_s	shaft angle relative to plane perpendicular to rotor translational velocity , rad
β	first harmonic flapping relative to a plane perpendicular to the shaft; $\beta = \beta_{1c}\cos\psi + \beta_{1s}\sin\psi$, rad
β_c	preconing angle, rad
Γ_k	total bound vorticity of blade section of k^{TH} segment, m^2/s
Γ_M	total stalled bound vorticity of blade section, m^2/s
γ_k	chordwise bound vorticity distribution at the k^{TH} collocation position, m/s
γ	ratio of specific heats (1.4 for air)
η_c	compressor efficiency
$\bar{\theta}$	angular coordinate used to specify chordwise position; $x = -b\cos\bar{\theta}$, rad
θ_B	built-in twist, rad
θ_i	generalized coordinate for i^{TH} torsion mode, rad
μ	advance ratio

ρ	air density, kg/m^3
σ	induced velocity coefficients of Γ -equations
ψ	azimuth, angle, rad
Ω	rotor angular velocity, rad/s
$\omega_{\beta i}$	natural frequency of β_i^{TH} mode, rad/s

2.0 DESCRIPTION OF ROTORS ANALYZED

The choice of the rotor configurations and the corresponding blade properties investigated were made recognizing that no typical jet-flap rotor exists. The rotor configurations and blade properties selected were based upon the following considerations:

1. jet-flap rotors currently being considered;
   a) Giravions-Dorand (References 2, 3, 4 and 16)
   b) Lockheed rigid rotor (Reference 17)
   c) The circulation control rotor of NSRDC (References 18 and 19)
   d) The Hughes Tool Company studies (Reference 20)
2. the primary missions for which jet-flap rotors might be used;
   a) heavy lift missions
   b) high speed missions
3. requirements for reduction of transmitted vibratory shears and for simplification of control mechanisms
4. existing rotor configurations

The choice for the "basic rotor configuration" was:

gross weight; 44482 N (10,000 lbs.)
number of blades; 2
articulation; flapping hinges for each blade--
hinge offset 0.369 m (1.21 ft.)
blade tip radius; 7.38 m (24.2 ft.)
blade root radius; 0.921 m (3.02 ft.)
blade chord (constant); 0.46 (1.51 ft.)
solidity; 0.0343
disc loading; 263 Pa (5.5 psf.)

$C_T/\sigma = 0.12$

The spanwise distributions of blade properties are basically those of the UHIA blade. The geometric properties used for the basic rotor blade are presented in Figure 1. The corresponding blade mass-elastic properties are presented in Figures 2 through 5. In each of the figures, the blade property plotted versus nondimensionalized radial position has been non-dimensionalized by the respective quantity at the blade root.

Presented in Figures 6 through 9 are the mode shapes and frequencies calculated for the mass-elastic properties assumed. The inflection in the mode shapes near the blade root is due to the hub inertia. The rotor operating frequency plot presented in Figure 10 is for no vertical hub motion (infinite vertical translational impedance).

The weight classification of 44482 N (10,000 lbs.) was chosen as representative of a large number of ships (relatively current) made by various manufacturers.

The number of blades was chosen as 2 because this number of blades transmits the widest frequency range of vibratory forces to the shaft. It is also representative of approximately one-half of the total number of ships in this weight classification.

Flap hinge articulation was selected because it represents approximately one third of the rotors in the noted weight classification.

The second rotor configuration analyzed was a four (4) bladed rotor in the 88964 N (20,000 lb.) class. The rotor blade characteristics were maintained the same as those for the "basic configuration" (see Figures 1 through 10). The solidity for this rotor is 0.0683, C_T/σ = 0.12, and the disc loading is 527 Pa (11.0 psf).

The assumed helicopter configuration is presented in Figure 11. Also shown in this figure are the trim forces and moments and the assumed sign convention. The parameters of the assumed configuration are:

Fuselage Flat plate drag area; 8.18 m^2 (26.8 ft^2.)

Tail rotor moment arm; 7.93 m (26.0 ft.)

A conventional control system having collective and cyclic degrees of freedom was used to achieve "no blowing" trim of the ship. To facilitate comparisons of the jet-on and jet-off results, it was required that the rotor trim conditions (i.e. forces and moments) be the same with the jet-on as with the jet-off. Thus an additonal rotor control is required when the jet is on.① The additional rotor control is provided by the 1P jet deflection angle.

① Turning the jet on (without deflecting it) significantly alters the distribution, over the disc, of the blade section lift, moment, and drag and thereby the rotor trim forces and moments. With a conventional system, at fixed rotor speed (via the throttle), there are only four controls available to control the six rotor forces and moments -- two must be left "free", they are the rotor pitch and roll moments. That is, the pilot accepts the pitch and roll attitudes required to achieve the desired side and propulsive forces. If, however, the moments are to be controlled in addition to the forces then it is clear that additional controls are required. (See Section 5.2.5)

This study assumed a "pure jet flap", as opposed to a blown flap or a circulation control device, to achieve control[1]. The jet blowing was assumed to be distributed over the outboard half of the rotor blade span. The detailed mechanics of the ducting, slot height etc. for the jet were not considered in this study.

---

[1] In a "pure jet flap", the jet is assumed to emanate from a fixed position in the vicinity of the trailing edge of the airfoil thereby fixing the rear stagnation point at that location. In a "blown flap", the jet passes over a short conventional mechanical flap. In a "circulation control" device the jet is blown over a round (or elliptical) trailing edge thereby allowing the rear stagnation point free to adjust to the local flow requirements.

3.0 PARAMETER VARIATIONS STUDIED

3.1 Flight Conditions

The operating conditions for the basic rotor configuration were:

Rotor tip speed; $R\Omega$ = 231 m/s (760.4 ft/sec.)

Ω = 3.4 rad/s (300 rpm = 5.0 HZ)

Rotor tip mach no.: M_T = 0.7 @ altitude of 762 m (2500 ft.)

Advance ratio: μ = 0.08, 0.20, 0.30

Forward Flight Velocity: V_f = 18.5 m/s (60.8 ft/sec.),
= 46.4 m/s (152.0 ft/sec.),
= 69.5 m/s (228.0 ft/sec.).

The second rotor configuration was investigated only at μ = 0.20.

The ship trim attitude (i.e. shaft angle, α_s) specified at each μ was determined, based on;

(i) an estimated fuselage drag which acted through the ship center of gravity (c.g.) at all μ and which was directly proportional to the freestream dynamic pressure, q ,

(ii) a c.g. which was assumed to lie on the rotor shaft axis,

(iii) the assumption that the resultant of the fuselage drag and weight was coincident with the rotor shaft axis

The resultant shaft angles, α_s , as a function of advance ratio, μ , are presented in Figure 12.

With the jet-off, the rotor trim forces were constrained, but the rotor pitching and rolling moments (PM and RM respectively) and the torque were allowed to be free.

The constrained trim forces are in the shaft plane and normal to it as shown in Figure 11. The constraint values were chosen consistent with requirements on the helicopter weight, drag force, rotor torque and shaft angle.

The rotor torque determined the value required on the side force through the constraints:

$$T_{rotor} = F_{tail} \times \ell_{tail} \quad (3.1.1)$$

$$Fy_{rotor} = F_{tail} \quad (3.1.2)$$

where;

T_{rotor} = rotor torque

F_{tail} = force generated by the tail rotor

Fy_{rotor} = rotor side force (in shaft plane)

ℓ_{tail} = distance from shaft axis to tail rotor center.

When the jet was turned on, not only were the rotor trim forces and shaft angle maintained but in addition the rotor PM and RM were constrained to the "jet-off" values. The rotor trim moments were maintained by allowing an extra control at 1P consisting of the jet deflection angle. The amplitude and phase of the 1P jet angle (τ) required to maintain trim at a given μ and jet blowing coefficient are a part of the resultant solution.

3.2 Rotor Blade Torsional Stiffness

The blade torsional stiffness assumed for the bulk of the cases studied was representative of the torsional stiffness found in conventional(i.e. "no blowing") rotor blades. Since relatively (with respect to conventional blades) large torsional moments are generated by blowing and because rotor blades employing some form of blowing are anticipated to be relatively stiff in torsion, additional calculations were made with the blade torsional stiffness increased by a factor of 10. The 1st and 2nd torsional mode frequencies were thus increased to 527 rad/s (16.7P) and 1373 rad/s (43.8P) respectively. The increased stiffness blade was investigated at μ = 0.20 with and without jet-on.

3.3 Shears Suppressed

Given the objective of this study, to determine the effectiveness of the jet flap for reducing the vertical and horizontal

transmitted blade root shears, the questions to be resolved were:

(i) What value should the shears be reduced to?

(ii) Should both components (i.e. vertical and horizontal) of the transmitted shears be suppressed simultaneously?

It was decided to suppress all harmonics (i.e. from 2nd to the 11th)[1] of the transmitted vertical and horizontal shears to zero for all cases studied. Several runs were also made to determine the effects on adjacent harmonics of shear when only one component of shear at a single harmonic was suppressed. One run was made in which only the significant blade root shears were suppressed (i.e. up to the 6th harmonic).

Suppression of the transmitted blade vertical and horizontal shears required only one jet flap control mode. This situation occurs for two reasons -- first, an n^{th} harmonic horizontal blade root shear (in the rotating system) appears in the non-rotating system at the $n \pm 1$ harmonic orders while the vertical blade root shear does not experience this frequency shift; second, in a multi-bladed rotor, both the horizontal and vertical blade root shears in the non-rotating system cancel at all harmonics except

$$n = m \cdot NB \qquad m = 0, 1, 2, \ldots$$

where NB is the number of blades. Thus the vertical and horizontal blade root shears which will be transmitted to the fixed system do not occur at the same frequency in the rotating system. Therefore at each frequency only one (either the horizontal or the vertical blade root shear) has to be suppressed and hence only one control mode is required. Although the simulation had a second jet flap control mode available, the simultaneous use of both control modes was not required during this study.

3.4 Jet Momentum Coefficient

The spanwise distribution of the jet velocity was assumed constant with radius and azimuth. Thus for a constant C_T (with μ) the jet velocity will be proportional to the rotor speed and advance ratio,

$$V_J = k_o \cdot (R\Omega) \cdot (1 + \mu) \qquad (3.4.1)$$

[1] The zeroth and first harmonics of the shears are constrained by the trim requirements (See Section 4.3)

For this study k_o was chosen as 1.2 which is in the lower end of the range to be considered a jet flap rather than boundary layer control.

It was also assumed that the spanwise distribution of the internal jet duct pressure was constant, arguing that the internal flow losses are just balanced by the centrifugal pumping action.

The local jet momentum coefficient is defined as

$$C_J = \frac{\text{jet momentum/unit span}}{\text{freestream momentum/ unit span}} \qquad (3.4.2)$$

$$= \frac{\left(\frac{d\dot{m}_J}{dr}\right) V_J}{\rho b (R\Omega)^2 (\bar{r} + \mu \sin\psi)^2} \qquad (3.4.3)$$

where;

$\frac{d\dot{m}_J}{dr} = (\rho h V)_J$ = jet mass flow rate per unit span, kg/s/m

ρ = freestream density, kg/m^3

ρ_J = jetstream density,

b = local blade semichord, m

h = slot height, m

ψ = blade azimuthal position, rad

$\bar{r} = r/R$, nondimensional spanwise distance

Defining

f_{C_J} = spanwise distribution of jet mass flow rate per unit span nondimensionalized to the tip value

$C_{J_{T_o}}$ = jet momentum coefficient at the blade tip based on the rotor speed, $R\Omega$

$$= \frac{\left(\frac{d\dot{m}_J}{dr}\right) V_J}{\rho b (R\Omega)^2}$$

equation (3.4.3) may be written as

$$C_J = C_{J_{T_0}} \frac{f_{c_J}}{(\bar{r} + \mu \sin\psi)^2} \qquad (3.4.4)$$

Thus both the jet momentum and its spanwise distribution could be varied during this study.

The values of $C_{J_{T_0}}$ selected for this study were:

$$C_{J_{T_0}} = 0.005,\ 0.01,\ 0.02,\ 0.03$$

These values were selected as being in the range of blowing coefficients which might be employed for the purpose of suppressing shears on a conventionally driven rotor.

The jet mass flow rate was assumed constant over the span of the jet for all of the cases presented herein.

The relationships between(C_J) , pressure ratio (P_0/P_{atm}),($\dot{m}_J/dr$), (V_J) and nozzle height are based on standard thermodynamic equations under the assumption of isentropic expansion. Plots of the compressor power required (P_c), total jet mass flow rate required ($\dot{m}_{J_T}$) and pressure ratio vs advance ratio are presented in Figure 13. The analyses for these quantities are presented in Appendix III. Presented in Figure 14 and 15 are typical plots of C_J variation with blade radius and azimuth respectively.

3.5 Jet Control Mode

As described previously the jet was assumed to be distributed over some spanwise extent of the rotor and emmanating from a slot at the airfoil trailing edge. The jet angle, τ , with respect to the airfoil chord was assumed to be controllable azimuthally. The spanwise variation of τ was treated as an independent parameter of the problem.

Two independent jet control modes were provided for. Hence, the jet control angle may be described by

$$\tau(r,\psi) = \sum_{j=1}^{2} f_{c_\tau}(r) \sum_{n=2}^{11} \left(\tau^c_{n_j} \cos n\psi + \tau^s_{n_j} \sin n\psi \right) \qquad (3.5.1)$$

where $f_{c_\tau}(r)$ — nondimensional spanwise mode shape for τ_j, $j = 1,2$

τ_{nj}^c, τ_{nj}^s — cosine, sine components of the τ_j mode at a given harmonic

n — harmonic order with respect to the rotor speed

The jet control mode at 1P is used as an additional control to allow the maintainence of jet-off trim forces and moments.

For this study only one jet control mode was required (see Section 3.3). Hence the simplest mode shape f_{c_j}; was selected,

$$f_{c_j} = 1.0$$

for all cases studied.

The values of τ_{nj}^c, τ_{nj}^s required to suppress shears are treated as unknowns in the computer program.

3.6 Jet Spanwise Extent and Jet Recovery Factor

Both the jet spanwise extent and the jet thrust recovery factor, T_R, are treated as variables in the program. For all cases studied T_R was assumed to be 0.5.

Two different jet spanwise lengths were analyzed. The bulk of the cases were done for a jet spanwise extent of 0.5R. The location of the jet was over the outer 50% of the blade. Several cases were analyzed for a shorter jet extent of approximately 0.167R located, again, over the outermost blade span (see Figure 1; jet extent, (1) and (2)).

3.7 Synopsis of Cases Run

A total of 20 cases involving variations of the above parameters are presented herein. An identification number sequence was specified to keep track of the various cases run: e.g.

Case No. 1. 20. 03. 03

- 03 — run number within the set
- 03 — designates tip jet momentum, $C_{J_{T_0}}$
- 20 — designates advance ratio, μ
- 1 — designates rotor configuration
  - (1) 2 bladed, 10,000 lb. rotor
  - (2) 4 bladed, 20,000 lb. rotor

Table I is a synopsis of all cases discussed herein.

4.0 ROTOR AEROELASTIC SIMULATION

The Rotor Aeroelastic Simulation (RAS) used in this study is described briefly in the following subsections. A more detailed presentation of the basic method of approach can be found in Reference 13, 14 and 21. Appendix I presents the details of the modifications to the aerodynamic portion of the model necessary to include the jet.

In addition to the modifications required to include the jet, an extensive effort was expended to include the rotor trim forces and moments as dependent variables. The effort followed the lead of Chang in Reference 22 and extended it to allow constraint of the rotor trim as an integral part of the computational procedure. The trim equations are presented in Appendix II.

This versatile simulation may be employed to solve the aeroelastic/trim problem in a direct, inverse or any combination there-of manner, i.e.

1) Given certain prescribed control inputs - determine the blade airloads, blade responses, and rotor trim forces and moments.

2) Given certain desired rotor trim conditions and blade respsonses - determine the airloads and required control inputs.

3) Any combination of the above (1) and (2).

It was operational mode (2) which was used during this study.

4.1 Description of Aerodynamic Simulation

The aerodynamic model of Reference 21 (essentially identical to that of Reference 13) was employed in the current effort. Modifications to the aerodynamic model were made to include the effects of the jet on the lift, moment and drag of a rotor blade section in forward flight.

The jet effects were included in the unsteady aerodynamics of Reference 21 in a quasi-steady fashion. It is believed that this quasi-steady representation of the jet flap aerodynamics is a reasonable approach because:

1) of the preliminary nature of this investigation;

2) the quasi-steady approximations for the jet flap are of the same order as the approximations made to define the rotor wake;

3) it is believed that the quasi-steady jet flap aerodynamics will adequately account for the major effects of the jet flap;

4) the quasi-steady formulation is adapatable to the computational procedures employed;

5) the theoretical unsteady jet flap aerodynamic solutions have been challenged as to their validity and this controversy remains unsolved.

Erickson in Reference 23, has shown that the unsteady jet flap aerodynamics are composed of the classical von Karman/Sears terms (L_0, L_1, L_2 ; M_0 , etc.) of Reference 24, plus similar terms describing the effects of the jet, and dependent upon the airfoil motions, jet momentum coefficient and shape.

Because of the above, the results of Reference 21 (and hence Reference 13) were followed directly with the appropriate modifications to account for a quasi-steady model of the jet. The quasi-steady approximation for the jet included the effects of airfoil pitching rate as an equivalent camber. The steady state camber effects for a jet flapped airfoil were derived by Hough in Reference 25 and provided the basis for the quasi-steady approximation.

No attempt was made to incorporate further approximations. for the unsteady jet effects because of the questionable validity of the unsteady results which left no means for evaluating estimates.

The jet off aerodynamic model which was used can be described as being composed of an adaptation of the classical theory for a thin airfoil executing unsteady motions in an inviscid flow. The adaptation to a rotor system models the rotor blade as a series of spanwise segments whose spanwise aerodynamic properties are assumed constant. Each segment was modeled as an equivalent chordwise distribution of bound vorticity whose strength distribution is determined by the chordwise boundary condition of no flow through the airfoil. Since the blade is in an unsteady (periodically varying) flow, it is continuously shedding a wake which varies both radially and azimuthally due to the radial and azimuthal variations of the total bound circulation of the blade segments.

This rotor blade wake is modeled as a mesh of concentrated line vortices whose strengths and thus induced velocities (non-uniform inflow) are always consistent with the azimuthal and spanwise variation of the blade total bound circulation and the blade dynamic

response. The periodicity of these variations in the blade bound circulation (integer multiples of the rotor speed) when coupled with the chordwise boundary condition on the blade airfoil results in a set of simultaneous equations in the unknown bound circulation.

Application of the unsteady linearized Bernoulli equation provides the relation between the chordwise distribution of bound vorticity of the airfoil and the resultant pressure distribution. From the unsteady chordwise pressure distribution may be obtained the unsteady local lift and moment and hence the spanwise and azimuthal variations of these quantities for the rotor blade.

Added to this model are the quasi-steady effects of a thin high velocity jet of air emanating from the airfoil trailing edge at an arbitrary angle with respect to the airfoil. The jet is modeled as a distribution of vortices and doublets along the jet centerline which in the limit of a thin-high speed jet becomes simply a single sheet of vorticity on the jet centerline. For the steady flow case the effect of this jet is shown by Spence (Reference 26) to affect the pressure distribution (and hence the airfoil load) in a fashion proportional to the jet momentum coefficient, airfoil angle and jet angle. Hough in Reference 25 included the camber effects in a similar fashion. Since a quasi-steady model for the jet flap airfoil was assumed, the instantaneous motions of the airfoil were treated, insofar as their direct effect on the pressure distributions, as though they had always existed. The indirect effect of the unsteady jet was approximately accounted for via the wake model in that changes in the total bound circulation due to the jet were reflected as changes in the wake vortex strengths and hence modified the impressed velocity distribution on the airfoil.

Thus the rotor blade section lift, drag and pitching moment are computed including the effects of a wake and nonuniform inflow which are always consistent with the coupled blade motions and the jet effects.

The details of the equations are presented in Appendix I.

4.2 Description of Blade Structural Model

To determine the inertia and elastic forces required for the aeroelastic problem, a Lagrangian approach was used. Following the development of Reference 27, the kinetic and potential energy of an elastic twisted rotating beam was written. A dissipation term proportional to the elastic displacement and in phase with the elastic velocity was written to account for structural damping forces. The elastic displacements were then expanded in terms of the normal modes of the blades, and the Lagrangian was applied. Since the forcing function of the system, i.e., response independent aerodynamic load, is periodic with its fundamental frequency being Ω, the steady-state response of the linearized system must be periodic of fundamental frequency Ω. Hence, both the motions and the generalized aerodynamic forcing functions were expanded in Fourier series on Ω. Then, by the uniqueness theorem for trigonometric series, corresponding coefficients must be equal. The result is a set of $2M$ (where M is the number of modes or degrees of freedom retained) simultaneous algebraic equations in the Fourier coefficients (of sine and cosine components) of the motions for each of p harmonics. The zeroth harmonic has only M simultaneous equations, since there are no corresponding sine terms in the series.

The following assumptions were made in defining the structural model:

(1) Simple beam theory was applicable.

(2) Airfoil cross sections were symmetrical with respect to the major neutral axis; hence, the center of gravity lies in this plane.

(3) Gravity forces were negligible.

(4) Flight conditions were steady state.

(5) Damping (structural) was proportional to the elastic displacement and in phase with the elastic velocity.

(6) Blade elastic deformations were small.

(7) Pitch axis, elastic axis and center of gravity were non-coincident.

The resultant set of linearized equations of blade motion include all the necessary mass, elastic, centrifugal, gyroscopic and aerodynamic force terms required to describe 7 fully coupled degrees

of freedom of the rotor blade. The equations have been constituted so as to be able to handle blade end conditions of flapping, teetering, lead-lag and cantilevered in any combination. The aerodynamic forces are described in Section 4.1 and Appendix I.

For the rotor configuration reported herein, flapping (h_1) plus 6 fully coupled elastic degrees of freedom were provided for. The elastic degrees of freedom were:

1) Two flatwise bending modes, h_2, h_3

2) Two chordwise bending modes, H_1, H_2

3) Two torsional modes, θ_1, θ_2

A discussion of the complete set of equations to be solved and the method of solution are presented in Sections 4.3 and 4.4.

4.3 Overall Problem Formulation

The overall problem formulation and solution procedure used for this study are based on those developed by Daughaday and reported in Reference 13. The aerodynamic simulation was modified to account for the influence of the jet flap as described in Section 4.1 and Appendix I. The problem formulation was changed to include the rotor trim parameters and allow them to be treated as dependent variables.

Daughaday's formulation of the rotor aeroelastic response problem represents a powerful and versatile tool. As presently formulated it allows the amplitude and phase of any two of eleven dependent variables of the rotor to be arbitrarily and independently constrained at each harmonic and the solution to be obtained for the remaining nine. Furthermore, it utilizes a sophisticated aerodynamic modeling of the blades and their wake which maintains the wake strength distribution and non-uniform inflow distribution consistent with the blade dynamic response and unsteady airloading.

The rotor trim parameters were included within the formulation as dependent variables (discussed in Appendix IV) as part of this effort. Thus the usefullness of the method has been expanded by allowing the rotor trim to be constrained (specified) if desired.

The set of eleven dependent variables are, at each harmonic (except the first), the seven blade degrees of freedom (Section 4.2), two components of blade root shear (horizontal and vertical), and two control variables. The exception at the first harmonic is that the rotor trim forces and moments are included as dependent variables in place of the blade root shear variables. This is possible when it is recognized that the first harmonic blade root shears determine the rotor trim parameters and therefore they cannot be independently specified. Furthermore, since these trim parameters are also functions of the other dependent variables, their equations can be incorporated into the equation set at the first harmonic in a manner similar to the blade root shear equations.

The two control variables at each harmonic (except the zeroth and the first) are the deflection angles of the two jet flap control modes. At the zeroth and first harmonic the first jet flap control mode is replaced by the rigid-body pitch control mode.

Because of the periodicity and the linearization of the structural representation as mentioned in Section 4.2 (Structural Model), the set of equations at each harmonic are independent. That is there is no structural/mechanical interharmonic coupling. However the aerodynamic interharmonic/intermodel coupling is included and enters through the aerodynamic forces on the right-hand-side of the equations (Section 4.4 on solution procedure).

The overall problem formulation is discussed in more detail in Appendix IV.

This formulation can be used to solve the direct rotor aeroelastic problem by constraining the rigid pitch control, i.e., given the rotor-operating condition and control setting, compute the resulting unsteady airloads, blade responses, rotor total loads and moments, and performance. It can also be used to determine control settings required in addition to the above loads and responses by constraining the rotor trim parameters. Or it can be used to perform either one of the above solutions with constraints impressed at any of the higher harmonics on any of the dependent variables.

4.4 Solution Procedure

The solution procedure employed is an iterative one. The rationale for this procedure is briefly described below and the logic flow depicted in Figure 16.

At each harmonic of the rotor speed, let the set of equations for the unconstrained variables be written as follows in matrix notations,

$$\hat{F}\bar{X}_o = \bar{y}_o \qquad (4.4.1)$$

or

$$(D+C)\bar{X}_o = \bar{y}_o \qquad (4.4.2)$$

where $\hat{F} = (D + C)$ is the matrix of coefficients relating the unconstrained variables and the forcing functions

D is the matrix of mass, spring and damping coefficients

C is the matrix of aerodynamic mass, spring and damping coefficients, i.e. coefficients of the response dependent air forces

$\bar{X}_o$ is the vector of unconstrained variables

$\bar{y}_o$ is the vector of driving forces (forcing functions).

If the aerodynamic forcing functions, $\bar{y}_o$, (forces independent of the blade responses, $\bar{X}_o$) and the aerodynamic response dependent forces, $C\bar{X}_o$, could be explicitly written as indicated above then a direct solution would be possible as

$$\bar{X}_o = \hat{F}^{-1}\bar{y}_o \qquad (4.4.3)$$

However because the "true" aerodynamic forcing function and the blade response aerodynamic forces cannot be accurately expressed explicitly, they are computed from an aerodynamic simulation in the time domain. But the computed blade section airloads, as obtained from the aerodynamic simulation, are the sum of the aerodynamic forces representing the "true" forcing function (independent of the blade response) and the response dependent aerodynamic forces. Thus for a given response vector, $\bar{X}_i$, the aerodynamic simulation yields the following force vector

$$\bar{GF}_i = (\bar{y}_o - C\bar{X}_i) \qquad (4.4.4)$$

which is the combination of both the forcing function and the response airloads, i.e., C exists only implicitly in the aerodynamic simulation.

Thus Equation (4.4.2) must be written

$$D\bar{X}_o = (\bar{y}_o - C\bar{X}_o) \equiv \bar{GF} \tag{4.4.5}$$

It is the above equation which must be solved.

If an approximation to the response dependent airloads, $C\bar{X}_o$, is written as $E\bar{X}_o$ then the set of equations can be written as follows for solution

$$(D + E)\bar{X} = (\bar{y}_o - C\bar{X}) + E\bar{X} \tag{4.4.6}$$

or

$$F\bar{X} = \bar{GF} + E\bar{X} \tag{4.4.7}$$

where

$$F = (D+E)$$

The solution would be

$$\bar{X} = F^{-1}(\bar{GF} + E\bar{X}) \tag{4.4.8}$$

It is obvious from Equation (4.4.6) that if E were equal to C then (4.4.8) would be the solution to Equation (4.4.1), however this is not the situation because it is not possible to express C explicitly. Equations (4.4.6) and (4.4.8) do however suggest a way to obtain the solution by successive approximations (iteration).

For a given (initial) approximation $\bar{X} = \bar{X}_i$, a new approximation to the $\bar{X}$ can be obtained from (4.4.5) and (4.4.6) as

$$(D + E)\bar{X}_{i+1} \approx (\bar{y}_o - C\bar{X}_i) + E\bar{X}_i \tag{4.4.9}$$

$$\bar{X}_{i+1} \approx F^{-1}(\bar{GF}_i + E\bar{X}_i) \tag{4.4.10}$$

This new approximation is then used in the aerodynamic simulation to re-evaluate the force vector which is represented by Equation (4.4.4) as,

$$\bar{GF}_{i+1} = (\bar{y}_o - C\bar{X}_{i+1}) \tag{4.4.11}$$

If this process of successive approximation is continued (as depicted in Figure 16) and it converges, that is

$$(\bar{X}_{i+1} - \bar{X}_i) \rightarrow 0$$

then the resulting $\bar{X}$ will be the solution. This is evident from Equation (4.4.9) which would then reduce to Equation (4.4.1) because $E\bar{X}_{i+1}$ would equal $E\bar{X}_i$. This is the iterative solution procedure used.

The E-Matrix of coefficients representing the explicit approximation to the response aerodynamic loads is based on quasi-steady aerodynamics. The D-Matrix represents all the non-aerodynamic forces. The F-Matrix ($F=(D + E)$) is pre-computed for each harmonic and inverted for use in calculating the successive approximations to the response vector, $\bar{X}_i$.

It should be noted that in this procedure the inflow distribution is always consistent with the blade response and airloads. The interharmonic aerodynamic coupling enters through the aerodynamic simulation.

Relative to convergence -- while no quantitive measure has been found for ascertaining convergence characteristics of a specific solution, it has been found that reducing the sensitivity of the right-hand-side of Equation (4.4.8) to the response, $\bar{X}$ (i.e., improving the E approximation to C) does improve the convergence.

5.0 RESULTS

Presented in this section are the synopsized results of the investigation. It is felt that the information presented here answers the main thrust of the study, namely "What are the transmitted shears and what is the corresponding jet control schedule and power required to suppress these shears?" This information is presented in the form of tables of amplitude and phase at each harmonic for all (transmitted and non-transmitted) shears and jet control angles. Also presented are plots of the azimuthal variations of the total jet control angle required.

The total power required is presented for both jet-on and jet-off cases. The jet-on power includes estimates for the required jet-flap control compressor power. Jet-off results are discussed first, followed by the comparable jet-on results. Special jet-on cases are then discussed.

Additional results in the form of blade responses, bending moments, lift load distributions, etc. are introduced only as needed to help clarify results or presented as representative indicators of what happened in general.

In all cases in which shear suppression was required, the shears were suppressed to zero.

5.1 GENERAL PRESENTATION OF RESULTS

5.1.1 Jet-Off Rotor Results

As described in Section 2.0 the two-bladed rotor was investigated at three advance ratios (μ = 0.08, 0.2 and 0.3) with jet-off. These cases provided the basic data on the values of the shears to be suppressed and the rotor trim conditions to be maintained. Presented in Tables 2 and 3 are all of the harmonics of the vertical and horizontal (respectively) blade root shears at each μ . (As used herein "vertical" and "horizontal" are in the shaft-axis system). Also presented are the jet-off shears for the four-bladed rotor (Case 2.20.00.02) and the torsionally stiff blade (Case 1.20.00.50).

In all results presented, the amplitude and phase referred to are defined by the following general expressions for the n^{th} harmonic variation with ψ of a quantity, $S(\psi)$:

$$S_n(\psi) = a_n \cos n\psi + b_n \sin n\psi$$

$$S_n(\psi) = A_n \cos(n\psi + \gamma_n)$$

$$A_n = \left[a_n^2 + b_n^2\right]^{1/2}$$

$$\gamma_n = -\tan^{-1}(b_n/a_n)$$

The zeroth and first harmonics (0P and 1P), of the blade root shears contribute to the trim of the craft as described in Section 4.3 and Appendix IV. For the two-bladed rotor, above the first harmonic, only the even harmonics of vertical blade root shears are transmitted, while only the odd harmonics of the horizontal blade root shears are transmitted.

The nominal acceleration level considered to be acceptable by pilots at 3P has been found to be about 0.015 g. This value is used herein as an approximate criterion of "acceptable" transmitted acceleration levels at all harmonics for purposes of the discussion only. For the investigation, the transmitted shears were all suppressed to zero.

For the two-bladed rotor at μ = 0.08, only the second and fourth harmonic transmitted vertical shears exceed the above criterion of 0.015 g while none of the horizontal transmitted shears (at 3P, 5P, 7P, 9P and 11P) exceed this level. At μ = 0.20 and 0.30 only the 2P vertical transmitted shear exceeds the criterion and, again, none of the horizontal transmitted shears exceed it.

The effect of increasing the torsional stiffness of the blades on the transmitted shears was, generally, to decrease them. The exceptions occurred at 4P vertical where the shears increased by approximately 5%, and at 7P horizontal where the shear increased by approximately a factor of 5. In both cases the increased values were still below the criterion.

The rotor configuration change from a two-bladed to a four-bladed rotor and increasing the weight from 44482 N to 88964 N kept the lift load per blade the same while increasing the disk loading and hence the mean downwash. The amplitude and frequency content of the downwash was correspondingly altered. Generally, the effect on the vertical and horizontal transmitted shears was to reduce (or exhibit no change in) their value. The exceptions were at 4P and 6P vertical and 7P horizontal where large increases are noted.

The changes in the 1P shears for the above discussed cases are reflected as changes primarily in the rotor rolling and pitching moments. These rotor trim moments are plotted vs μ and

presented in Figure 17. These are the values to which the jet-on cases were constrained. Presented in Figure 18 are the corresponding jet-off rotor power requirements. A minimum in rotor power required is noted at about $\mu = 0.125$.

The required control angles (collective and cyclic) are presented in Figure 19. Note the slightly larger values of control angles required for the torsionally stiffer blade. This is the result, at least in part, of the smaller contribution of the torsional blade response to the effective angle of attack; thus since the rotor is constrained to maintain trim forces in both cases, increases are required in the control angles. Note that for the case in hand the elastic axis (e) is aft of the quarter chord (aerodynamic center for jet-off) over most of the blade span (See Figure 1) and hence the aerodynamic pitching moment with respect to the e is nose up (positive).

A slight decrease in the power required was noted for the torsionally stiff blade.

5.1.2 Jet-On Transmitted Shears Suppressed Results

5.1.2.1 Basic Rotor Configuration

5.1.2.1.1 Advance Ratio Variation

Presented in Tables (4a-c) and (5a-c) are the jet-on vertical and horizontal (respectively) blade root shears at all harmonics (transmitted and nontransmitted) for each case run. Presented in Table (5a-c) are the corresponding data for the jet angle required. See Table I for the case designation.

The azimuthal variations of the required jet angles for each case presented in the Tables are presented in Figures 20 to 26.

The transmitted vertical shears for the two-bladed rotor which were to be suppressed at each μ are presented in Figure 27 (Cases 1.08.00.03, 1.20.00.09 and 1.30.00.04). The total amplitude (from Table 4) at 2P, 4P, 6P, 8P and 10P only is plotted. Similar plots are presented for the transmitted horizontal shears (at 3P, 5P, 7P, 9P and 11P) in Figure 28. These are the values which were to be suppressed. Also presented are the 1P shears which determine the trim of the helicopter -- they are termed "TRIM SHEARS".

The transmitted shears presented in Figures 27 and 28 were suppressed to zero at $\mu = 0.08$ and $\mu = 0.20$ (See Tables 4 and 5). The values of the jet control amplitude required at each harmonic to achieve this suppression are presented in Table 6 for several

values of $C_{J_{T_0}}$. The azimuthal variation of the total jet control angle (τ) at the tip required to suppress these shears is presented in Figures 20, 21 and 22. As can be seen from these plots, the maximum value of τ required to suppress all the transmitted shears and maintain the trim forces and moments to the jet-off values never exceeded 60°. Furthermore, from Table 6, the principal harmonic contributors were the 1P and 2P components. Trim requirements alone always produced large 1P τ values as is evident in Figure 22. (See Section 5.2.5)

It was observed that for the vertical shears, the trend of the required τ to suppress vertical shears at a given harmonic followed the trend of the vertical shear with μ . Thus, for example, the trend of the vertical shears vs μ for the 4P harmonic indicates a decrease in amplitude from μ = 0.08 to μ = 0.20, hence the τ's required would exhibit the same trend. This is true for all harmonics except at 2P where it is true only for $C_{J_{T_0}}$ = 0.01. No such pattern was observed for the horizontal transmitted shears.

No results were obtained with the jet-on at an advance ratio of 0.3 because it was not possible to obtain a converged solution for this operating condition. The divergence was dominated by the 7P response of the second chordwise bending mode which has natural frequency of 7.45 P at the rotor operating speed (see Figure 10). This problem could be a numerical/computational instability of the iterative procedure or it could be indicative of proximity to an unstable operating condition for the rotor system simulated. It is noted that with the jet-off, at μ =0.3, a converged solution was obtained but a large region of blade stall was encountered on the retreating blade. This could also be a significant ingredient in the instability of the solution for this operating condition when the jet is on.

A method to improve convergence was applied to this case which had in similar cases allowed converged results to be obtained. The technique involved the determination of correction elements to be used in the offending degree of freedom and harmonic which aided only the convergence characteristics of the iterative solution technique but did not affect the solution once convergence was obtained. This method was unsuccessful in the present cases.

5.1.2.1.2 Jet Momentum Coefficient Variation

Several values of $C_{J_{T_\theta}}$ were studied at $\mu = 0.08$ and $\mu = 0.20$ (See Table 1). The azimuthal variation of the required τ to suppress shears at $\mu = 0.08$ indicates a larger peak τ for the lower blowing coefficient ($C_{J_{T_\theta}}$). However at $\mu = 0.20$ the opposite is observed. The principal harmonic contributions to τ at all μ are the 1P and 2P components as can be seen in Figure 29. In Figure 29 are plotted the jet control amplitudes required at each harmonic to suppress the transmitted shear at that harmonic versus jet tip momentum coefficient.

No obvious trends with $C_{J_{T_\theta}}$ can be observed except at 1P. There, for both $\mu = 0.08$ and 0.20, the amplitude of the jet control angle required increases with increasing blowing coefficient values. As will be discussed more fully subsequently (See Section 5.2.3), this trend is attributable to the fact that the lower $C_{J_{T_\theta}}$, upset trim (i.e., rolling and pitching moments) less from the jet-off values and hence require smaller τ to restore trim to the jet off values.

If only $C_{J_{T_\theta}} = 0.01$ is considered, Figure 29 shows that at all harmonics the required τ trend with μ follows the corresponding flapwise or chordwise shears trend with μ as pointed out in Section (5.1.2.1.1). However for increased $C_{J_{T_\theta}} = 0.03$ it is observed that these trends are reversed at 2P, 3P, 5P and 7P. These results provide some small indication as to the complex nature of the interaction which occur between the influence of the jet and the blade responses. The effects of blade resonances, interharmonic couplings and the manner in which shear suppression is achieved via the balancing of inertia, spring, damping and aerodynamic forces change with $C_{J_{T_\theta}}$ and μ. Though not definitive, a discussion of these interelations is presented in Section 5.2.3.

Presented in Figure 30, as indicative of what happens to blade responses when the jet is activated, is the azimuthal variation of the tip deflection of the 6 elastic blade degrees of freedom for the jet off and $C_{J_{T_\theta}} = 0.03$ case at $\mu = 0.20$. Note in particular the greatly increased torsional response of the blade with the jet on. Both first and second torsion are affected (note scale change between 1st and 2nd torsion). If the variation of first torsion in Figure 30 is compared to the τ of Figure 22

for all shears suppressed (the torsion and τ both result from Case 1.20.03.08) the following are noted:

1) a very strong similarity in the azimuthal variation between θ_1 and τ
2) approximately a factor of 10 difference in the θ_1 and τ peak amplitudes
3) an approximate 180° shift in phase between θ_1 and τ .

5.1.2.1.3 Torsionally Stiff Blade

The observations in the preceeding section concerning the blade torsional response led to the speculation that a torsionally stiffer blade would require larger jet deflection angles, τ , to accomplish the shear suppression. The results for a torsionally stiff blade (Case 1.20.03.58) are presented in Tables 4, 5 and 6 and in Figure 23. The torsionally stiff blade did require significantly more, τ , to suppress the shears at all harmonics except 2P and 8P (see Table 6). However, the stiff blade required less τ at 1P for trim but the 1P is still the dominant frequency component. A discussion of these results is presented in Sections 5.2.1 and 5.2.2.

5.1.2.1.4 Selected Shear Suppression

Several cases were run to determine the effects on the transmitted shears when only selected shears were suppressed. The cases considered were at μ = 0.20 for $C_{J_{T_0}}$ = 0.03. The shears chosen for suppression were the 2P vertical and the 5P vertical shears. Also run was a case in which the 2P, 4P and 6P vertical shears and the 3P and 5P horizontal shears were suppressed (i.e., all transmitted shears through the 6P). In all cases, trim was maintained at the jet-off values. The required τ azimuthal variation for these cases is presented in Figure 25. Also presented in that figure is the τ for suppressing all transmitted shears through the 11P harmonic. The τ variation required for suppressing all transmitted shears compared with that required for suppressing only the first six transmitted shears can be seen to differ mostly at the 7P and 9P components. These 7P and 9P components of τ are those required to suppress the horizontal shears at 7P and 9P.

Several interesting observations can be made from these cases, namely;

1) interharmonic effects may be quite strong

2) suppression of one harmonic of shear (flapwise or chordwise) will affect the magnitude of all others -- generally the shears at harmonics immediately above and below the suppressed harmonics are most affected.

A quick scan down the vertical and horizontal shears of Tables 2, 4 and 5 for Cases 1.20.00.09, 1.20.03.09 and 1.20.03.10 will verify the above. Also observe Case 1.20.03.20 where only rotor trim was constrained; note especially the very large change in the 2P components and the substantial changes in the chordwise shears induced by the jet at the 6P and 7P harmonics. Thus simply turning on the jet and using only a 1P variation to maintain trim caused large changes in blade root shears at other harmonics. It is speculated that the large changes at the 2P and 7P harmonic are at least in part related to the fact that the chordwise bending mode resonances are in these ranges (See Figure 10).

5.1.2.1.5 The Short Span Jet

To determine the effect of changing the spanwise extent of the jet a "short jet" case (1.20.03.S6) was run suppressing only the 5P harmonic of the vertical shear. This harmonic was chosen because it was closest to the first torsional natural frequency. When compared to the long jet (See Figures 25 and 26 and Table 6) -- 5P shear suppression (1.20.03.10), a smaller 1P variation to maintain trim was required by the short jet; however almost twice the τ amplitude at 5P was required to suppress the vertical shear. The more important aspect of this case is the fact that the power is much reduced for the short jet (See Section 5.1.3)

5.1.2.2 Four Bladed Rotor Configuration

The four-bladed, 88964 N rotor results are presented in Figure 24 and Tables 4 through 6 to Case 2.20.03.02. All transmitted shears were reduced to zero. Relative to the two-blade rotor, large changes in τ requirements occurred at virtually all harmonics; except for 2P all even harmonic requirements were substantially increased. No pattern for τ required to suppress the horizontal shears emerged.

5.1.3. Total Power Considerations

As discussed previously, the analysis computes the basic rotor power required jet-on or jet-off due to the aerodynamics and inertial loads of the blades. To this power was added the estimated compressor power required to supply the jet (See Section 3.4 and Appendix III for details). Thus the total power required was given by

$$P_T = P_R + P_c \qquad (5.1.3.\ 1)$$

The compressor power P_c was derived as a function of $C_{J_{T_o}}$ and μ and is presented in Figure 13. The rotor shaft power, P_R, was determined as

$$P_R = \frac{N\Omega}{2\pi(550)} \int_0^{2\pi} \int_0^R \left[\mathcal{L} \cdot \alpha_i + \mathcal{D} \right] r\, dr\, d\psi \qquad (5.1.3.\ 2)$$

P_R = power supplied to the shaft (SHP)

$\mathcal{L}$ = blade section lift including jet contributions

$\mathcal{D}$ = blade section drag including jet contributions

α_i = blade section induced angle

N = number of blades

Ω = rotor speed

(See Appendix I, Equations I-31 and I-37 and Appendix III, Equation III-2) Recognizing that equation (5.1.3. 2) can be written as

$$P_R = P_{C_D} + P_I - P_{C_J} \qquad (5.1.3.\ 3)$$

where

P_{c_p} =power due to the profile drag

P_I =power due to induced effects

P_{c_J} =power (propulsion) due to the jet

Equation (5.1.3. 1) can be then written as

$$P_T = (P_{c_p} + P_I - P_{c_J}) + P_c \qquad (5.1.3.\ 4)$$

Recognizing that

$$P_{c_p} \propto \alpha_g^2$$

$$P_I \propto \mathcal{L} \cdot \alpha_i$$

$$P_{c_J} \propto \cos(\alpha_g + \tau)$$

and that α_g , α_i , τ and $\mathcal{L}$ may be represented by a Fourier Series on ψ, it can be shown that the "mean" total power, P_T, in the Fourier sense, depends not only on the steady valves of α_g , α_i , τ and $\mathcal{L}$ but also on the higher harmonic amplitudes of these quantities. For example,

$$P_{c_J} = \frac{N\Omega}{2\pi(550)} \cdot (\rho b R^2 \Omega^2)(C_{J_{T_0}})(f_{c_J}) \int_0^{2\pi} \int_{r_J}^{R} r \left[T_R + \right. \qquad (5.1.3.\ 5)$$

$$\left. + (1 - T_R)\cos\theta \right] dr\, d\psi$$

$$P_{c_J} \approx C_1 - \sum_n C_{2_n} \int_{r_J}^{R} r \left[(\theta_n^c)^2 + (\theta_n^s)^2 \right] dr \qquad (5.1.3.\ 6)$$

where

C_1 =function of only the steady valves of θ

C_2 =constant of integration

$\theta_n^{c,s}$ =cosine, sine components of the n^{th} harmonic of the sum $(\alpha_g + \tau)$

Thus while ordinarily the jet-off harmonic variation of α_y, α_i and $\mathcal{L}$ may be ignored with regard to power, with the jet-on they may become important. Further it should be noted that there is a power penalty to be paid for activating τ which is proportional only to the jet deflection amplitude required regardless of the harmonic. Also keep in mind that $C_{J_{T_o}}$ and τ also influence $\mathcal{L}$ and α_i. Hence the overall interaction is quite complex as discussed in the following paragraphs.

The total power, P_T, required at $\mu = 0.20$ to maintain trim and suppress all transmitted shears is presented in Figure 31 as a function of $C_{J_{T_o}}$. It is observed that this total power is a monotonically increasing function of $C_{J_{T_o}}$, i.e., in these results, there is no indication of a minimum with respect to $C_{J_{T_o}}$. However these results do not necessarily rule out the possibility of such a minimum. The lack of a minimum with respect to $C_{J_{T_o}}$ may be the result of the trim philosophy adopted for this study (see Section 5.2.5).

The following observations can be made concerning the various contributions to the total power required. It is helpful if Equation (5.3.1 4) is rewritten as the following two groups of terms,

$$P_T = P_c\left(1 - P_{c_J}/P_c\right) + \left(P_{C_D} + P_I\right) \qquad (5.1.3\ 7)$$

Concerning the first group of terms, it is first recalled that the compressor power required, P_c, is a monotonically increasing function of $C_{J_{T_o}}$ as in Figure 13, and that the jet reaction/recovery power, P_{c_J}, is that portion of P_c recovered (i.e., $P_{c_J}/P_c < 1$). Second, it is recalled (Equation 5.3.1 5 and 6) that P_{c_J} increases with $C_{J_{T_o}}$ and decreases with τ (regardless of the harmonic) —— the required τ's, however, depend on $C_{J_{T_o}}$. That is the τ's required to suppress the shears, τ_S, decrease with increasing $C_{J_{T_o}}$ and the τ's required to maintain the jet-off trim, τ_T, increase with $C_{J_{T_o}}$. Thus, if only the τ required for trim, τ_T, is considered, then the net power resulting from the first group of terms is a monotonically increasing function of $C_{J_{T_o}}$. It is not possible, apriori, to determine the variation of this net power with $C_{J_{T_o}}$ due to the τ's required for shear suppression, τ_S, because it will depend on the relative rate of change of τ_S and P_c with $C_{J_{T_o}}$.

However, for the trim philosophy used, the increase of τ_T with $C_{J_{T_o}}$ is much greater than the decrease of the τ_s, and furthermore, because P_{c_J} varies as the square of τ (Equation 5.1.3. 6), it is believed that the τ_T influence dominates and thus the total power P_T increases monotonically with $C_{J_{T_o}}$.

The influence on the total power represented by the second group of terms (Equation 5.1.3. 7) is more obscure than the first group of terms. Both the "profile power", P_{c_o}, and the "induced power", P_I, will be indirectly influenced by $C_{J_{T_o}}$ and τ. It is expected that $C_{J_{T_o}}$ would reduce the profile power, P_{c_o}, but the magnitude of the influence would depend on the operating state of the local airfoil section (i.e. Reynolds number, Mach number, angle of attack, etc.). The influence of $C_{J_{T_o}}$ on the induced power, P_I, would be through the lift distributions and thus the induced velocities. However it is believed that it would, to a larger extent, be determined by the specific application of the jet-flap. That is, it would depend on the redistribution of the lift required (and thus the τ required) for the specific application.

Also plotted on Figure 31 is the total power, P_T, required to turn the jet on and only maintain trim at $\mu = 0.2$ and $C_{J_{T_o}} = 0.03$; it is,

$$P_T = 1193 \text{ HP.}$$

Of this total, 872 HP was the compressor power required. The jet-off shaft power, P_T, was 892 HP.

Thus a 34% power increase was required just to maintain rotor trim at its jet-off value when the jet was turned on. Further it is noted that for this case, the compressor power required just about equals the jet-off power required. It has been speculated that, if trim had not been required to be maintained in the manner of this study, the power penalty indicated herein may have been substantially reduced.

Even with the adverse power requirement (relative to trim maintainance), Figure 31 implies that the job of suppressing all transmitted shears can be accomplished simply by reducing the jet tip momentum sufficiently. The increment in power required (See Figure 31) to go from maintaining trim

only to trim plus full shear suppression is indicative of the effect of higher harmonic τ contributions. An additional 117 HP was required just to suppress all transmitted shears while maintaining trim (compressor power held constant for $C_{J_{T_o}} = 0.03$ and $\mu = 0.2$). Thus the total power required was increased by 47% over that required jet-off, but only 13% of the increased power required was attributable to the requirement to suppress all transmitted shears.

What was not definitively ascertained in this study was the corresponding limits on the resulting jet control angle amplitudes. For the lower, $C_{J_{T_o}}$ (0.005) studied the total value of τ , required to maintain trim and suppress all shears was not large (see Figure 21). This was due to the fact that as $C_{J_{T_o}}$ was decreased the rotor trim was upset less and less and hence the 1P-τ required to maintain trim was smaller. Thus because the 1P-τ component is by far and away the largest term in the series representation of τ , the increased values of τ required at the higher harmonics to suppress shears at this low $C_{J_{T_o}}$ were more than compensated for by the reduced 1P-τ requirements.

At some sufficiently small value of $C_{J_{T_o}}$ it is expected that, even though the 1P-τ required for trim would be very small, the required τ to suppress higher harmonic shears would begin to become prohibitively large from a practical standpoint. Once the jet angles become sufficiently large, the analysis employed herein begins to suffer from certain small angle assumptions made in the aerodynamic modeling.

The effect on power required for suppressing selected shears is presented in Table 7. There it is seen that for a fixed μ and $C_{J_{T_o}}$(0.3 and 0.03 respectively) requiring successively more shears to be suppressed increases the P_T required. The cases suppressing the 2P and 5P flap-wise shears tend to substantiate that the power required to suppress a given harmonic of shear at a given C_{J_T}, and μ goes like the τ required.

The power required for the torsionally stiffer blade is considerably reduced over the power required for the less stiff blade (Figure 31). This power difference is

attributable to the large changes in the τ required and the large changes in torsional response. The jet-off power requirements for the torsionally stiff blade were also found to be slightly lower, 874 HP, than for the less stiff blade. Thus stiffening the blade had a beneficial effect on the power required.

The reduced 1P torsional response is reflected directly in the reduced τ requirement at 1P (see Table 6b and 6c - Cases 1.20.03.08 and 1.20.03.58). A large reduction in the 2P component is also noted. Although not explicitly identifiable, it is believed that the large power reduction observed is due to the reduced 1P-τ and the reduced shear load to be suppressed at 2P because of the reduced torsional response. The τ requirements at all the remaining higher harmonics are significaltly increased. The reduced 1P and 2P τ requirements more than outweigh the increased higher harmonic τ requirements. Thus the overall result is the large reduction in power required. These explanations are somewhat speculative because the requirement for maintaining trim tends to obscure the influence of the other participants.

Similarly, the comparison of P_T between the long jet and short jet cases (1.20.03.10 and 1.20.03.56) in Table 7 indicates a much reduced power requirement. Thus, although a much larger τ is required (but not excessively large), the same trim balance and shear suppression was achieved at a much smaller power.

Presented in Figure 32 is a crossplot of P_T vs μ for the cases run. Power jet-on trends follow the jet-off trends as might be expected.

The power required jet-on and off for the four bladed rotor is presented in Table 7 (Cases 2.20.00.02 and 2.20.03.02). A comparison of the jet-on power for the two bladed rotor and the four bladed rotor indicates that approximately the same power penalty is paid to suppress all shears for both configurations.

5.2 Discussion of Results

The results as presented in Section 5.1 encompass the complete scope of this investigation to assess the theoretical potential of a jet-flap control system for reducing the vertical and horizontal transmitted blade root shears. In this section, some of the more pertinent or interesting aspects of these results are noted and discussed. It should be recalled that the rotor aeroelastic response problem is not a simple one. The many parameters, forces, and variables are intimately interrelated, therefore, simple explanations may not always exist. Furthermore those which are presented may not necessarily be generalized beyond the specific problem in-hand.

5.2.1 The Role of the Blade Torsional Response

The results of some of the inital calculations for suppression of the transmitted blade root shears on the basic rotor configuration, suggested that the blade torsional response may be a primary element in the jet flap control system. It was observed that because of the effectiveness of τ in generating blade section aerodynamic pitching moments (relative to the elastic axis), it was the dominant driving "force" on the torsion response. That is, τ was controlling the first torsion mode.

The question was then raised as to which was the "effective" aerodynamic force control in reducing the shears--the jet deflection angle, τ , or the blade torsional deflection angle, θ ? Actually τ is the "primary" control (because it is the input to the rotor) and both τ and θ influence the aerodynamic loads but what are their "effective" aerodynamic roles? Is the torsional response reducing the effectiveness of τ or is it a beneficial influence on the efficiency of the jet flap control system relative to shear reduction? With the objective of obtaining information relative to the above kinds of questions, additional calculations were made.

In order to assess the importance of the torsional response relative to τ , the torsion response was virtually eliminated by increasing the generalized stiffness in torsion by a factor of 10 (so that ω_{n_1} @ 16.7P and ω_{n_2} @ 43.8P). The τ control schedule required to suppress all the transmitted blade root shears was then re-calculated. The resulting azimuthal variation of τ is presented in Figure 23 and the corresponding harmonics in Table 6c (Case 1.20.03.58). The harmonics of the resulting blade root shears are presented in Table 5c. The corresponding results

for the standard blade are in Figure 22 and Tables 6b and 5b, (Case 1.20.03.08). It is observed that, virtually eliminating the blade torsional response has increased the τ -amplitude requirement at all harmonics except 1, 2 and 8. This would seem to indicate that the torsional response of the standard blade is generally beneficial relative to the effectiveness of the jet flap in shear suppression. However it degrades the effectiveness relative to trim at 1P as described below. This result further supports the conjecture that (for the standard blade) the jet flap is controlling torsion and the torsion is the "effective" aerodynamic force control. That is the jet flap is operating as a control tab (trim tab) similar to the Kaman "controllable-twist" rotor (Reference 33).

The above exception at the 1st and 2nd harmonic (n = 1 and 2) are not really understood. However it should be noted that the constraints are different at n=1, i.e., the rotor trim force and moment are constrained rather than the blade root shears. It may be that, relative to rotor trim, τ is the dominant influence and the torsion influence is opposing that of τ , i.e. reducing its effectiveness. It is noted that, at n = 1, torsion is nearly 180 degrees out of phase with τ (i.e., θ is negative when τ is positive). Thus, for the stiff blade at n = 1, the reduced torsion response (from 4.8° to 0.4°) would increase the effectiveness of τ relative to trim and thereby explain the reduced τ requirement (from 31.1° to 27.4°). No rationalization of the anomalous results relative to the τ requirement at n = 2 and n = 8 can be offered.

The greater effectiveness of the blade section angle-of-attack θ , over that of the jet-deflection angle, τ , in controlling the aerodynamic forces arises because the τ- dependent force coefficient slopes (e.g., $\bar{C}_{L_\tau}$) go to zero as C_{J_τ} goes to zero while the θ -dependent slopes (e.g., C_{L_α}) go to their jet-off values (see Appendix I). Thus for example, the variation of the ratio, $C_{L_\alpha} / \bar{C}_{L_\tau}$, (the respective α and τ lift curve slopes) with C_J is as sketched below. In the low range of

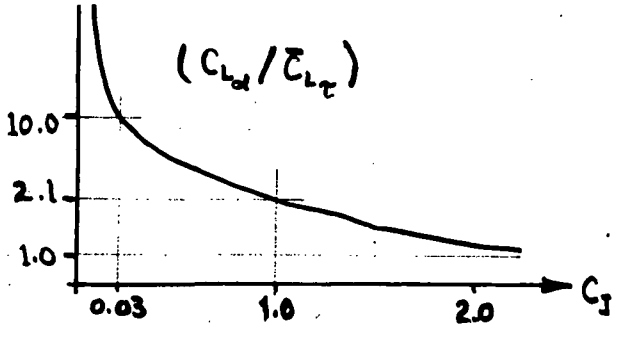

blowing coefficient, of interest herein, it is observed that the effectiveness of θ is very much greater than τ . The situation is similar for the blade section drag and moment.

The above results suggest the possibility of a "jet-flap torsionally controlled rotor" (JF/TCR), similar to the Kaman CTR, that is, a rotor designed so the primary function of the jet flap is to "drive" the blade torsional response at each harmonic. The aerodynamic force control would be obtained from the angle of attack variation due to the torsional response at each harmonic. The efficiency of the jet-flap control system may be improved by this mode of operation. For a given blowing coefficient reducing the span of the jet will reduce the total mass flow rate required and thus the compressor power. By locating the jet at the blade tip where the torsion deflection is maximum, its effectiveness (generalized force in torsion mode) is maximized.

5.2.2 Jet Flap Torsionally Controlled Rotor

To obtain an initial assessment of the potential of the JF/TCR described above, the span of the jet was reduced by two-thirds. This configuration was then used to repeat a previous case (1.20.03.10) where only the dominant 5th harmonic vertical blade root shear is suppressed.

The required azimuthal variation of τ is presented in Figure 26 and the corresponding harmonics in Table 6C (Case 1.20.03.S6). The corresponding blade root shears are presented in Tables 4C and 5C. The comparative results for the basic configuration are presented in Figure 25, and Tables 6B, 4B and 5B (Case 1.20.03.10).

The results are very encouraging --- for this case, the power required was reduced from 1200 HP to 892 HP and, while the required τ at the fifth harmonic increased from 3.4 degrees to 7.3 degrees, the torsion response only increased 20 percent (from 1.23 degrees to 1.48 degrees). This result further illustrates that the torsion response is the fundamental aerodynamic control and τ is controlling torsion as a control flap. The first harmonic component of τ required to maintain the jet-off trim was reduced from 28.2 degrees to 24.5 degrees. Apparently the shorter span jet upsets the trim less and thus requires less first harmonic control to maintain the jet-off trim (see Section 5.2.5).

5.2.3 Mechanism of Shear Suppression

At each harmonic of the rotor speed, there are spanwise distributions of aerodynamic and inertia loads proportional to the blade response in each of its degrees of freedom. There is also a spanwise distribution of the aerodynamic loads which are independent of the blade response (i.e., the aerodynamic forcing function). The blade root shears (vertical and inplane) are the sum of these spanwise distributions of aerodynamic and inertia loadings.

There are conceptually two possible ways of eliminating a given harmonic component of shear. The first is, to effectively cancel the aerodynamic forcing function in each blade degree of freedom--this would obviously reduce all the blade response at that harmonic to zero and thereby eliminate the response dependent aerodynamic and inertia

loadings in addition to the forcing function airloading. The number of independent control modes required for this conceptual approach would have to equal the number of blade-degrees-of-freedom -- this seems impractical at the present.

The second obvious and more practical way of eliminating a given harmonic component shear is to only require that the aerodynamic and inertial contributions sum to zero. This requires only one independent control for each component of shear to be constrained at each harmonic and is the method used in this study.

Only as an example to illustrate how the various contributions to a blade root shear can change to make sum zero at a given harmonic, these components are presented in the vector plots of Figure 33 for case (1.20.03.S6) of suppressing the dominant 5th harmonic vertical blade root shear with the shortened jet span. Individual aerodynamic contributions for each blade mode and the forcing function are not available separately (as explained in Appendix IV) but only their sum. Thus presented in Figure 33A are all the significant contributions to the 5th harmonic blade root shear before it was suppressed, i.e., with the jet off (Case 1.20.00.09) -- they are:

A - the total aerodynamic component

I_β - flapping inertia load

I_{ϕ_1} - 1st flapwise bending mode inertia load

I_{ϕ_2} - 2nd flapwise bending mode inertia load

I_{θ_1} - 1st torsion mode inertia load.

When this 5th harmonic shear is suppressed with the short jet the components re-adjust as shown in Figure 33 B. With the jet off, the largest contribution to this shear was the 2nd flapwise bending mode inertial load -- this mode is near resonance ($\omega_n = 5.27$). When this shear is suppressed to zero, the components change as follows:

A - increases by a factor of 5.5

I_β - increases by a factor of 7.6

I_{ϕ_2} - increases by a factor of 8.1

I_{ϕ_1} - decreases by a factor of 0.85

I_{θ_1} - increases by a factor of 5.0

Thus, all the components increased except that due to the bending response near resonance.

This general increase in the magnitude of the individual components of the reduced total shear implies that the resulting total shear could be sensitive to the amplitude and phase of the jet control angles. That is, open-loop operation may be unsatisfactory because it could result in an increase in the level of the shears if the jet control angles were not properly chosen.

5.2.4 Blade Dynamic Response to Shear Suppression

As was illustrated in the previous section, when the blade root shears are constrained, the blade dynamic response in all modes is required to re-adjust so that the appropriate aerodynamic and inertia contributions sum up to the constrained values. In general, this resulted in an increase in the blade bending responses at frequencies away from resonance and a reduction of these responses at frequencies nearest resonance. This can be observed in Figure 30 where the azimuthal variations (time histories) of the response in each blade mode are presented for the jet off case, and for the case with all the transmitted shears suppressed. It is observed that the 1st flap-bending mode ($\omega_n = 2.94$) response at $n = 3$ is reduced, the 2nd flap-bending ($\omega_n = 5.38$) response at $n = 5$ is about the same, the 1st edgewise-bending ($\omega_n = 0.98$) response at $n = 1$ is reduced, but the 2nd edgewise-bending ($\omega_n = 7.45$) response increased. As discussed in Section 5.2.1, the blade torsion is strongly coupled to the jet deflection angle, τ, so that the jet control drives the torsion response. Therefore, as observed in Figure 30 the blade response in both torsion modes is increased when the jet flap control is used to suppress all the transmitted shears.

5.2.5 Jet Influence on the Rotor Trim

In this study the tip jet momentum coefficient, $C_{J_{T_0}}$ is constant with azimuth, ψ, however, as explained in Appendix I, the blade section jet momentum coefficient, C_J, varies through relatively large amplitudes as depicted in Figure 15. Because of this large variation of C_J with ψ there is a significant redistribution of the blade airloads over the disk and a resulting change in the rotor total forces and moments (especially the moments) when the jet is turned on, i.e. the rotor trim is upset.

With the jet off, the three rotor trim forces are controlled by the three components of blade rigid body pitch, i.e., the collective pitch, lateral, and longitudinal cyclic pitch. The yawing moment is controlled by the "pedals" (tail rotor collective). The resulting rotor pitch and roll moments are accepted and thus determine the rotor shaft orientation (attitude). With the jet on, the philosophy adopted for this investigation was that the rotor forces and moments shall be the same as for the jet off.

To control the rotor moments in addition to the rotor forces requires two additional controls -- in this study, they are the 1st harmonic sine and cosine components of the jet deflection angle, τ (see Section 4.3 and Appendix IV).

This requirement, for the rotor moments to remain unchanged, results in the same rotor shaft angles (i.e., fuselage attitude) with the jet on as with the jet off. This trim procedure is not necessary -- the resulting, different, jet-on moments could alternatively have been accepted as an attitude change.

It should be noted that the first harmonic blade pitch and jet angle control requirements are uniquely determined for a specific rotor trim condition. That is they are not interchangeable when both the forces and the moments of the rotor are specified because the jet angle control results in a different distribution of blade lift, drag, and moment over the disk than does the blade pitch control. However if only the rotor forces (or only the moments) were specified then either control could be used independently or they could be used on arbitrary combinations. Thus the specified rotor forces (or moments) can be obtained with any combination of pitch and jet control but then unconstrained forces (or moments) would be different for each combination.

Because the amplitude of the variation of C_J with Ψ (Figure 15) increases with increasing $C_{J_{T_o}}$, the change in the rotor trim due to the jet increases and therefore the amplitude of 1st harmonic τ required to restore trim also increases with $C_{J_{T_o}}$. This variation (with $C_{J_{T_o}}$) of the 1st harmonic τ required for trim is presented in Figure 22. It is observed that amplitude of τ required at $n = 1$ to maintain the jet off trim is quite large, varying from 13.6 degrees at $C_{J_{T_o}} = 0.005$ to 31.1 degrees at $C_{J_{T_o}} = 0.03$. These relatively large jet deflections for trim result in signifcant power penalties as explained below. They are also believed to be the source of the relatively large τ requirement generally required at $n = 2$ (via the inter-harmonic aerodynamic coupling).

When the thrust recovery factor, T_R, is less than one, the jet provides a steady propulsive torque to the rotor which is a function of the total angle of the jet relative to the shaft plane. (A value of $T_R = 0.5$ was used for this study). This total angle is the sum of the blade section geometric angle relative to the shaft plane and the jet deflection angle, τ, relative to the blade section chord. As a result of the inter-harmonic coupling, when the total jet angle, α_n, at each harmonic is less than one radian, the steady propulsive torque, Q_τ, derived from the jet decreases approximately as the square of each harmonic of the jet angle, θ_n, i.e.,

$$Q_\tau \propto \left\{ 1 - \sum_n 1/4\, \theta_n^2 + \sum_n 3/192\, \theta_n^4 - \cdots \right\}$$

That is, the rate of decrease of Q_τ increases with the larger angles. Thus the relatively large τ required to maintain the jet off trim resulted in large power increments -- for example, at $\mu = 0.2$ and $C_{J_{T_o}} = 0.03$ this power increment was about 200 horsepower. This is the total increment in power which includes the profile and induced components as well as the Q_τ component.

These results, relative to the "trim-power", raise the following question. Would the total power required with the jet on be less if the rotor total moments were accepted an an attitude change? A proper answer to this question, of course, would be dependent on the drag variation, with attitude, of the specific fuselage considered. This is the main reason, for the choice made herein, to require the rotor moments to be the same with jet on and jet off. However, this alternate trim procedure should be investigated, at least for a typical fuselage drag-characteristic because the procedure used herein may represent an unnecessary power penalty.

6.0 CONCLUSIONS

The general overall conclusion of this study is that the rotor jet-flap control system appears to be (theoretically) a practical means of achieving efficient higher harmonic control which could be used for many applications.

The results indicate that a jet flap control system has the potential of reducing all of the vertical and inplane transmitted (non-cancelling) blade root shears simultaneously with a single jet control mode. Furthermore the results indicate that the control angle schedule and additional power required are within practical limits (indicated below).

It was found that the blade torsional response can be an essential, beneficial element of the jet flap control system. That is a jet-flap "torsionally controlled" rotor may be much more efficient than a "pure" (torsionally stiff) jet flap rotor where the aerodynamic control is primarily from the jet angle rather than the blade angle.

Because the "mechanics" of implementing the jet-flap control systems were not considered, the conclusions of this study are independent of such practical considerations.

The specific conclusions of this study are summarized as follows:

1) The jet-flap control system can suppress all the transmitted blade root shears to zero

2) Only one independent jet-flap control mode is required to suppress all the transmitted shears.

3) The jet deflection angles and additional power required are within practical limits.

   For example, the total jet deflection angle required (exclusive of the re-trim requirement) to suppress all the transmitted vertical and horizontal blade root shears never exceeded approximately 30°. Similarily the additional power required for the two-blade rotor was 117 HP, exclusive of that required to re-trim (301 HP).

4. It was possible to suppress all the transmitted shears with the $C_{J_{T_o}}$ as low as 0.005 and the jet deflection angles were still practical (at μ = 0.20, less than 30° including requirement for re-trim).

5) The jet-on trim requirement adopted for this study may be resulting in an unnecessary power penalty for trim.

The power required to maintain trim was greater than that required to suppress all the transmitted shears. The trim requirement adopted was that the rotor moments (and thus the shaft angles and fuselage attitudes) in addition to the forces shall be the same with the jet-on as with the jet-off. Accepting the small attitude changes may require significantly less power. The penalty may be due to the fact that the flapping rotor (with 5% hinge off-set) is an inefficient moment generator. Thus for a semi-rigid rotor this trim requirement may be a reasonable one.

6) Generally the blade dynamic bending response increased at all harmonics except that nearest the mode resonant frequency--there it generally decreased! However, the net result was that peak to peak bending stresses did not increase significantly.

7) Generally the more shear suppression required the greater the power required.

8) Interharmonic aerodynamic coupling due to the jet may be quite pronounced.

9) Suppression of one harmonic of shear affects the magnitude of all remaining shears--generally the shears at harmonics immediately above and below the suppressed harmonic are most affected.

10) For the rotor studied (1st torsion at $(\omega_\alpha/\Omega) = 5.3$) torsion is an essential and beneficial element in the jet flap control system.

The blade is behaving similar to the Kaman CTR with the jet acting as the control flap. For the shaft driven rotor where the jet is being used primarily for control (i.e., low $C_{S_{T_o}}$), the blade angle-of-attack is very much more effective in controlling the aerodynamic forces than is the jet deflection angle.

11) The power required to suppress shears and trim was significantly reduced by reducing the span of the jet by two-thirds and maintaining the same blowing coefficient.

7.0 RECOMMENDATIONS

The objective of this study was to investigate the theoretical potential of a jet-flap control system for reducing the vertical and horizontal transmitted shears. It was shown that the potential appears good based on the computer simulation employed and the specific rotor configurations and problem parameters studied. Obviously many questions arise as to the effects on the results of this study of the modeling employed to represent the aerodynamics and structure as well as to the limiting assumptions made. Other questions arise relative to the range of specific parameters looked at;

1) were they adequate
2) were they representative
3) should others be considered, etc.

These questions obviously present valid reasons for further studies.

Of all the many possible recommendations which could be made as a result of this study it is felt that the following are most important:

1) In view of the behavior of the jet flap rotor as a torsionally controlled rotor, TCR, further studies to evaluate this possible mode of operation are recommended wherein the influence of the following parameters is investigated:

   a - Blade torsional stiffness

   b - Spanwise extent of the jet

2) Because one of the ground rules of this study required that the "jet-on" rotor be trimmed(both forces and moments) to the corresponding values of trim jet-off, very large control angles and hence power were required just to maintain trim. This may be unduly penalizing the jet flap control rotor and hence the effect of removing the moment trim constraint should be investigated.

3) Because only one calculation was made at $C_{J_{TO}}$ =0.005 and the jet deflection angles required to suppress shear were not excessive, it is recommended that

further calculations be made to determine the practical lower bound on the jet momentum coefficient, $C_{J_{T_0}}$, and the jet deflection angle, τ, as a function of advance ratio.

4) Because no results on shear suppression were obtained above $\mu = 0.20$, it is recommended that further effort be made to obtain results at a higher advance ratio.

5) It is recommended that this investigation of the potential of the jet-flap for shear suppression be extended to include the rigid rotor configuration. This would provide information relative to the question of the possible benefits of this type of rotor configuration (with its greater control power) over the articulated rotor of the present study.

6) Because the calculated power required to suppress shears is influenced by the value of the thrust recovery factor, T_R, it is recommended that calculations be made at additional values of T_R. A value of 0.5 was used for this study, thus calculations with $T_R = 0.0$ and 1.0 would establish bounds on its influence.

7) This study has shown that the rotor blade responses play a very important role in suppression of shears. It was also noted that torsion was driven directly by large jet generated moments. Furthermore the large inherent azimuthal variations of the jet momentum coefficient (due only to the dynamic pressure variations) significantly alter the jet-off aerodynamic mass, stiffness and damping of the blade while at the same time altering the motion independent forcing function. These observations lead to the speculation that aeroelastic stability problems associated with such rotor systems may be significant. Thus investigation of such systems from a stability point of view is recommended.

REFERENCES

1. Richards, E.J. and Jones, J.P.: The Application of the Jet Flap to Helicopter Rotors. Journal of the Helicopter Association of Great Britain, Vol. 9, No. 3, January 1956, pp. 414-423.

2. Dorand, R.: The Application of the Jet Flap to Helicopter Rotor Control. Journal of the Helicopter Association of Great Britain, Vol. 13, No. 6, December 1959, pp. 323-367.

3. Evans, W.T. and McCloud, J.L.,III: Analytical Investigation of a Helicopter Rotor Driven and Controlled by a Jet Flap. NASA TN D-3028, September 1965.

4. McCloud, J.L.,III, Evans, W.T. and Biggers, J.C. Performance Characteristics of a Jet-Flap Rotor NASA SP-116 (Conference on V/STOL and STOL Aircraft, Ames Research Center, April 4-5, 1966).

5. Lewis, R.B.,III Jet Flap Rotor Research Proceedings of the V/STOL Technology and Planning Conference, Las Vegas, Nevada 23-25 September 1969.

6. Cheeseman, I.C. The Application of Circulation Control by Blowing to Helicopter Rotors Journal of the Royal Aeronautical Society Vol. 71, No. 679 July 1967, pp. 451-467.

7. Smith, M.C.G. The Aerodynamics of a Circulation-Controlled Rotor Proceedings, Third CAL/AVLABS Symposium on Aerodynamics of Rotary Wing and V/STOL Aircraft Vol. II, Cornell Aeronautical Laboratory, Inc., Buffalo, N.Y. June 1969.

8. Yuan, S.W. Jet Circulation Control Airfoils for VTOL Rotors AIAA Paper No. 69-741 (CASl/AIAA Subsonic Aero-and Hydro-Dynamics Meetings Ottawa July 2-3, 1969).

9. Williams, R.M. Some Research on Rotor Circulation Control Proceedings Third CAL/AVLABS Symposium on Aerodynamics of Rotary Wing and V/STOL Aircraft, Vol. II Cornell Aeronautical Laboratory, Inc., Buffalo, New York June 1969.

10. Stewart, W. Second Harmonic Control on the Helicopter Rotor Aeronautical Research Council R & M 2997 August 1952.

11. Payne, P.R. Higher Harmonic Rotor Control Aircraft Engineering, Vol. 30, No. 354 August 1958, pp. 222-226.

12. Arcidiacono, P.J. Theoretical Performance of Helicopters Having Second and Higher Harmonic Feathering Control Journal of the American Helicopter Society, Vol. 6, No. 2 April 1961 pp. 8-19.

13. Daughaday, H. Suppression of Transmitted Harmonic Rotor Loads by Blade Pitch Control Journal of the American Helicopter Society Vol. 13, No. 2, April 1968, pp. 65-82, Also USAAVLABS TR 67-14, November 1967.

14. Balcerak, J.B., Erickson, J.C.,Jr. and McGarvey, J.H. Higher Harmonic Pitch Control Proceedings, Third CAL/AVLABS Symposium on Aerodynamics of Rotary Wing and V/STOL Aircraft, Vol. II, Cornell Aeronautical Laboratory, Inc., Buffalo, N.Y June 1969.

15. Dorand, R. and Tararine, S. Determination Through Wind-Tunnel Tests and Analytical Methods of the Optimum Deflection Devices Suitable for Use on Jet-Flap Helicopter Rotor Blades European Research Office, U.S. Department of Army Report No. DE-1203, December 30, 1960.

16. Trenka, A.R. and White, R.P.,Jr.: Theoretical Investigation of the Flutter Characteristics of a Jet-Flap Helicopter Rotor in Hovering and Forward Flight. CAL Report BB-1493-S-2, TRECOM TR 63-9, April 1963.

17. Kuczynski, W.R. and Lewis, R.B.II Jet Flap Cyclic Twist Feasibility Research Program Lockheed-California Co. Report No. LR22973 March 31, 1970.

18. Williams, R.M. Some Research on Rotor Circulation Control Proceedings, Third CAL/AVLABS Symposium on Aerodynamics of Rotary Wing and V/STOL Aircraft, Vol. II, Cornell Aeronautical Laboratory, Inc., Buffalo, N.Y. June 1969.

19. Williams, R.M. and Bernitt, C.L. Theoretical Performance of a Pure Jet Flap Rotor at High Advance Ratios NSRDC-Aviation and Surface Effects Department Tech. Note AL-189 December 1970.

20. Sullivan, R.S., LaForge, S., Holchin, B.W. A Performance Application Study of a Jet-Flap Helicopter Rotor (Hughes Tool Co.) NACA CR-112030 May 1972.

21. Piziali, R.A. Method for the Solution of the Aeroelastic Response Problem for Rotating Wings Presented at Symposim on the Noise and Loading Actions on Helicopter V/STOL Aircraft

and Ground Effect Machine Institute of Sound and Vibration Research, University of Southampton, Hampshire, England, August 30 - September 3, 1965. (Also as USAAVLABS TR 65-74)

22. Chang , T.T. A Method for Predicting the Trim Constants and and the Rotor Blade Loadings and Responses of a Single-Rotor Helicopter Cornell Aeronautical Laboratory Report No. BB-2205-5-1 (USAAVLABS TR 67-71). 1967

23. Erickson, J.C., Jr. A Theory for Unsteady Motions of Jet-Flapped Thin Airfoils Ph.D. Thesis and AFOSR Technical Note, Cornell University September 1962, also available from University Microfilms, Inc., Ann Arbor, Michigan

24. Von Karman, Th. and Sears, W.R. Airfoil Theory for Non-Uniform Motion Journal of the Aeronautical Sciences, Vol. 5, No. 10 August 1938 pp. 379-390.

25. Hough, G.R. Cambered Jet Flap Airfoil Theory Graduate School of Aeronautical Engineering, Cornell University, Ithaca, New York. MS Thesis September 1959.

26. Spence, D.A. The Lift Coefficient of a Thin Jet-Flapped Wing Proceedings of the Royal Society, A, Vol. 238, No. 121, 4 December 1956, pp. 46-68.

27. Houboult, J.C. and Brooks, G.W. Differential Equations of Motion for Combined Flapwise Bending, Chordwise Bending, and Torsion of Twisted Nonuniform Rotor Blades National Advisory Committee for Aeronautics, Langley Field, Virginia NACA TN 3905 February 1957.

28. Tanner, W.H. Charts for Estimating Rotary Wing Performance in Hover and at High Forward Speeds (United Aircraft Corp.) NASA CR-114, November 1964.

29. Chang , T.T. A Method for Predicting the Trim Constants and the Rotor Blade Loadings and Responses of a Single Rotor Helicopter (Cornell Aeronautical Laboratory) USAAVLABS TR 67-71, September 1967.

30. Lanczos, C. Applied Analysis Prentice Hall, Inc. Englewood Cliffs, New Jersey 1956.

31. Kizilos, A.P. and Rose, R.E. Experimental Investigations of Flight Control Surfaces Using Modified Air Jets St. Paul, Minn., November 1969 Honeywell, Inc. Document 12055-FR 1 (DDC AD 864-2716).

32. Kretz, M., Aubrun, J. and Larche, M. March 1971 Wind Tunnel Tests of the Dorand DH 2011 Jet Flap Rotor June 1973 NASA CR 114694 Vol. I and II.

33. Lemnios, A.Z. and Smith, A.F. An Analytical Evaluation of the Controllable Twist Rotor Performance and Dynamic Behavior USAAMRDL TR 72-16 May 1972.

Table 1. CASES PRESENTED

$C_{J_{T_o}}$ \ μ	0.08	0.20	0.30
0	1.08.00.03	1.20.00.09 1.20.00.50 ⑤ 2.20.00.02	1.30.00.04
0.005		1.20.005.01	
0.01	1.08.01.01	1.20.01.01	1.30.01.01 ✱
0.02		1.20.02.01	
0.03	1.08.03.02	1.20.03.06 ② 1.20.03.56 ③ 1.20.03.08 1.20.03.09 } 1.20.03.10 } ① 1.20.03.20 ④ 1.20.03.58 ⑤ 2.20.03.02	1.30.03.01 ✱

NOTES: ① Only vertical shear suppressed at 2nd and 5th harmonic respectively

② Non-cancelling shears suppressed at 2nd through 6th harmonics only

③ Short jet, only vertical shear suppressed at 5th harmonic

④ No shears suppressed, only jet off rotor trim-forces and moments-required

⑤ Increased torsional stiffness, jet off and jet on

✱ Convergence not obtained

Case No. 1. 20. 03. 03

- 03 — run number within the set
- 03 — designates tip jet momentum, $C_{J_{T_o}}$
- 20 — designates advance ratio, μ
- 1 — designates rotor configuration
  - (1) 2 bladed, 44,482 N (10,000 lb.) rotor
  - (2) 4 bladed, 88,964 N (20,000 lb.) rotor

TABLE 2

JET OFF VERTICAL BLADE ROOT SHEARS - AMPLITUDE AND PHASE (N /DEGREES)

CASE	1.08.00.03		1.20.00.09		1.30.00.04		220.00.02		1.20.00.50	
HARMONIC	AMP	PHASE	AMP	PHASE	AMP	PHASE	AMP	PHASE	AMP	PHASE
0	22240.	.0000	22299.	.0000	22512.	.0000	22299.	.0000	22299.	.0000
1	1044.	39.27	3732.	-72.09	11427.	-93.37	1027.	-20.17	3839.	-74.74
2	1278.	8.295	584.0	166.7	3191.	171.6	503.5	53.29	402.5	175.0
3	785.6	92.62	2065.	153.4	2107.	151.3	1442.	92.89	2355.	154.9
4	445.7	-3.597	136.0	-25.96	251.5	77.17	566.3	31.67	142.8	-8.660
5	295.1	-24.91	1306.	-95.57	476.0	-38.15	1435.	-74.16	1299.	-90.11
6	862.5	-2.465	265.6	5.526	109.0	146.9	328.0	-7.315	215.8	39.53
7	31.56	-8.790	78.29	-36.61	48.04	87.02	69.35	-27.14	26.88	-110.3
8	9.715	24.23	74.46	-16.55	4.946	16.17	16.02	25.04	49.46	-4.367
9	12.86	158.0	90.57	167.9	16.47	156.7	41.07	-168.4	90.39	-88.31
10	9.924	-169.5	117.1	93.59	23.49	62.79	59.47	106.9	82.65	154.7
11	8.020	-13.89	86.78	-71.66	21.19	5.632	53.16	-92.56	94.44	55.95

TABLE 3

JET OFF HORIZONTAL BLADE ROOT SHEARS - AMPLITUDE AND PHASE (N/DEGREES)

CASE	1.08.00.03		1.20.00.09		1.30.00.04		2.20.00.02		1.20.00.50	
HARMONIC	AMP	PHASE	AMP	PHASE	AMP	PHASE	AMP	PHASE	AMP	PHASE
0	1834.	.0000	1940.	.0000	3434.	.0000	2394.	.0000	1930.	.0000
1	2578.	-1.950	2439.	-3.775	3834.	.1456	3370.	-1.982	2385.	-3.384
2	192.5	-6.125	47.64	-6.128	445.3	-175.0	205.2	1.466	107.6	-31.68
3	33.71	105.1	29.64	82.24	45.24	146.9	30.93	81.55	17.17	-43.95
4	45.55	145.1	27.94	118.9	38.09	-48.93	70.19	114.1	28.32	-167.7
5	12.28	148.5	62.27	37.94	52.22	60.89	31.43	121.9	30.47	118.4
6	15.74	7.529	3.575	-133.9	65.43	69.95	49.86	-15.15	51.47	-67.78
7	68.15	.4709	16.24	48.75	73.35	93.58	198.0	-6.192	49.73	-33.86
8	11.47	-79.61	77.71	177.9	44.53	59.59	71.17	-121.1	83.94	177.5
9	10.84	-6.350	49.86	-28.91	14.49	11.34	50.13	-5.018	38.57	-16.33
10	4.895	26.26	37.83	-89.36	3.998	-178.0	20.36	-16.83	27.33	-71.86
11	2.555	144.8	29.00	110.3	5.618	116.7	22.41	110.0	13.10	168.7

TABLE 4a

JET ON VERTICAL BLADE ROOT SHEARS - AMPLITUDE AND PHASE (N /DEGREES)

CASE	1.08.01.01		1.08.03.01		1.20.005.01		1.20.01.01		1.20.02.01	
HARMONIC	AMP	PHASE	AMP	PHASE	AMP	PHASE	AMP	PHASE	AMP	PHASE
0	22241.	.0000	22241.	.0000	22299.	.0000	22299.	.0000	22299.	.0000
1	1403.	-58.13	5498.	-70.22	5191.	-72.63	6561.	-74.15	8683.	-67.98
2	.0000	.0000	.0000	.0000	.0000	.0000	.0000	.0000	.0000	.0000
3	1221.	78.83	1992.	71.68	2120.	155.7	1899.	160.4	853.6	115.3
4	.0000	.0000	.0000	.0000	.0000	.0000	.0000	.0000	.0000	.0000
5	65.43	-43.48	100.4	-111.5	1031.	-91.05	1021.	-93.44	1118.	-95.89
6	.0000	.0000	.0000	.0000	.0000	.0000	.0000	.0000	.0000	.0000
7	249.9	-29.55	196.7	-27.15	87.36	-151.4	126.6	-146.8	33.32	74.74
8	.0000	.0000	.0000	.0000	.0000	.0000	.0000	.0000	.0000	.0000
9	28.88	-48.82	23.60	-53.59	68.46	-41.09	89.36	-16.69	71.48	23.20
10	.0000	.0000	.0000	.0000	.0000	.0000	.0000	.0000	.0000	.0000
11	5.240	-.8015	2.581	3.834	30.25	98.19	30.05	121.8	52.27	73.20

TABLE 4b

JET ON VERTICAL BLADE ROOT SHEARS - AMPLITUDE AND PHASE (N /DEGREES)

CASE	1.20.03.08		1.20.03.20		1.20.03.06		1.20.03.09		1.20.03.10	
HARMONIC	AMP	PHASE	AMP	PHASE	AMP	PHASE	AMP	PHASE	AMP	PHASE
0	22299.	.0000	22299.	.0000	22299.	.0000	22299.	.0000	22299.	.0000
1	10502.	-64.78	11218.	-86.97	10026.	-67.08	10631.	-72.72	11072.	-86.43
2	.0000	.0000	2022.	-108.9	.0000	.0000	.0000	.0000	1957.	-108.3
3	1382.	72.38	2052.	153.5	1189.	80.12	2050.	-170.8	2128.	153.2
4	.0000	.0000	182.2	.5144	.0000	.0000	232.2	-45.07	353.5	-9.509
5	1270.	-97.21	1398.	-96.54	1257.	-99.57	1316.	-96.57	.0000	.0000
6	.0000	.0000	267.1	8.251	.0000	.0000	239.2	14.49	152.8	13.29
7	488.4	70.18	79.31	-30.98	178.8	-90.35	72.59	-38.11	66.77	-40.29
8	.0000	.0000	72.37	-24.37	180.6	-.2882	78.91	-10.81	67.70	-30.04
9	99.55	51.35	195.8	175.1	201.1	157.6	93.37	174.9	103.3	170.4
10	.0000	.0000	124.0	91.27	20.32	63.03	121.7	94.11	124.6	87.42
11	50.98	54.62	91.99	-68.24	110.0	2.467	82.91	-70.48	97.37	-66.44

TABLE 4f

JET ON VERTICAL BLADE ROOT SHEARS - AMPLITUDE AND PHASE (N /DEGREES)

CASE	1.20.03.58		1.20.03.56		2.20.03.02		1.30.01.—		1.30.03.—	
HARMONIC	AMP	PHASE	AMP	PHASE	AMP	PHASE	AMP	PHASE	AMP	PHASE
0	22299.	.0000	22299.	.0000	22299.	.0000				
1	10809.	-83.48	6677.	-79.02	6245.	-61.50				
2	.0000	.0000	637.0	-126.3	.0000	.0000				
3	879.0	-151.1	2317.	156.3	2757.	58.92	NO RESULTS OBTAINED	NO RESULTS OBTAINED	NO RESULTS OBTAINED	NO RESULTS OBTAINED
4	.0000	.0000	196.7	43.50	.0000	.0000				
5	549.4	-2.450	.0000	.0000	1447.	-72.13				
6	.0000	.0000	223.1	-6.286	.0000	.0000				
7	141.5	-140.3	86.56	-32.42	1013.	103.8				
8	.0000	.0000	81.18	-16.43	.0000	.0000				
9	238.7	-109.1	91.05	167.3	34.56	38.41				
10	.0000	.0000	120.5	93.48	.0000	.0000				
11	171.5	-50.00	96.39	-74.61	68.06	-164.5				

TABLE 5a

JET-ON HORIZONTAL BLADE ROOT SHEARS - AMPLITUDE AND PHASE (N /DEGREES)

CASE	1.08.01.01		1.08.03.02		1.20.005.01		1.20.01.01		1.20.02.01	
HARMONIC	AMP	PHASE	AMP	PHASE	AMP	PHASE	AMP	PHASE	AMP	PHASE
0	1415.	.0000	548.0	.0000	1697.	.0000	1471.	.0000	1177.	.0000
1	1822.	-3.064	281.3	-32.32	1963.	-5.586	1531.	-6.946	1004.	-19.18
2	788.2	-178.2	833.1	177.5	394.6	8.483	355.5	28.92	350.8	76.66
3	.0000	.0000	.0000	.0000	.0000	.0000	.0000	.0000	.0000	.0000
4	77.18	-2.292	121.3	13.32	20.21	-117.4	37.62	-83.10	83.98	-22.35
5	.0000	.0000	.0000	.0000	.0000	.0000	.0000	.0000	.0000	.0000
6	22.17	39.13	19.75	20.75	46.88	-1.045	40.92	-8.956	63.39	-25.26
7	.0000	.0000	.0000	.0000	.0000	.0000	.0000	.0000	.0000	.0000
8	27.41	157.5	51.42	153.4	52.53	-176.8	55.60	-165.4	46.35	-114.5
9	.0000	.0000	.0000	.0000	.0000	.0000	.0000	.0000	.0000	.0000
10	2.418	160.4	2.478	176.2	2.660	2.241	5.756	103.1	4.800	-121.8
11	.0000	.0000	.0000	.0000	.0000	.0000	.0000	.0000	.0000	.0000

TABLE 5b

JET-ON HORIZONTAL BLADE ROOT SHEARS - AMPLITUDE AND PHASE (N/DEGREES)

CASE	1.20.03.08		1.20.03.20		1.20.03.06		1.20.03.09		1.20.03.10	
HARMONIC	AMP	PHASE	AMP	PHASE	AMP	PHASE	AMP	PHASE	AMP	PHASE
0	908.3	.0000	704.6	.0000	869.2	.0000	707.7	.0000	715.3	.0000
1	628.1	-44.49	114.6	-105.8	574.7	-43.05	363.8	-69.68	112.2	-91.32
2	378.2	103.1	572.5	-119.3	358.7	99.85	247.5	126.0	566.3	-116.3
3	.0000	.0000	61.39	63.07	.0000	.0000	210.1	-26.67	527.1	84.82
4	114.7	6.450	30.47	-146.9	112.4	3.375	60.45	163.2	30.74	166.2
5	.0000	.0000	62.81	12.15	.0000	.0000	75.57	-3.967	264.3	-116.7
6	99.86	-30.27	50.22	-126.1	104.4	-41.04	16.79	-84.51	97.50	-2.135
7	.0000	.0000	62.32	158.1	102.2	85.51	22.08	-107.7	54.89	-132.4
8	90.92	-90.26	67.61	-160.2	55.87	-163.6	56.49	-148.0	67.21	-165.1
9	.0000	.0000	40.06	-14.03	40.95	-13.84	48.57	-.6387	61.21	-5.256
10	8.852	-135.3	27.34	-78.35	15.07	-78.57	24.80	-80.77	26.76	-90.02
11	.0000	.0000	26.66	114.7	26.08	144.2	27.56	118.9	30.38	116.0

TABLE 5c

JET ON HORIZONTAL BLADE ROOT SHEARS - AMPLITUDE AND PHASE (N /DEGREES)

CASE	1.20.03.58		1.20.03.56		2.20.03.02		1.30.01.—		1.30.03.—	
HARMONIC	AMP	PHASE	AMP	PHASE	AMP	PHASE	AMP	PHASE	AMP	PHASE
0	688.6	.0000	1423.	.0000	1217.	.0000				
1	171.9	-104.9	1283.	-9.039	1267.	-13.29				
2	346.5	-86.59	233.4	-92.79	722.4	151.3	NO RESULTS OBTAINED	NO RESULTS OBTAINED	NO RESULTS OBTAINED	NO RESULTS OBTAINED
3	.0000	.0000	26.90	123.5	.0000	.0000				
4	22.22	-129.7	30.65	-118.1	298.1	33.27				
5	.0000	.0000	319.8	-23.62	.0000	.0000				
6	196.7	-97.45	22.98	-139.5	139.8	-.6610				
7	.0000	.0000	73.48	-130.1	.0000	.0000				
8	317.3	-128.5	75.35	-172.0	112.6	141.8				
9	.0000	.0000	39.00	-34.11	.0000	.0000				
10	42.40	-40.89	31.03	-70.79	7.402	41.33				
11	.0000	.0000	30.60	105.7	.0000	.0000				

TABLE 6a

HARMONICS OF TIP JET ANGLE REQUIRED TO SUPPRESS SHEARS - AMPLITUDE AND PHASE
(DEGREES/DEGREES)

CASE	1.08.01.01		1.08.03.02		1.20.005.01		1.20.01.01		1.20.02.01	
HARMONIC	AMP	PHASE	AMP	PHASE	AMP	PHASE	AMP	PHASE	AMP	PHASE
0	.0000	.0000	.0000	.0000	.0000	.0000	.0000	.0000	.0000	.0000
1	10.71	-1.529	19.96	23.33	13.64	23.31	20.19	21.48	27.73	36.23
2	28.32	-167.7	15.26	176.6	15.28	43.52	13.73	72.40	18.50	108.3
3	3.840	-92.02	3.424	-122.3	1.971	160.4	2.551	160.0	6.458	-170.8
4	3.249	40.51	1.798	40.36	1.716	-.3825	1.313	3.638	1.853	-4.351
5	.6837	84.03	.5681	99.65	1.561	-29.48	1.115	29.50	.2106	37.28
6	.4660	164.8	.2738	158.1	2.842	169.0	1.958	168.4	.9288	-155.0
7	2.205	-39.70	.9806	-38.20	2.066	166.7	1.724	175.9	3.630	74.26
8	.1502	-166.0	.0164	-158.4	.9029	169.7	.5520	169.3	1.384	-167.1
9	.5073	-38.03	.2195	-41.16	3.216	-22.89	2.603	12.64	2.463	-7.412
10	.1414	32.12	.0703	34.83	2.049	-77.54	1.294	83.10	.2899	-178.0
11	.0477	165.1	.0425	171.3	3.109	116.5	2.098	127.0	1.226	162.7

TABLE 6b

HARMONICS OF TIP JET ANGLE REQUIRED TO SUPPRESS SHEARS - AMPLITUDE AND PHASE
(DEGREES/DEGREES)

CASE	1.20.03.08		1.20.03.20		1.20.03.06		1.20.03.09		1.20.03.10	
HARMONIC	AMP	PHASE	AMP	PHASE	AMP	PHASE	AMP	PHASE	AMP	PHASE
0	.0000	.0000	.0000	.0000	.0000	.0000	.0000	.0000	.0000	.0000
1	31.12	42.65	28.94	-2.466	30.37	40.16	27.33	29.07	28.17	-2.255
2	19.94	120.1	.0000	.0000	19.09	117.7	12.42	114.7	.0000	.0000
3	7.753	-161.6	.0000	.0000	7.215	-165.0	.0000	.0000	.0000	.0000
4	1.691	-5.440	.0000	.0000	1.533	-6.253	.0000	.0000	.0000	.0000
5	.3158	116.9	.0000	.0000	.3840	100.9	.0000	.0000	3.402	-6.946
6	.7016	-141.1	.0000	.0000	.9597	-154.3	.0000	.0000	.0000	.0000
7	3.874	68.85	.0000	.0000	.0000	.0000	.0000	.0000	.0000	.0000
8	1.330	-166.9	.0000	.0000	.0000	.0000	.0000	.0000	.0000	.0000
9	2.105	-.4500	.0000	.0000	.0000	.0000	.0000	.0000	.0000	.0000
10	.3465	152.3	.0000	.0000	.0000	.0000	.0000	.0000	.0000	.0000
11	.9368	-178.1	.0000	.0000	.0000	.0000	.0000	.0000	.0000	.0000

TABLE 6c

HARMONICS OF TIP JET ANGLE REQUIRED TO SUPPRESS SHEARS - AMPLITUDE AND PHASE
(DEGREES/DEGREES)

CASE	1.20.03.58		1.20.03.56		2.20.03.02		1.30.01.—		1.30.03.—	
HARMONIC	AMP	PHASE	AMP	PHASE	AMP	PHASE	AMP	PHASE	AMP	PHASE
0	.0000	.0000	.0000	.0000	.0000	.0000	NO RESULTS OBTAINED	NO RESULTS OBTAINED	NO RESULTS OBTAINED	NO RESULTS OBTAINED
1	27.36	7.457	24.47	4.225	21.23	35.25				
2	2.508	-160.9	.0000	.0000	17.89	151.0				
3	12.72	166.8	.0000	.0000	5.597	-128.1				
4	2.877	-60.18	.0000	.0000	3.028	66.24				
5	6.539	-81.75	7.290	74.17	.4590	162.6				
6	8.426	-120.0	.0000	.0000	1.451	86.44				
7	6.460	42.47	.0000	.0000	6.108	106.9				
8	1.012	64.84	.0000	.0000	1.385	-57.05				
9	2.512	67.00	.0000	.0000	1.216	83.90				
10	1.891	158.2	.0000	.0000	1.654	-94.03				
11	2.015	165.1	.0000	.0000	1.550	72.11				

TABLE 7

TOTAL POWER REQUIRED TO SUPPRESS SPECIAL SHEAR CASES

CASE	DESCRIPTION	P_T (HP)
1.20.00.09	JET OFF.	892
1.20.03.20	JET ON - USED ONLY TO MAINTAIN JET OFF TRIM	1193
1.20.03.10	JET ON - TRIM AND 5P VERT. SHEAR SUPPRESSED.	1200
1.20.03.09	JET ON - TRIM AND 2P VERT. SHEAR SUPPRESSED.	1216
1.20.03.06	JET ON - TRIM AND 2P TO 6P TRANSMITTED SHEARS SUPPRESSED.	1290
1.20.03.08	JET ON - TRIM AND ALL TRANSMITTED SHEARS SUPPRESSED.	1310
1.20.03.56	JET ON - SHORT JET - TRIM AND 5P VERT. SHEAR SUPPRESSED.	892
2.20.00.02	JET OFF - 4 BLADED ROTOR	2202
2.20.03.02	JET ON - TRIM AND ALL TRANSMITTED SHEARS SUPPRESSED. - 4 BLADED ROTOR	2885

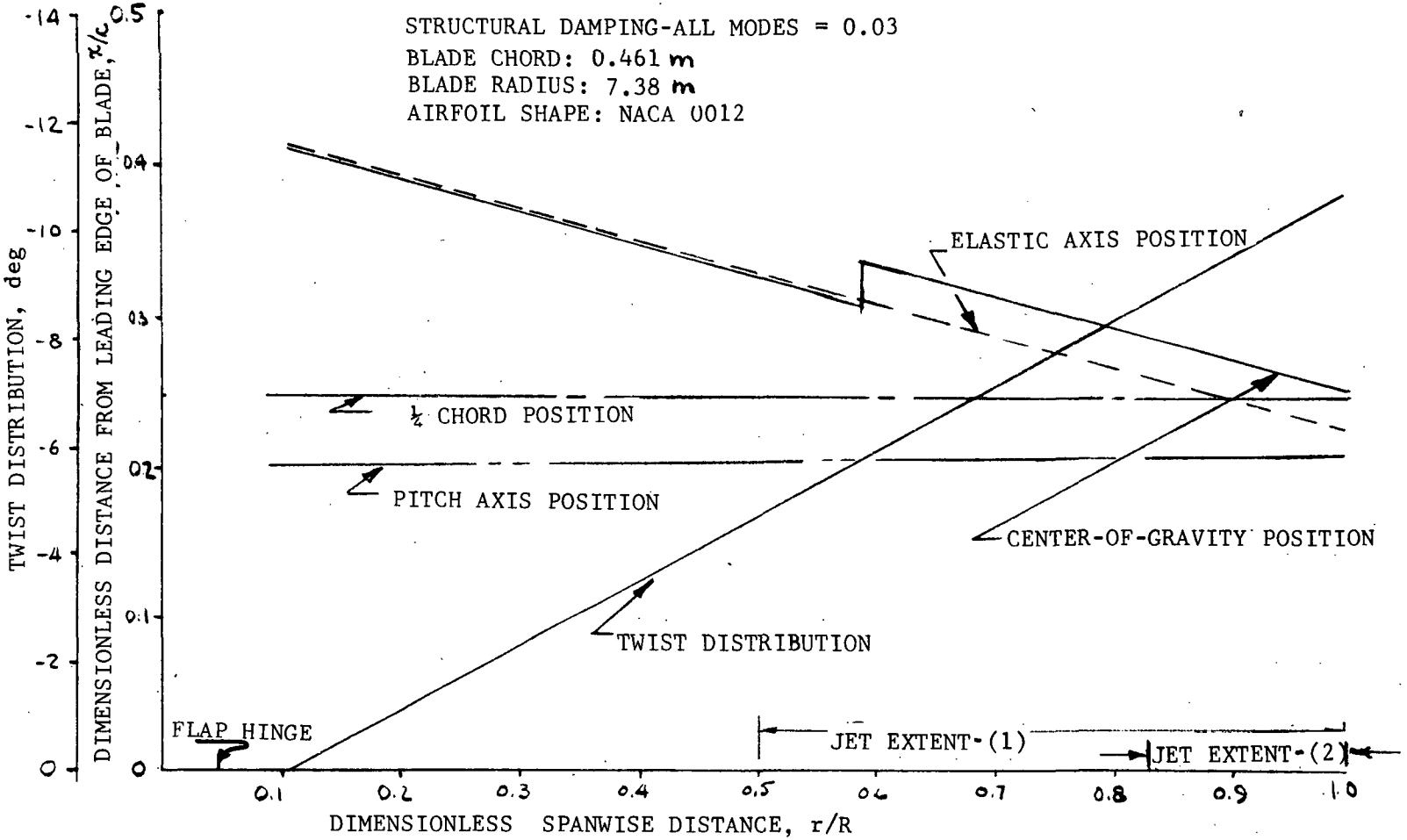

Figure 1. GEOMETRIC PROPERTIES OF ROTOR BLADES

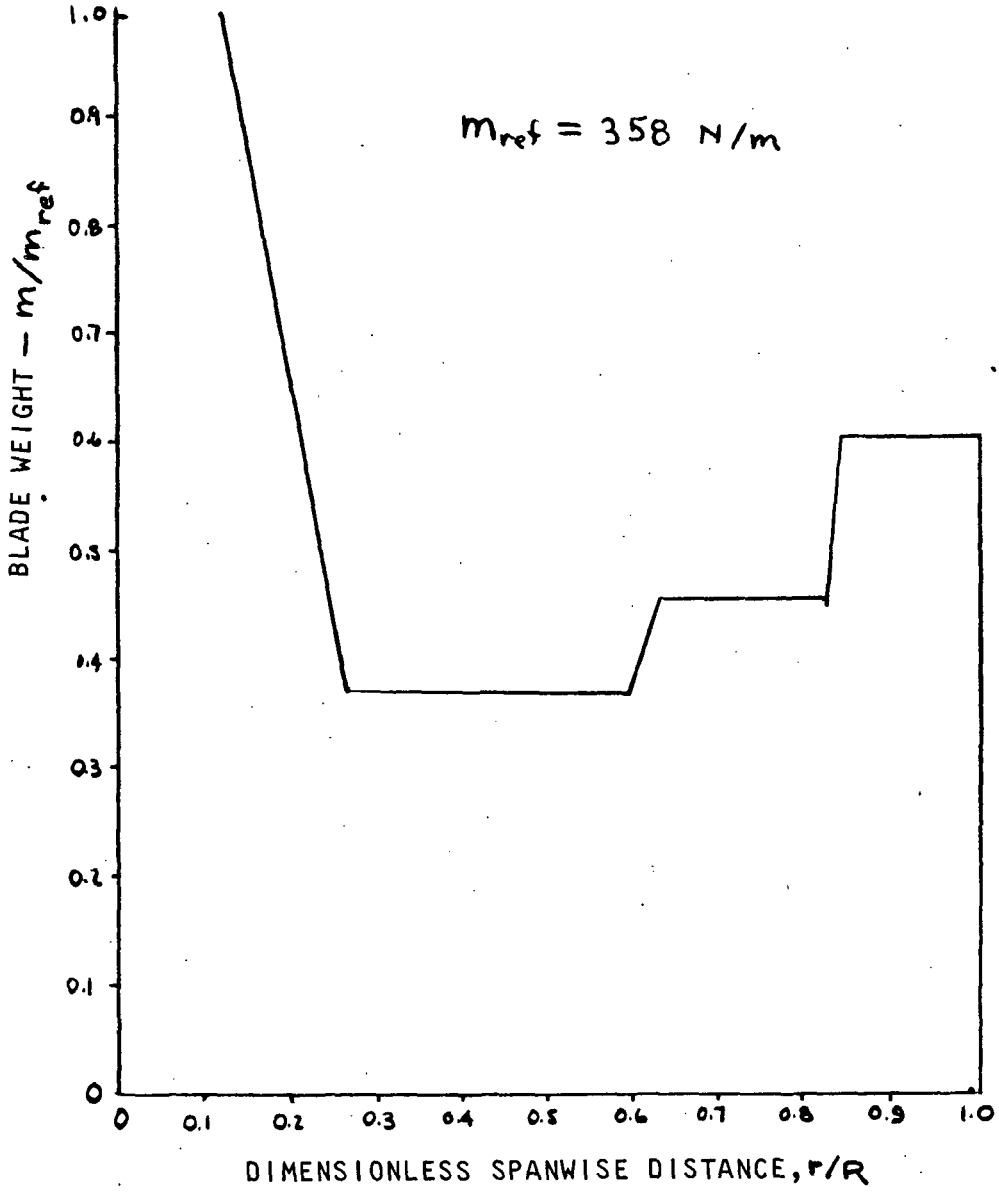

Figure 2. BLADE WEIGHT DISTRIBUTION

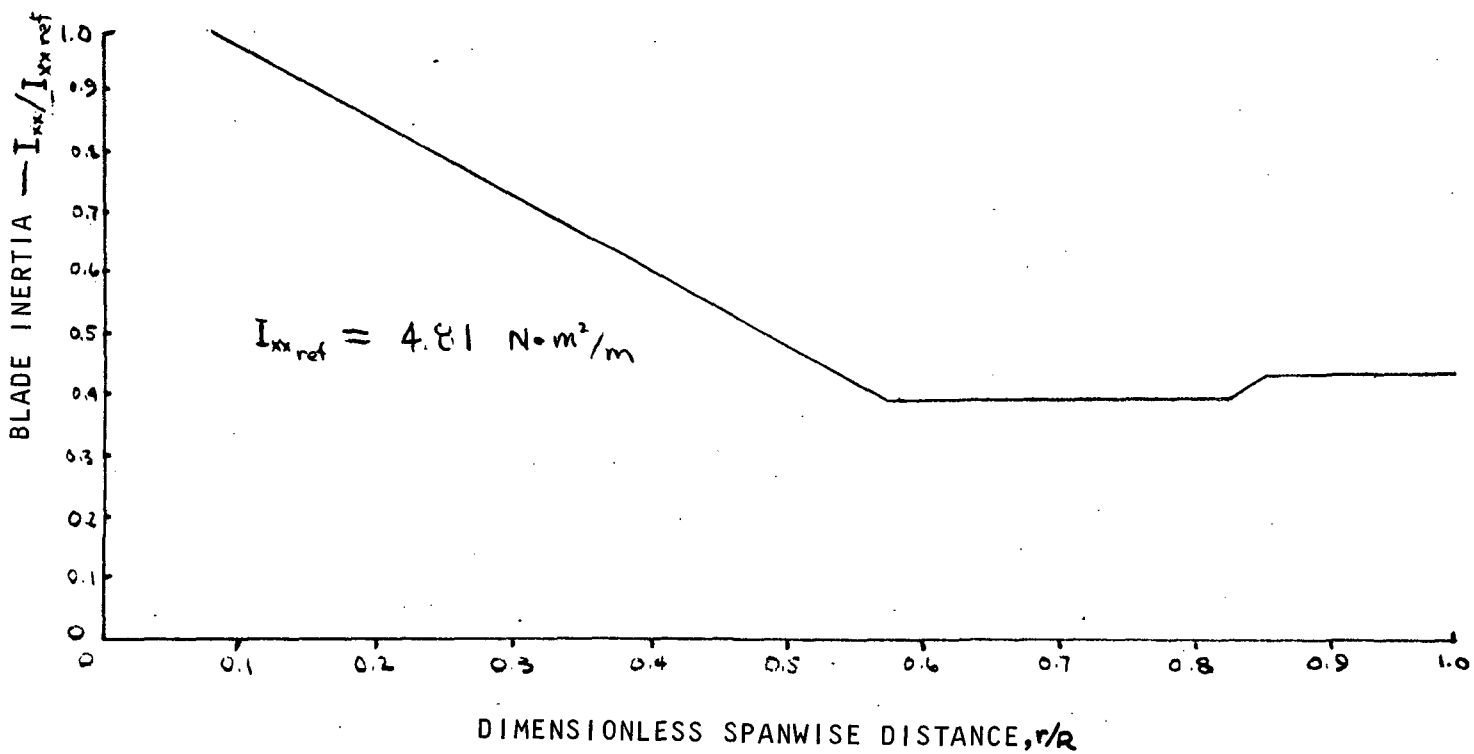

Figure 3. BLADE PITCH INERTIA DISTRIBUTION

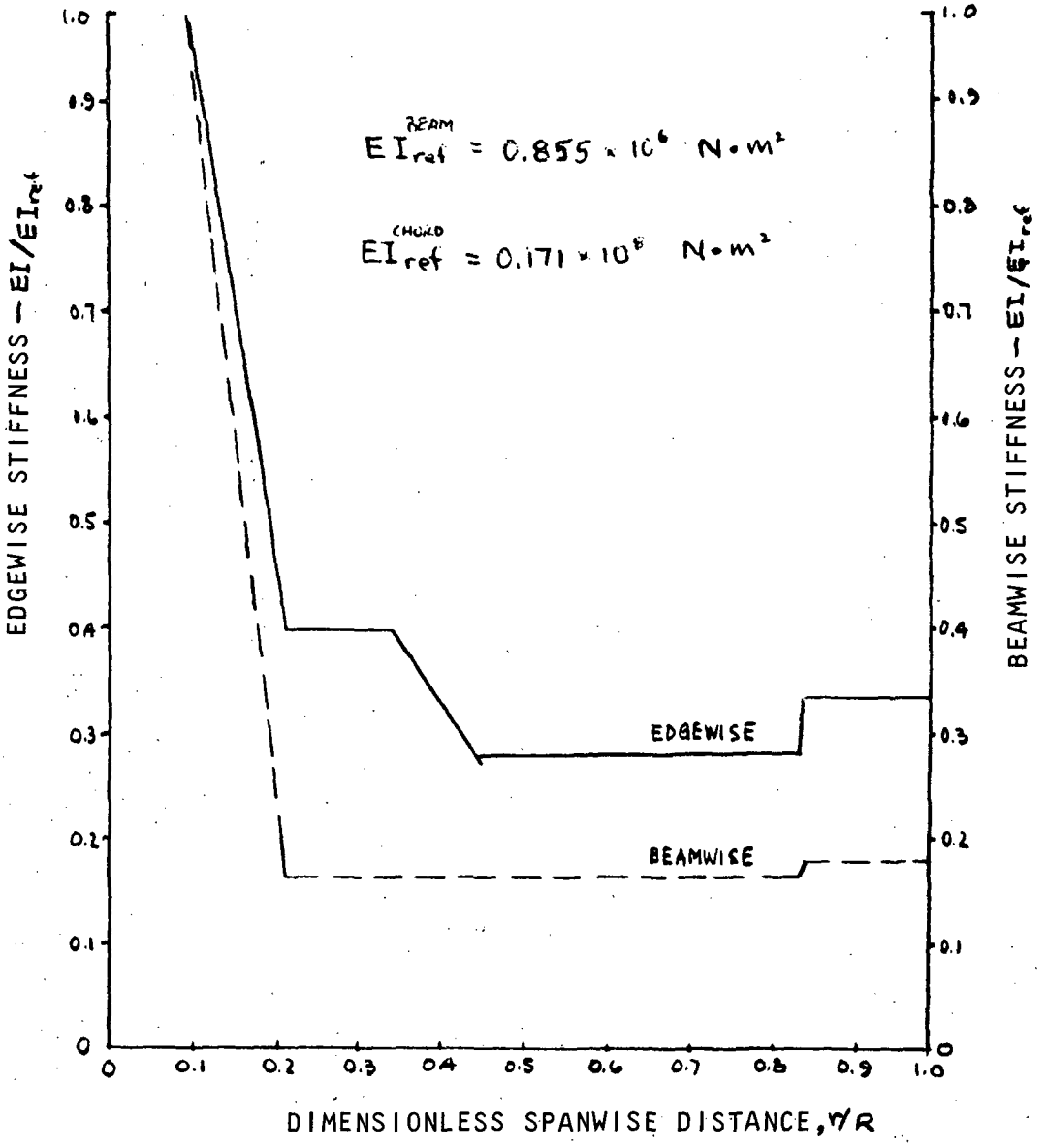

Figure 4. BLADE BENDING STIFFNESS DISTRIBUTION

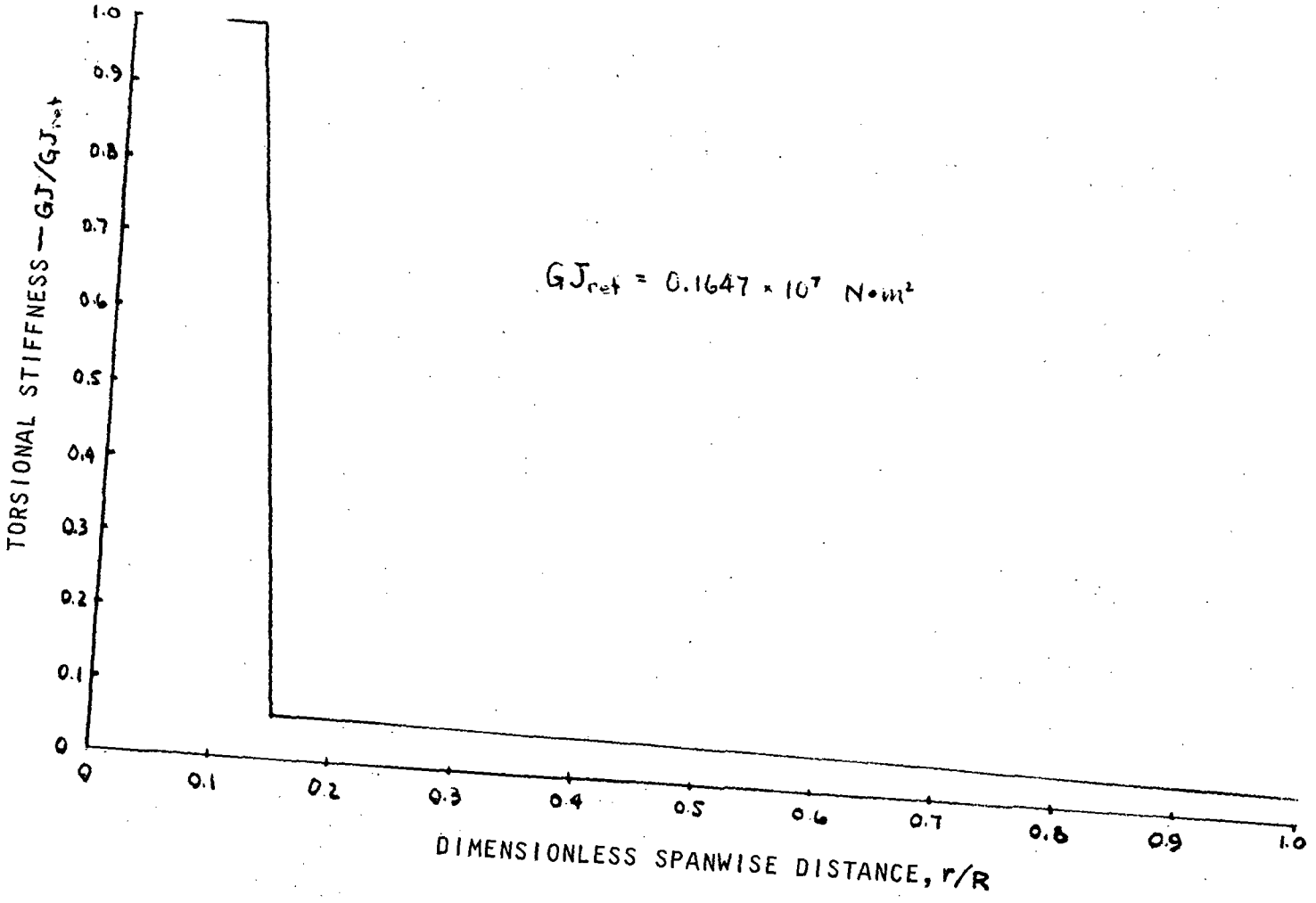

Figure 5. BLADE TORSIONAL STIFFNESS DISTRIBUTION

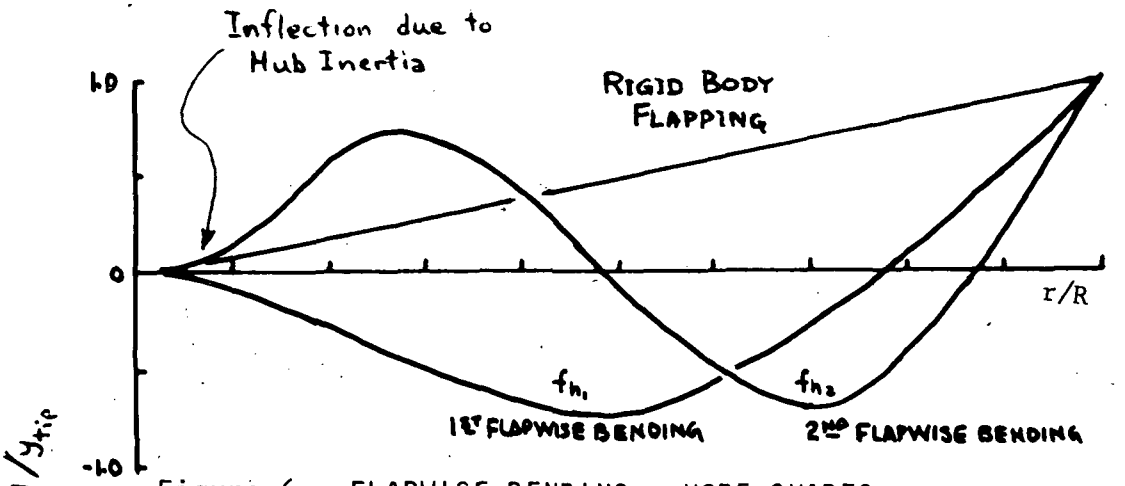

Figure 6. FLAPWISE BENDING - MODE SHAPES

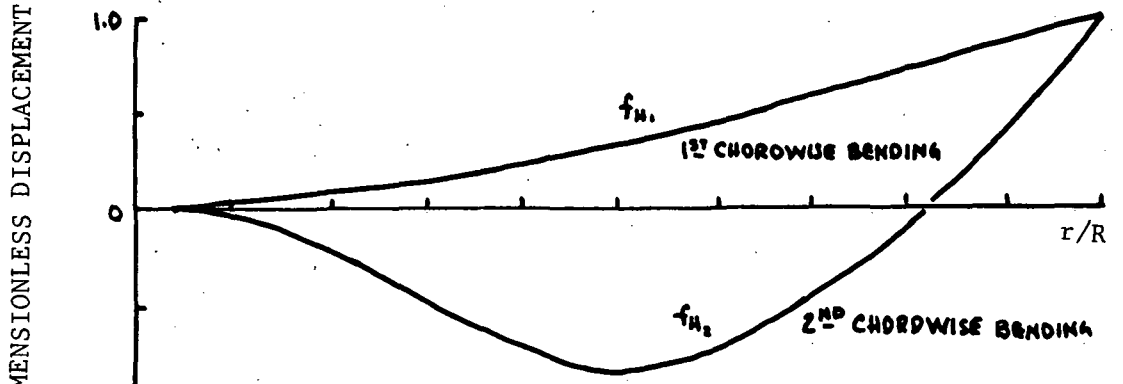

Figure 7. CHORDWISE BENDING - MODE SHAPES

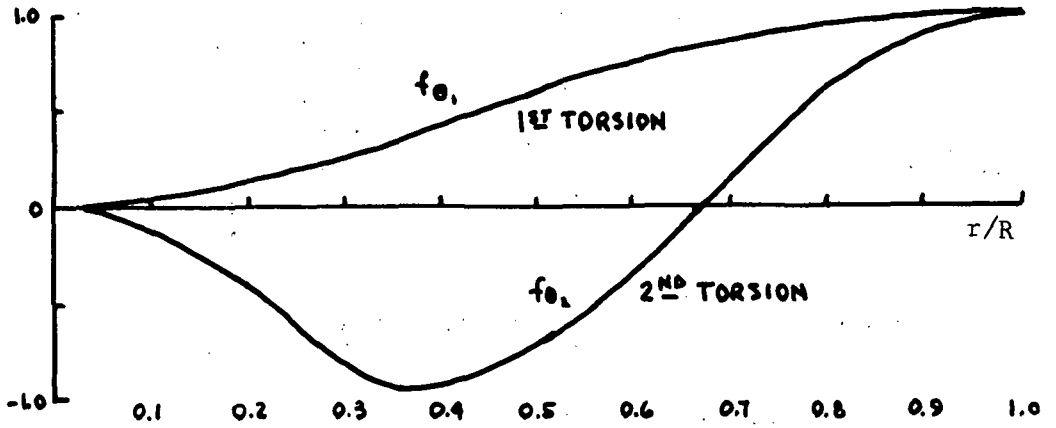

Figure 8. FIRST & SECOND TORSION - MODE SHAPE

	FREQUENCY AT Ω = 5 HZ	HARMONIC (ω/Ω)
RIGID FLAPPING	5.18 HZ	1.037
1st FLAPWISE BENDING	14.7 HZ	2.94
2nd FLAPWISE BENDING	26.4 HZ	5.28
1st EDGEWISE BENDING	5.92 HZ	1.18
2nd EDGEWISE BENDING	37.3 HZ	7.46
1st TORSION	26.5 HZ	5.30
2nd TORSION	69.3 HZ	13.86
STIFF BLADE: 1st TORSION	84.1 HZ	16.7
2nd TORSION	219. HZ	48.3

Figure 9. BLADE FREQUENCIES

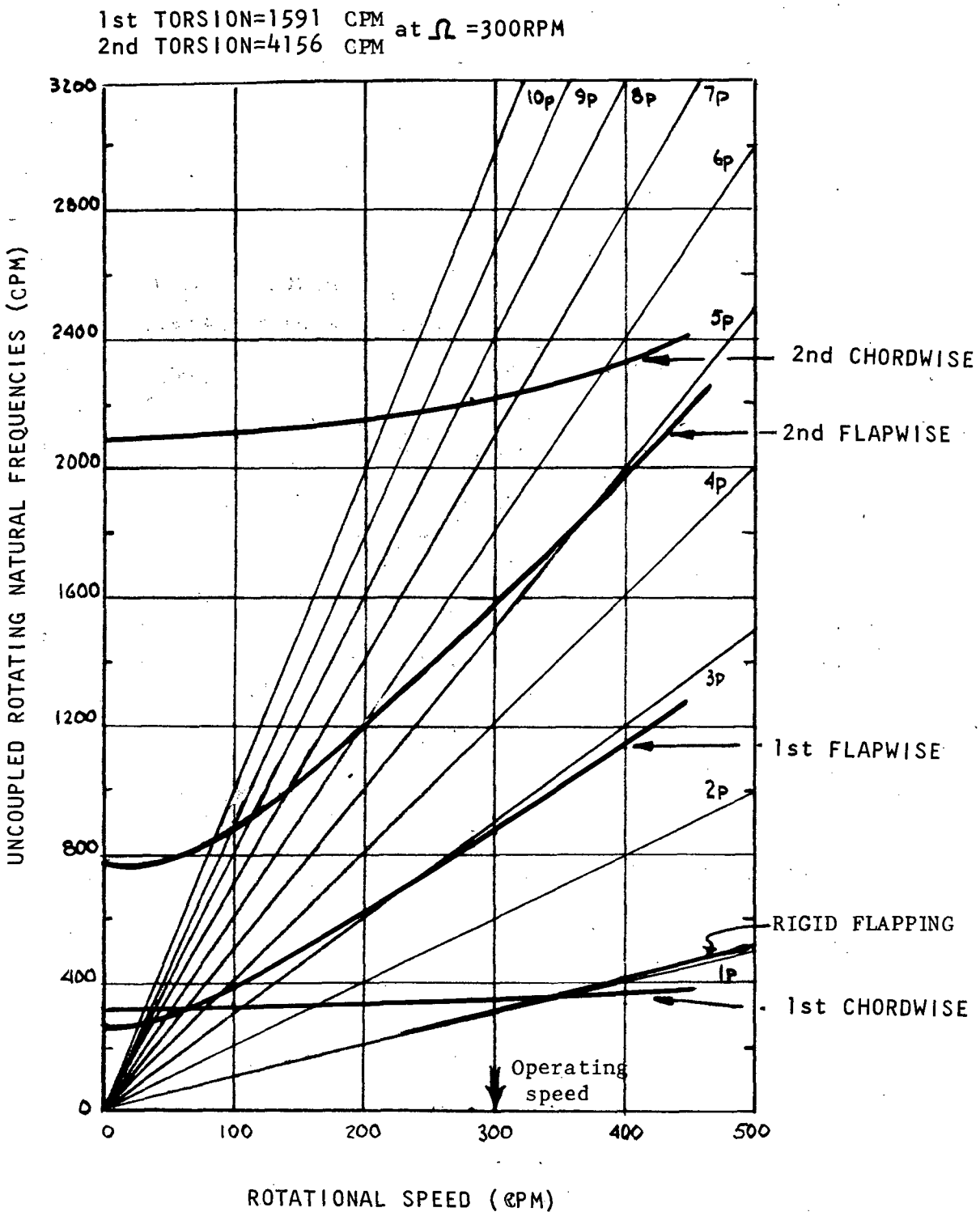

Figure 10. ROTATING BLADE FREQUENCY PLOT

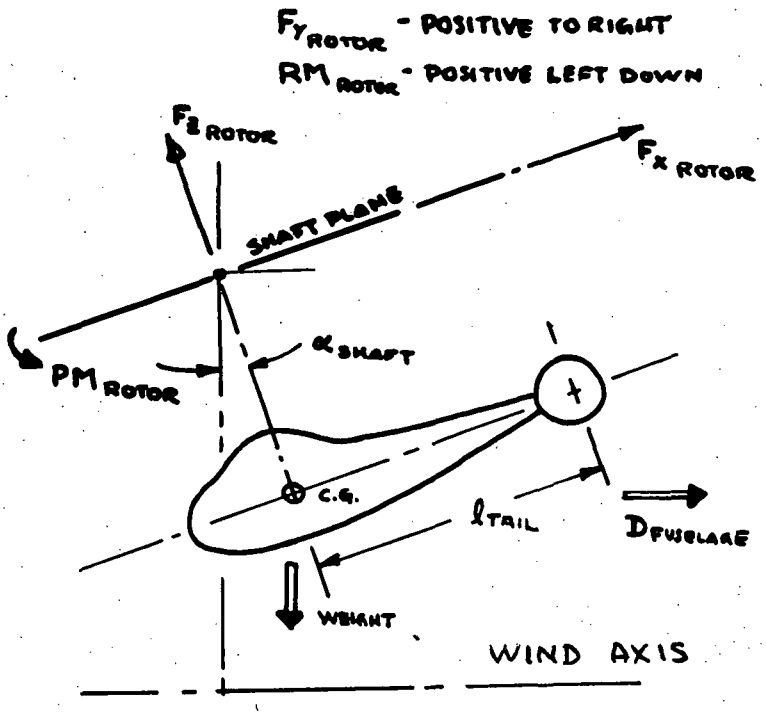

Figure 11. FORCES & MOMENTS ACTING ON THE HELICOPTER

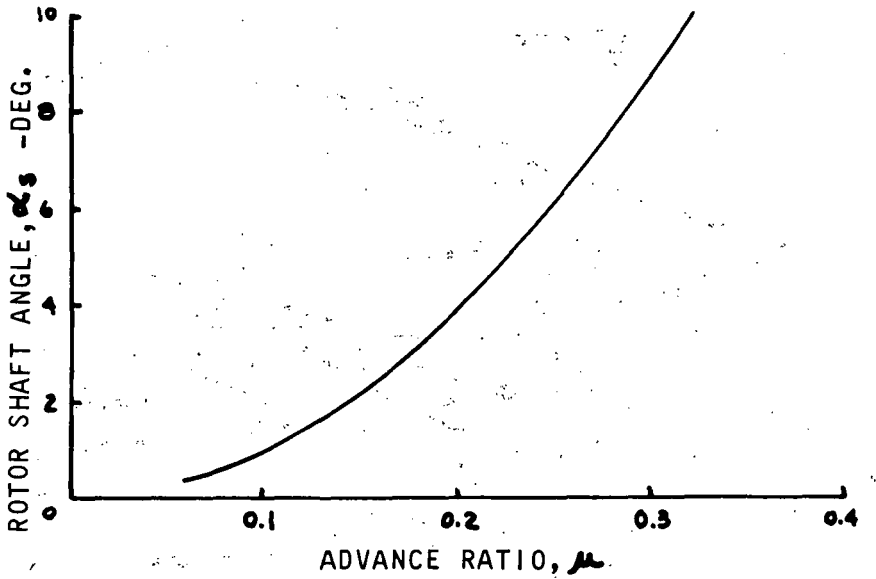

Figure 12. ROTOR SHAFT ANGLE vs ADVANCE RATIO

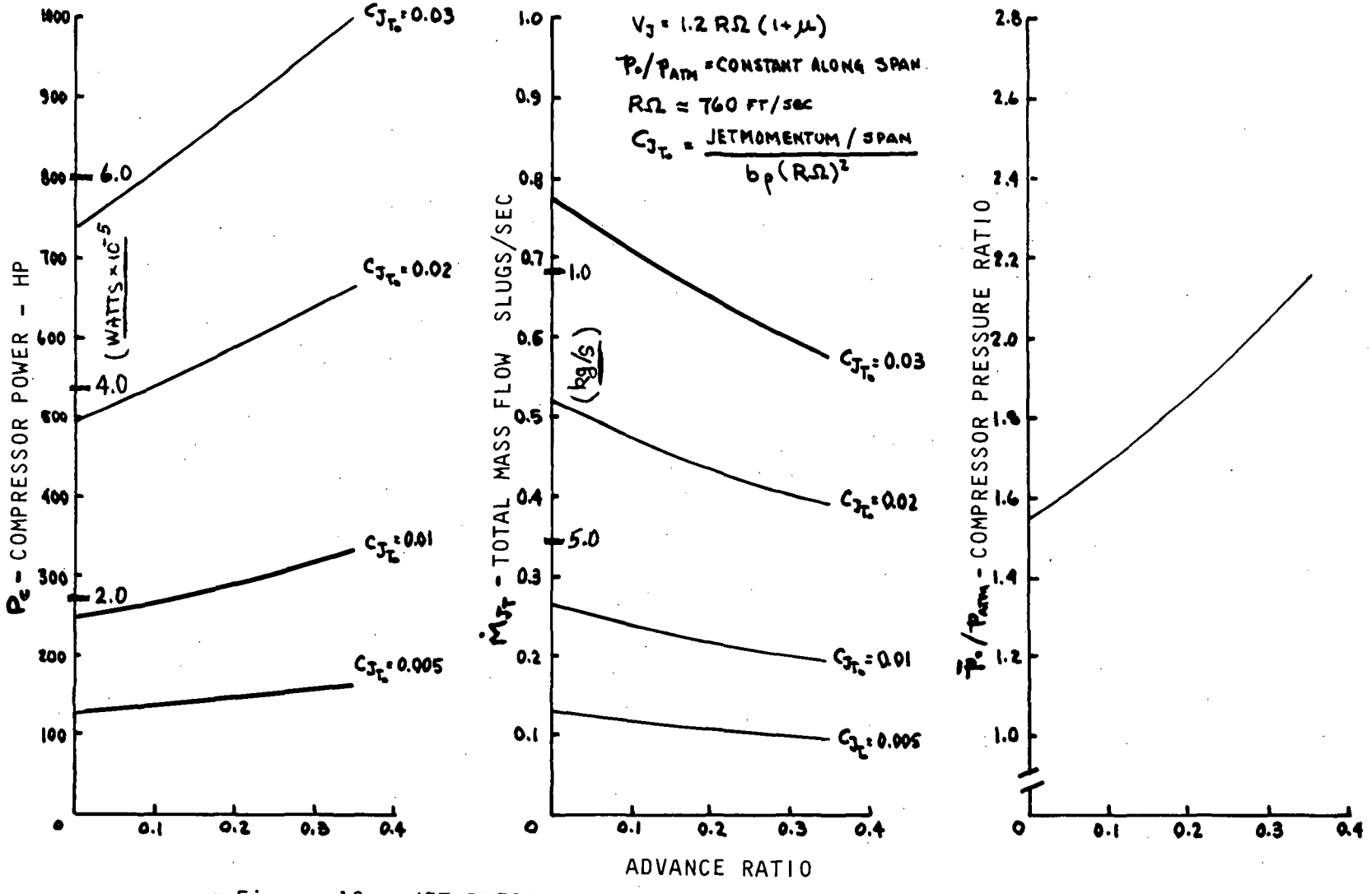

Figure 13. JET PRESSURE RATIO, VELOCITY AND COMPRESSOR POWER PLOTS.

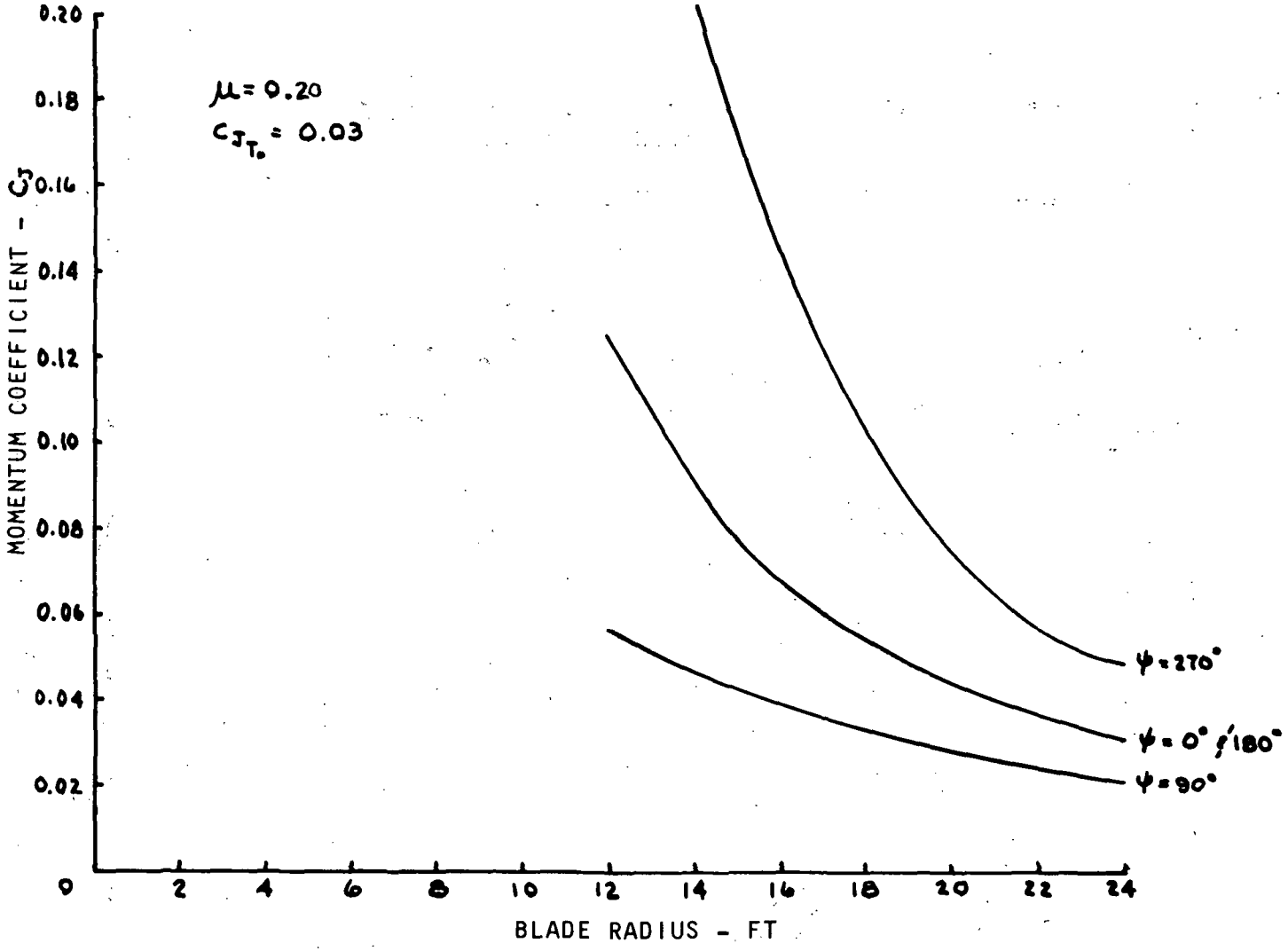

Figure 14. RADIAL VARIATION OF JET MOMENTUM COEFFICIENT AT SEVERAL AZUMUTHAL STATIONS.

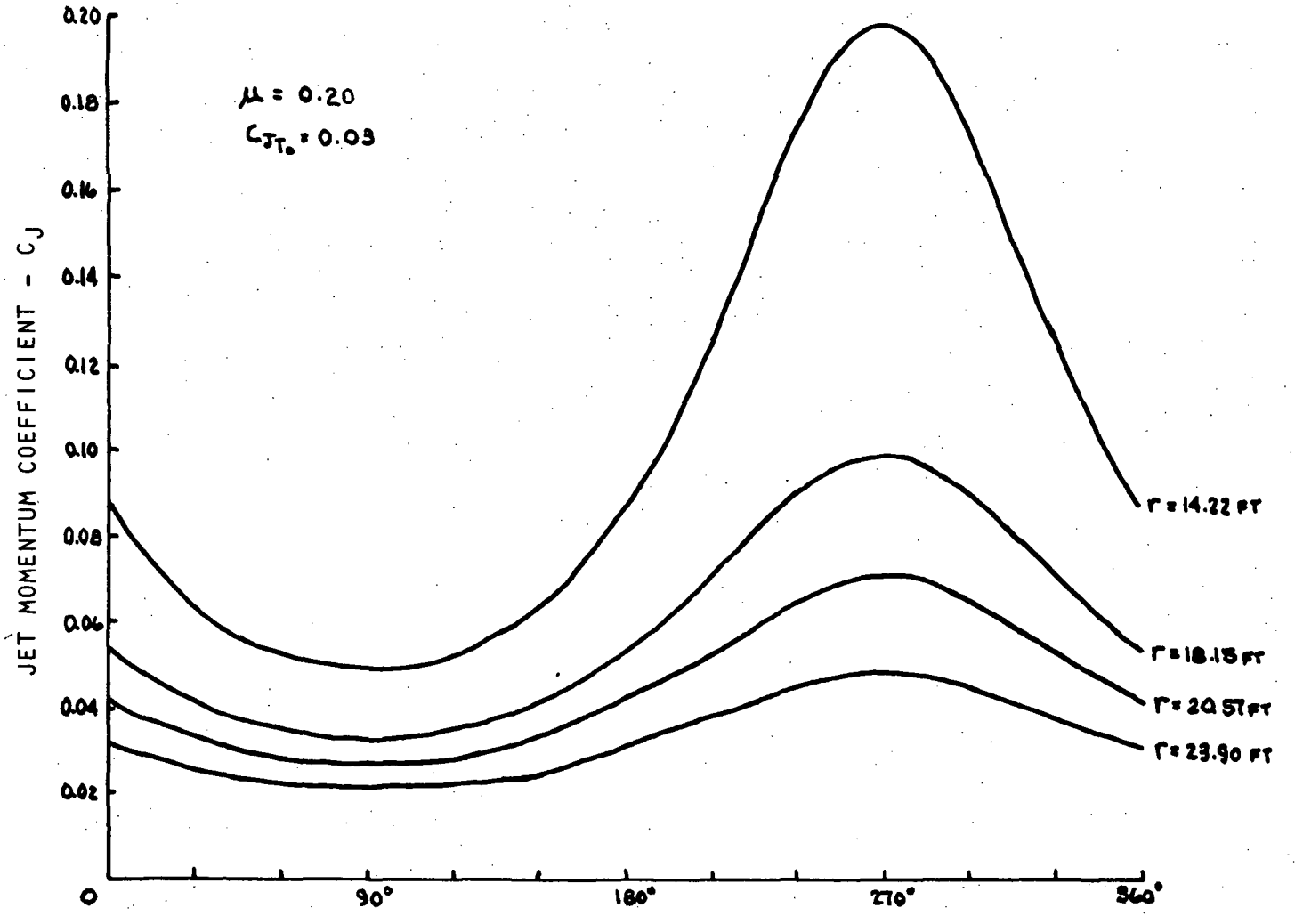

Figure 15. AZIMUTHAL VARIATION OF JET MOMENTUM COEFFICIENT AT SEVERAL RADIAL STATIONS

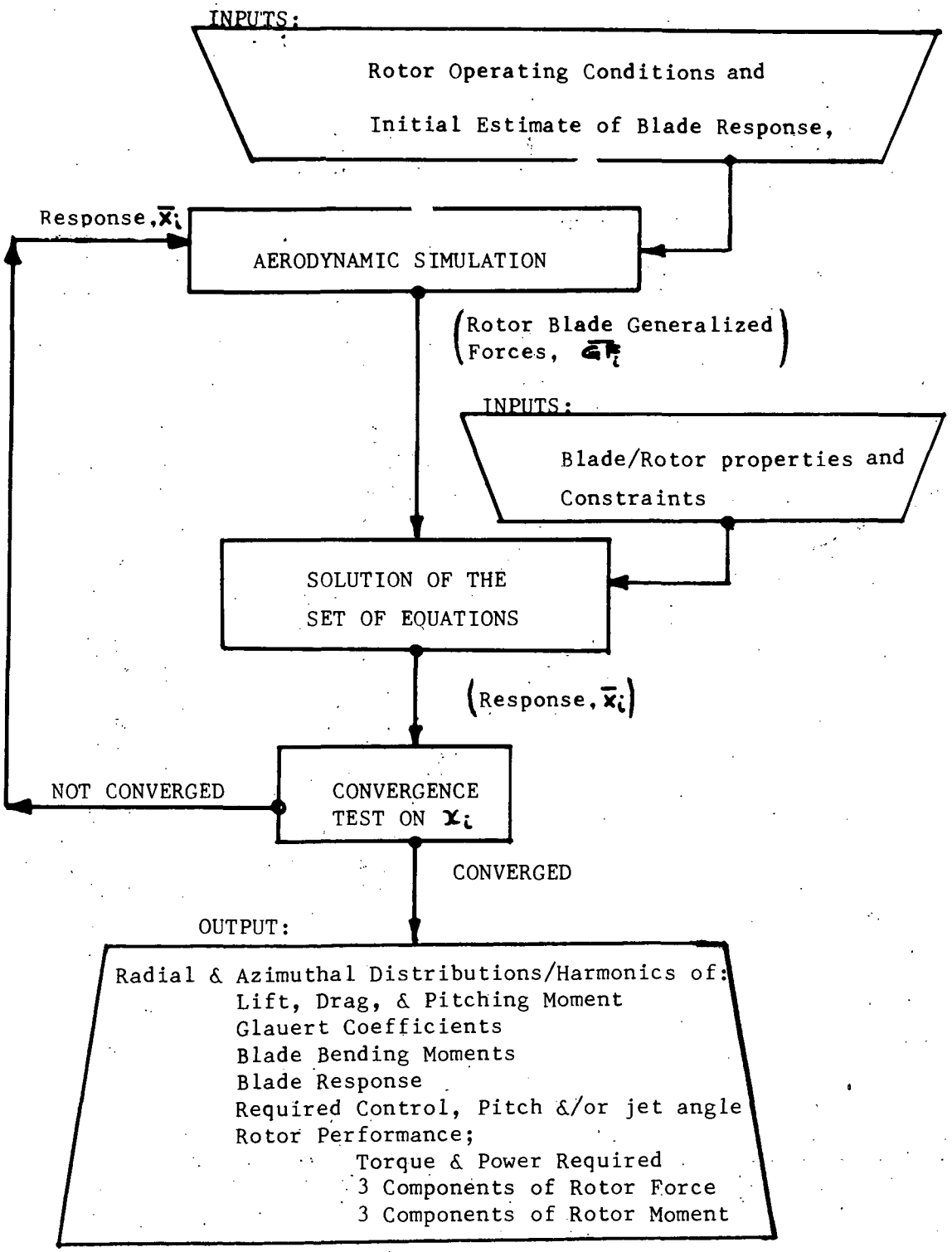

Figure 16. PROGRAM LOGIC FLOW

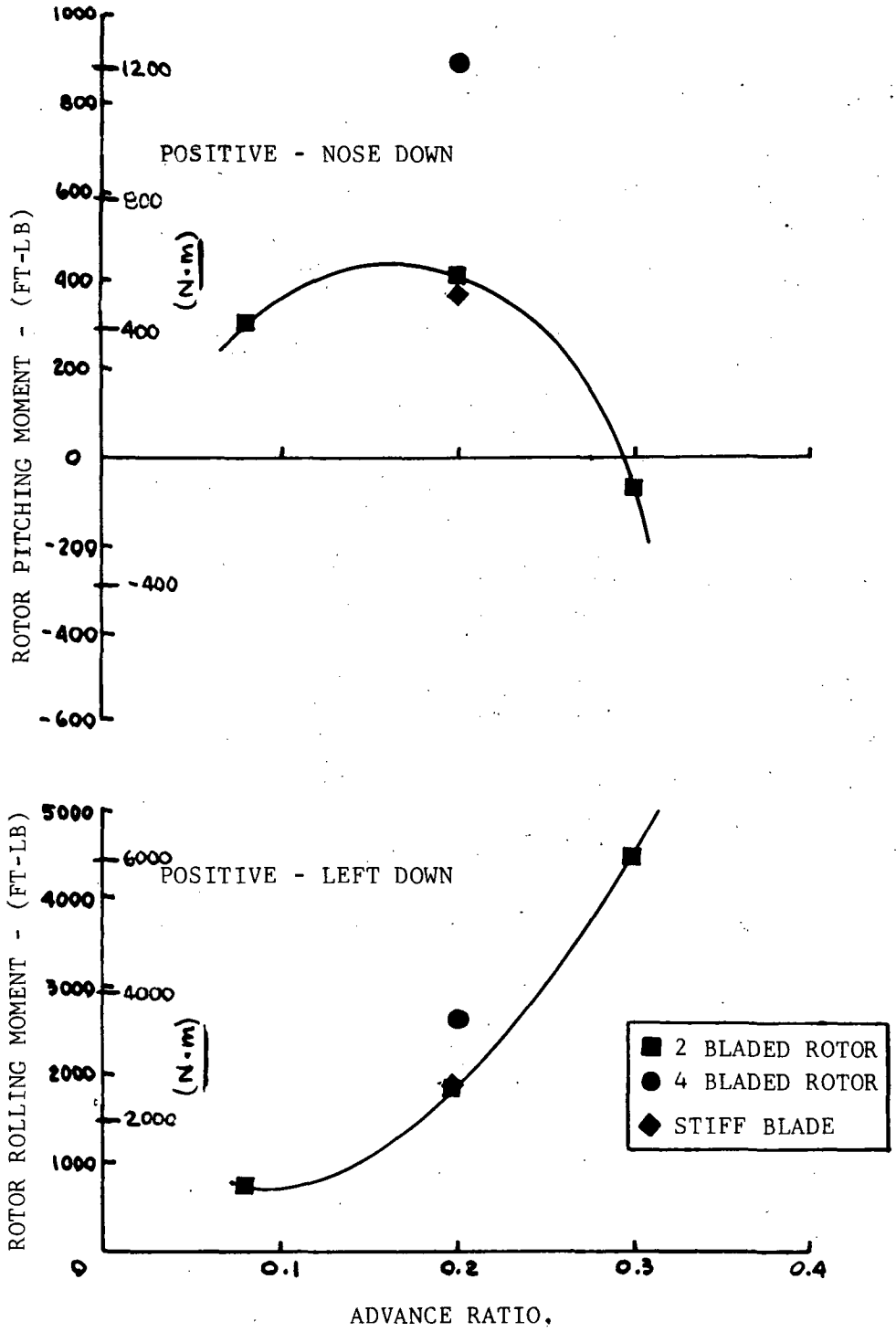

Figure 17. ROTOR TRIM MOMENTS JET-ON & OFF vs ADVANCE RATIO

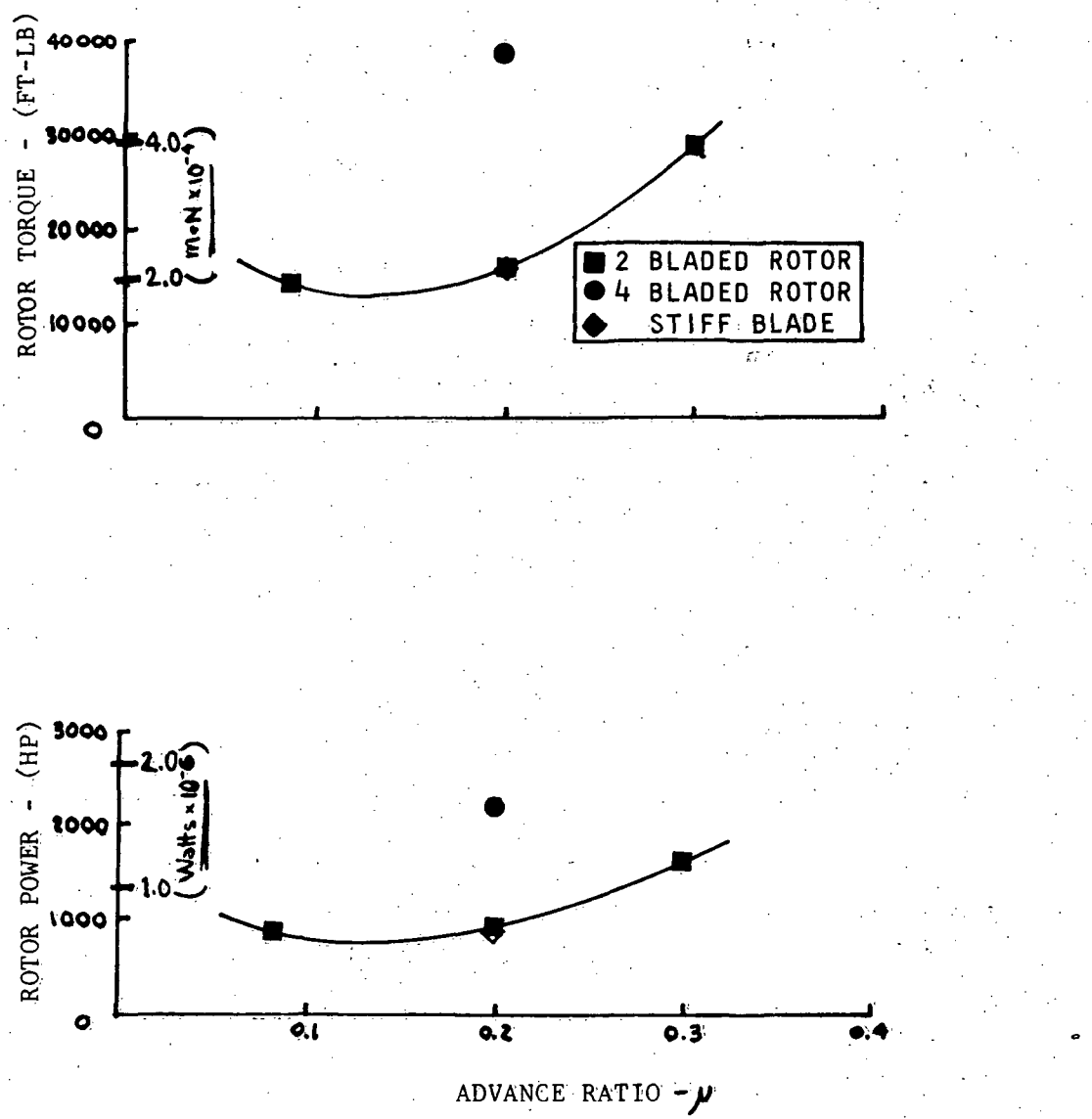

Figure 18. JET-OFF ROTOR TORQUE & POWER vs ADVANCE RATIO

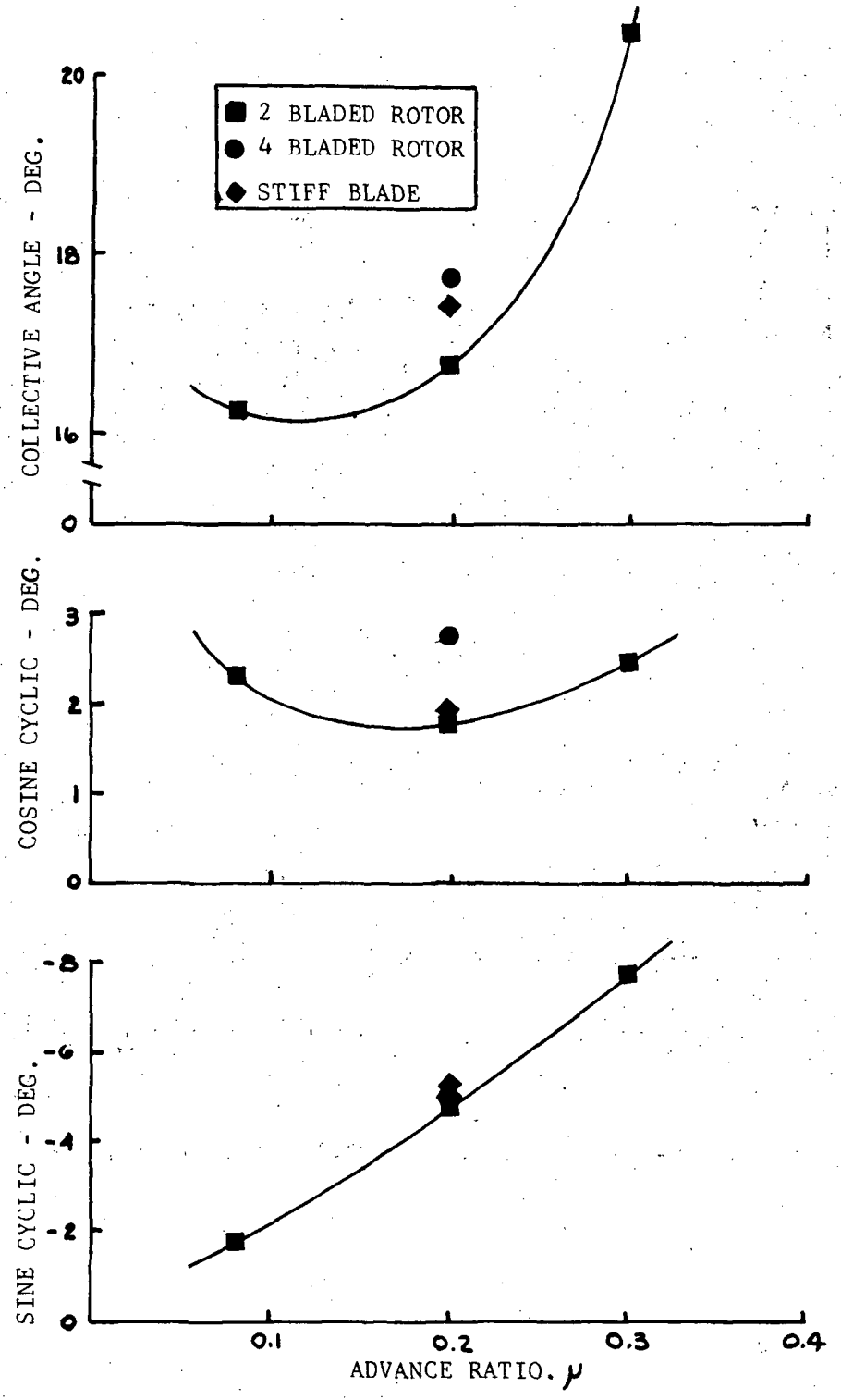

Figure 19. CONTROL ANGLE VALUES vs ADVANCE RATIO - JET-OFF

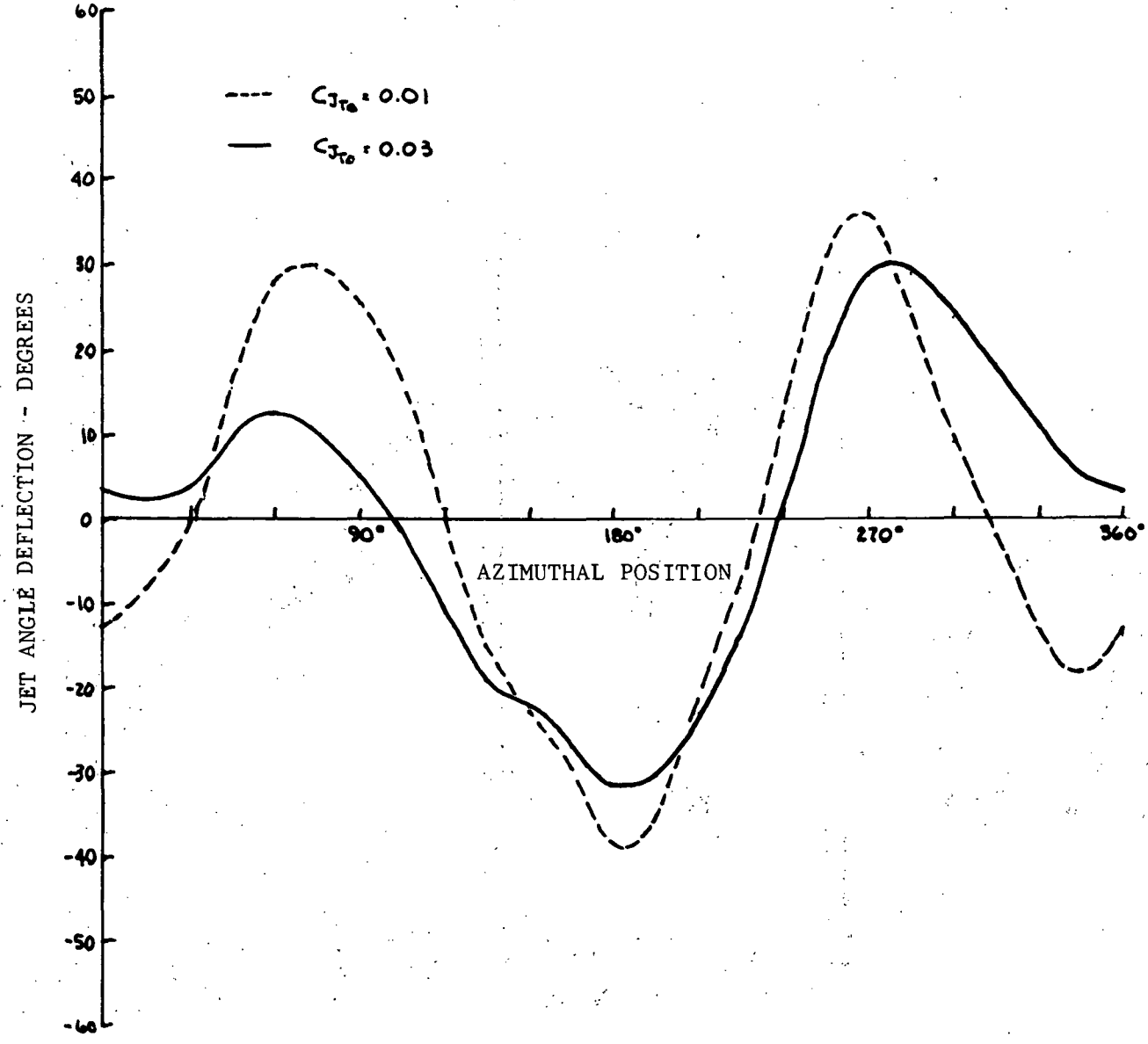

Figure 20. AZIMUTHAL VARIATION OF REQUIRED JET ANGLE TO SUPPRESS ALL TRANSMITTED SHEARS TO ZERO FOR μ =0.08, $C_{J_{T_0}}$ =0.01, 0.03

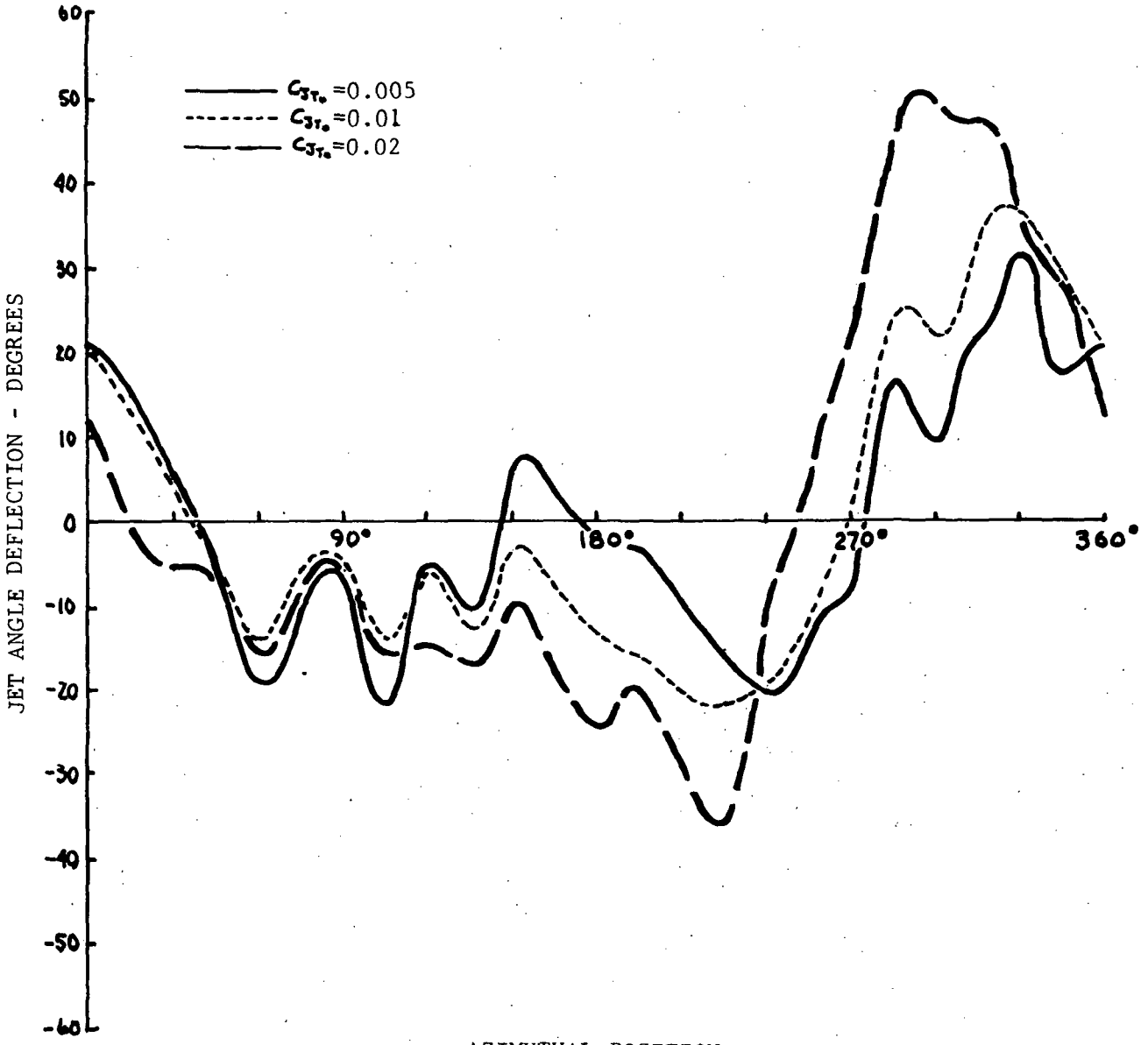

Figure 21. AZIMUTHAL VARIATION OF REQUIRED JET ANGLE TO SUPPRESS ALL TRANSMITTED SHEARS TO ZERO FOR μ =0.20, $C_{J_{T_o}}$ =0.005, 0.01, 0.02.

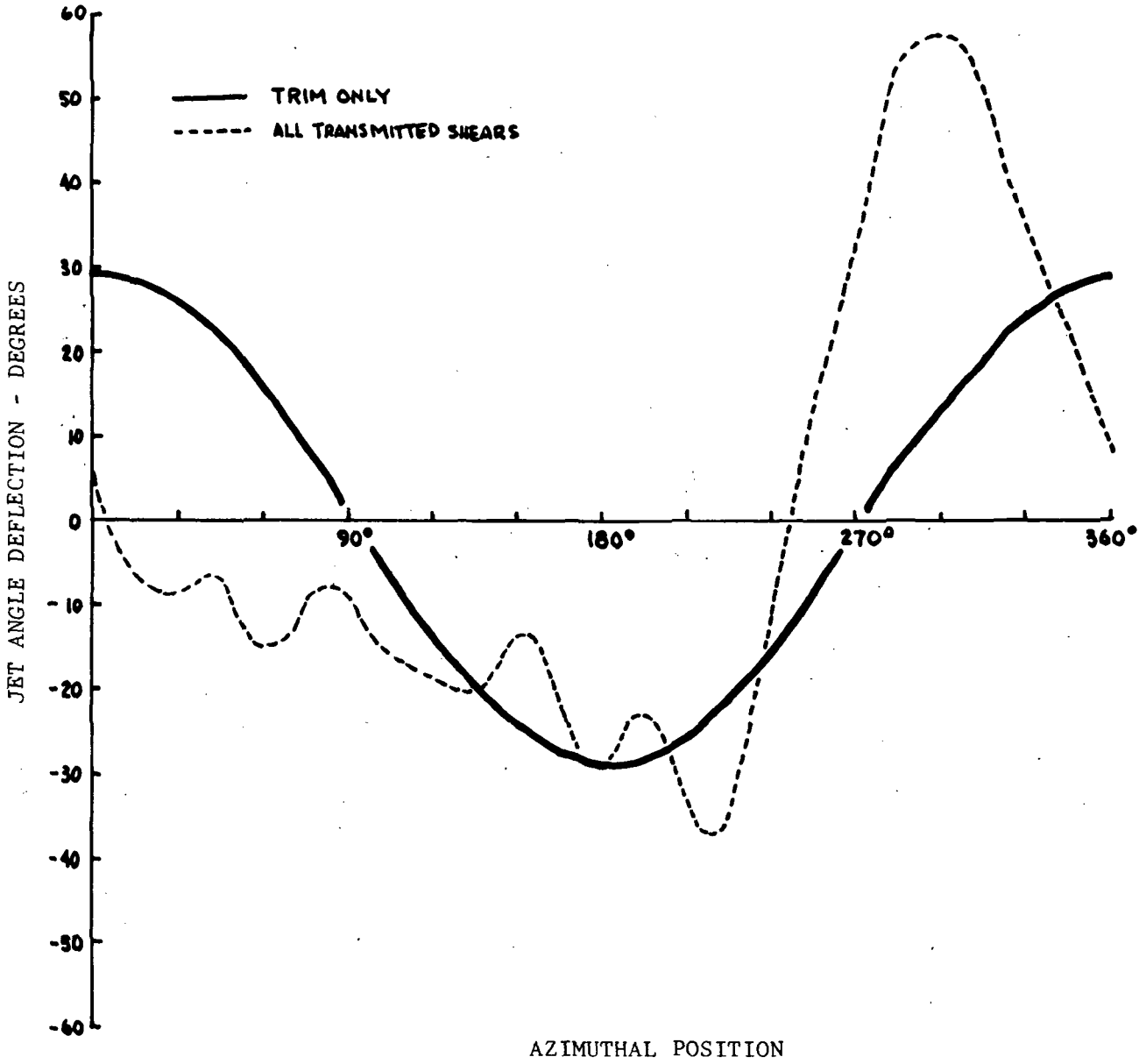

Figure 22. COMPARISON OF AZIMUTHAL VARIATION OF REQUIRED JET ANGLE TO MAINTAIN TRIM ONLY WITH REQUIRED JET ANGLE TO SUPPRESS ALL TRANSMITTED SHEARS, $\mu = 0.20$, $C_{J_{T_o}} = 0.03$.

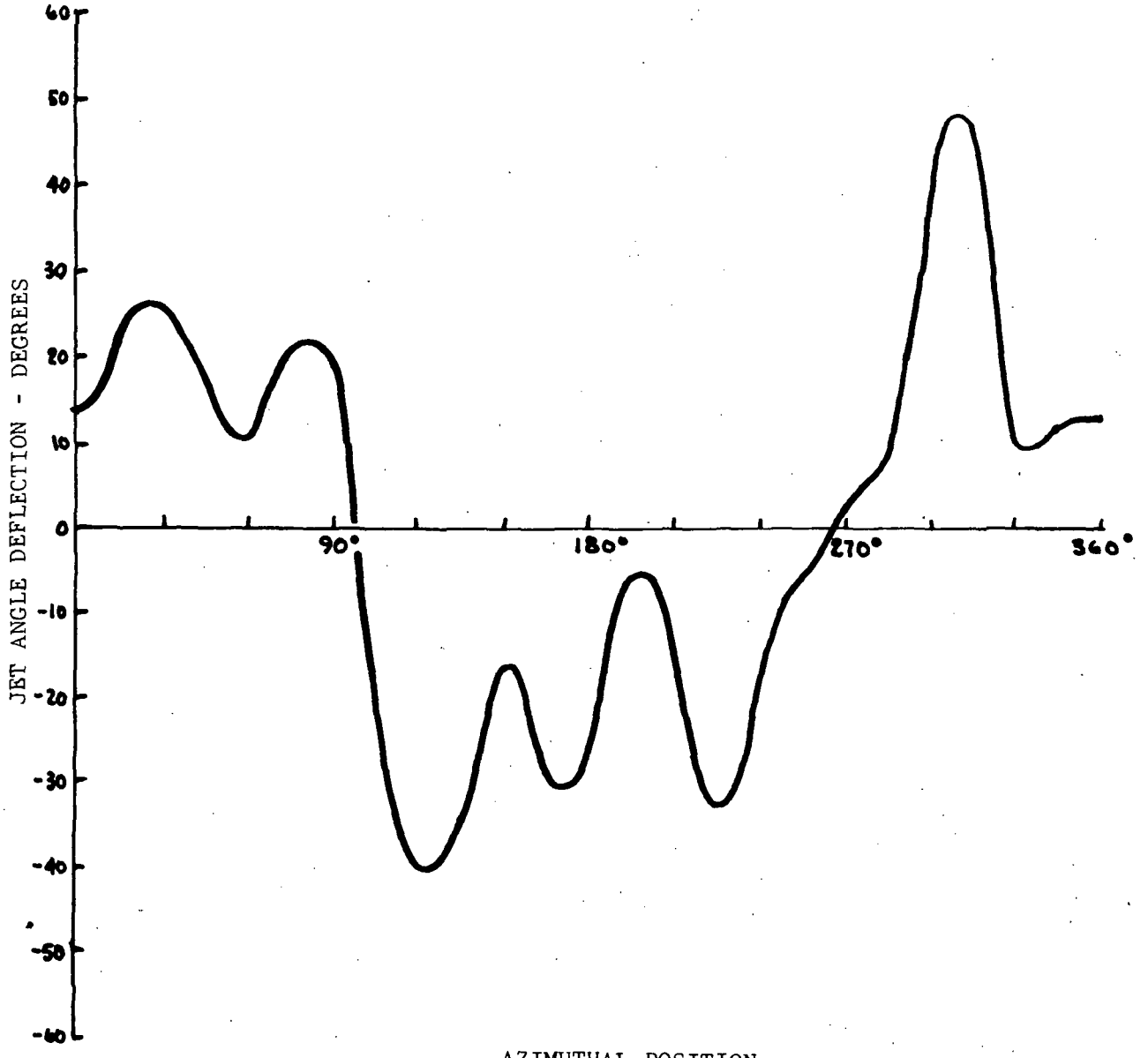

Figure 23. AZIMUTHAL VARIATION OF REQUIRED JET ANGLE TO SUPPRESS ALL TRANSMITTED SHEARS TO ZERO FOR STIFF BLADE AT μ =0.20, C_{T_0} =0.03.

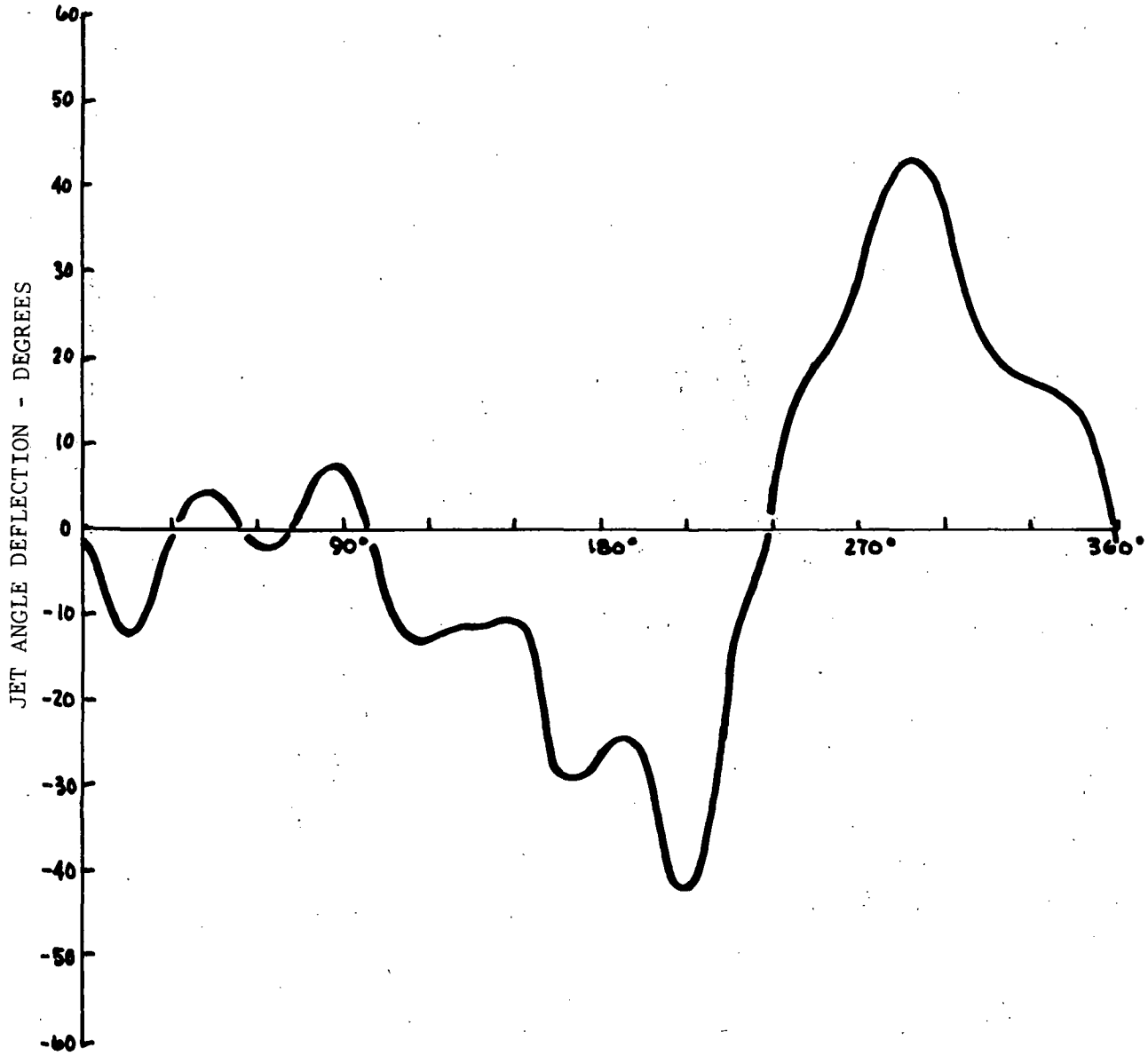

Figure 24. AZIMUTHAL VARIATION OF REQUIRED JET ANGLE TO SUPPRESS ALL TRANSMITTED SHEARS TO ZERO FOR FOUR BLADED ROTOR AT μ =0.20, $C_{J_{T_0}}$ =0.03.

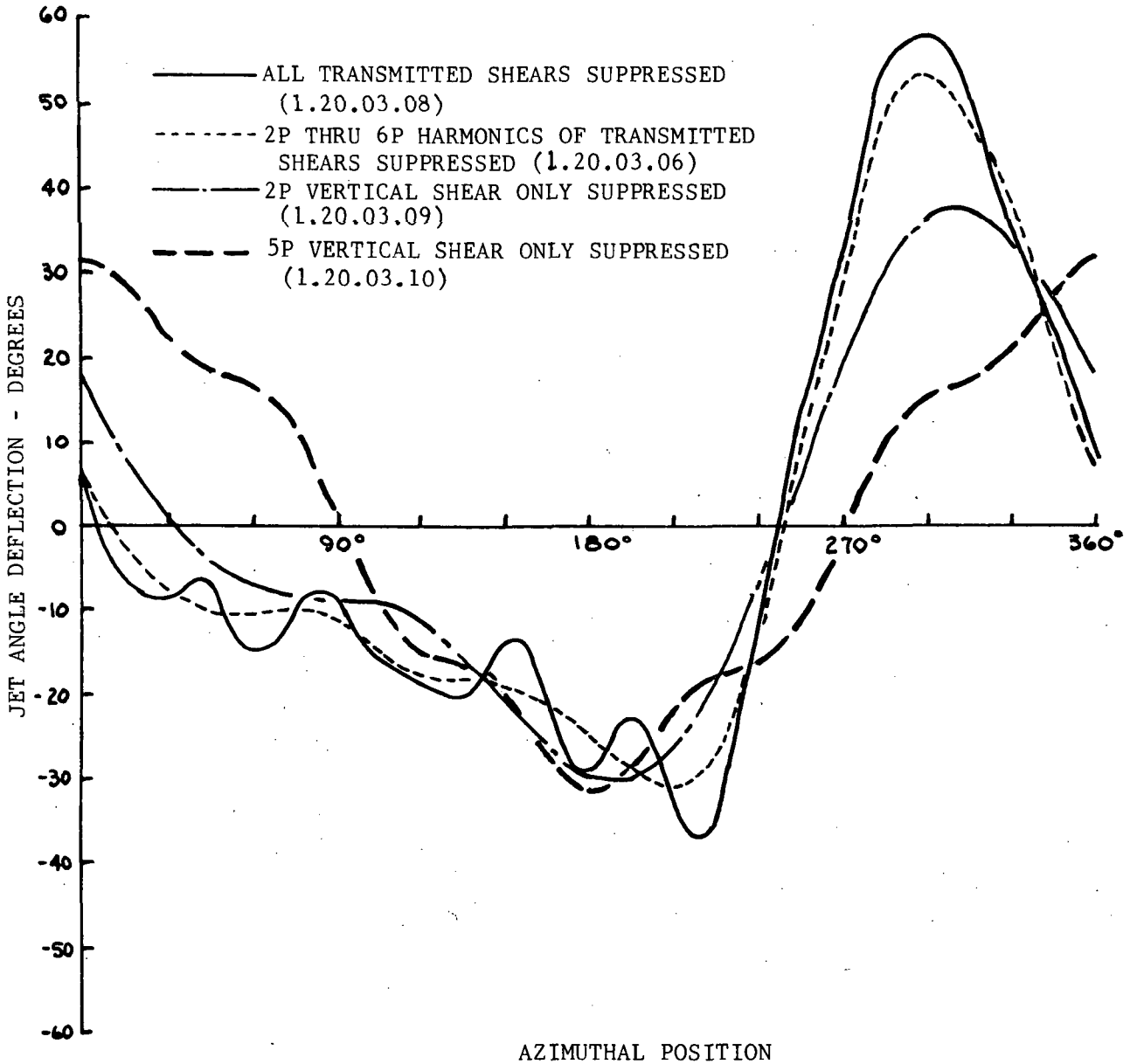

Figure 25. AZIMUTHAL VARIATION OF REQUIRED JET ANGLE - ALL AND PARTIAL SHEAR SUPPRESSION FOR μ =0.20 and $C_{J_{T_c}}$=0.03.

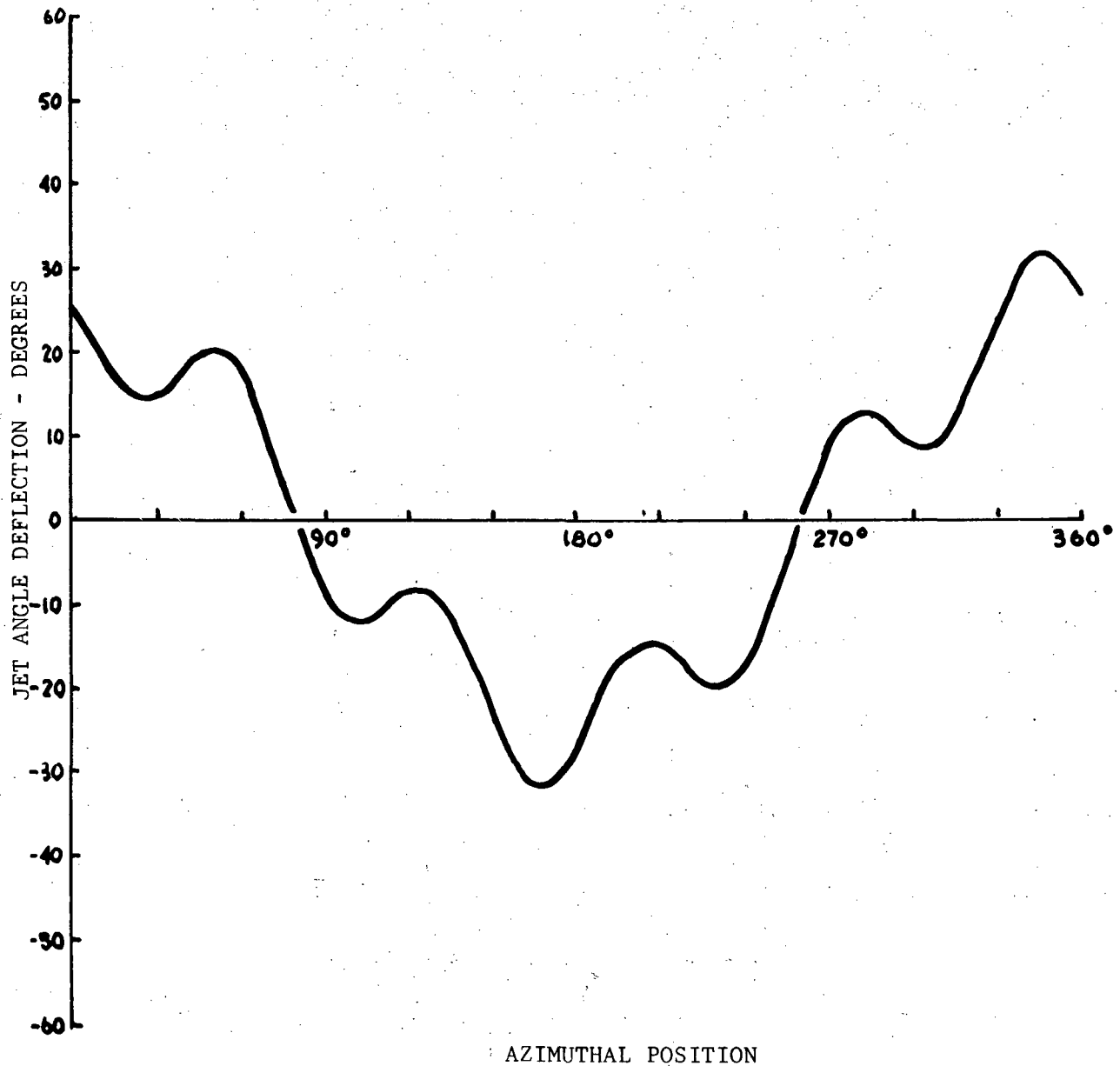

Figure 26. AZIMUTHAL VARIATION OF REQUIRED JET ANGLE TO SUPPRESS ONLY 5P VERTICAL SHEAR USING "SHORT JET", μ =0.20, $C_{J_{T_o}}$ =0.03.

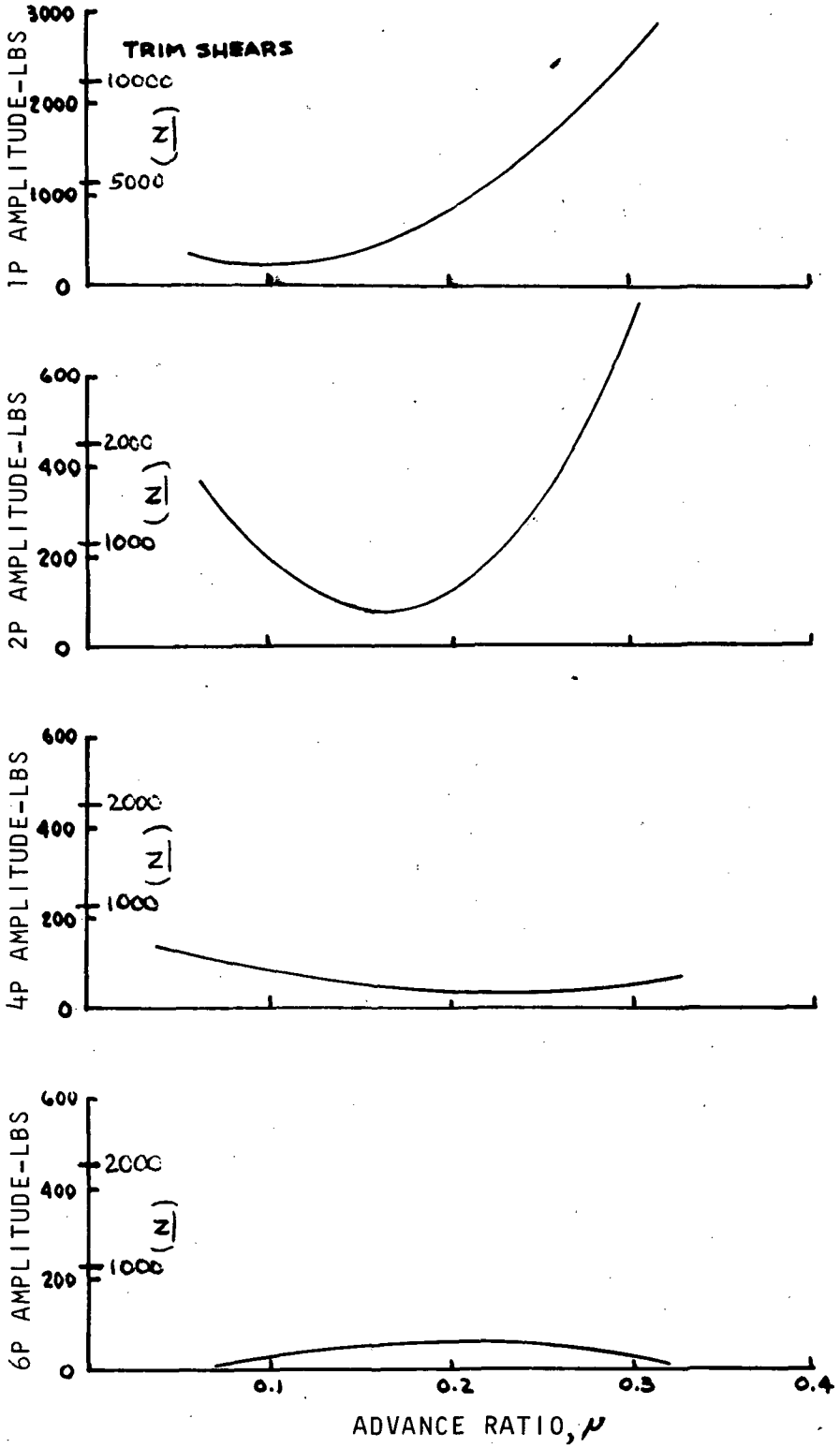

Figure 27. AMPLITUDE OF TRIM & TRANSMITTED FLAPWISE SHEARS vs ADVANCE RATIO, JET OFF.

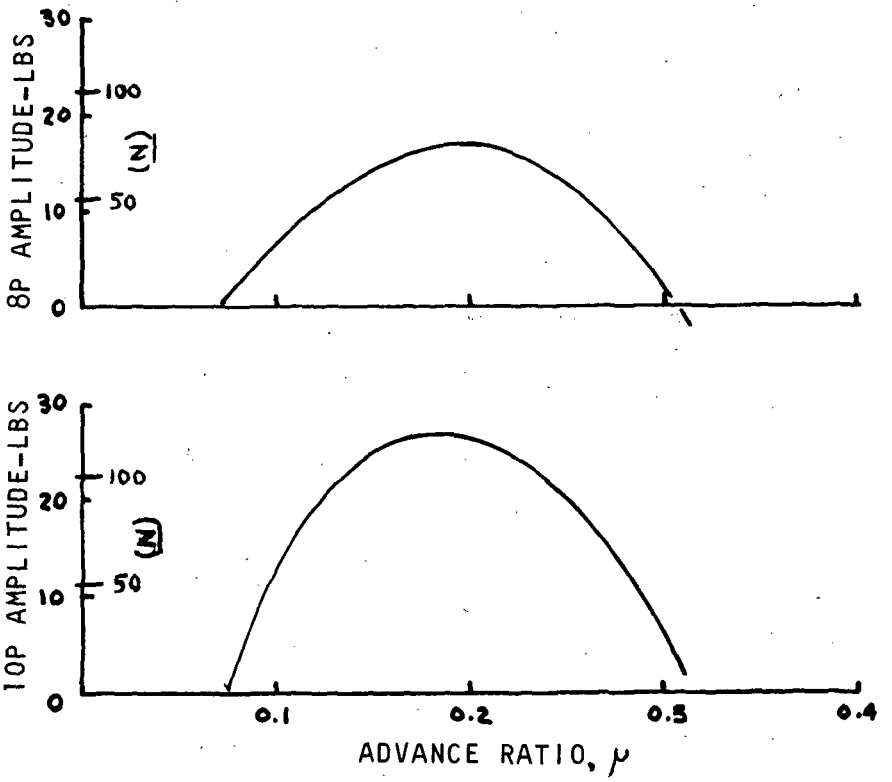

Figure 27. (CONTINUED)

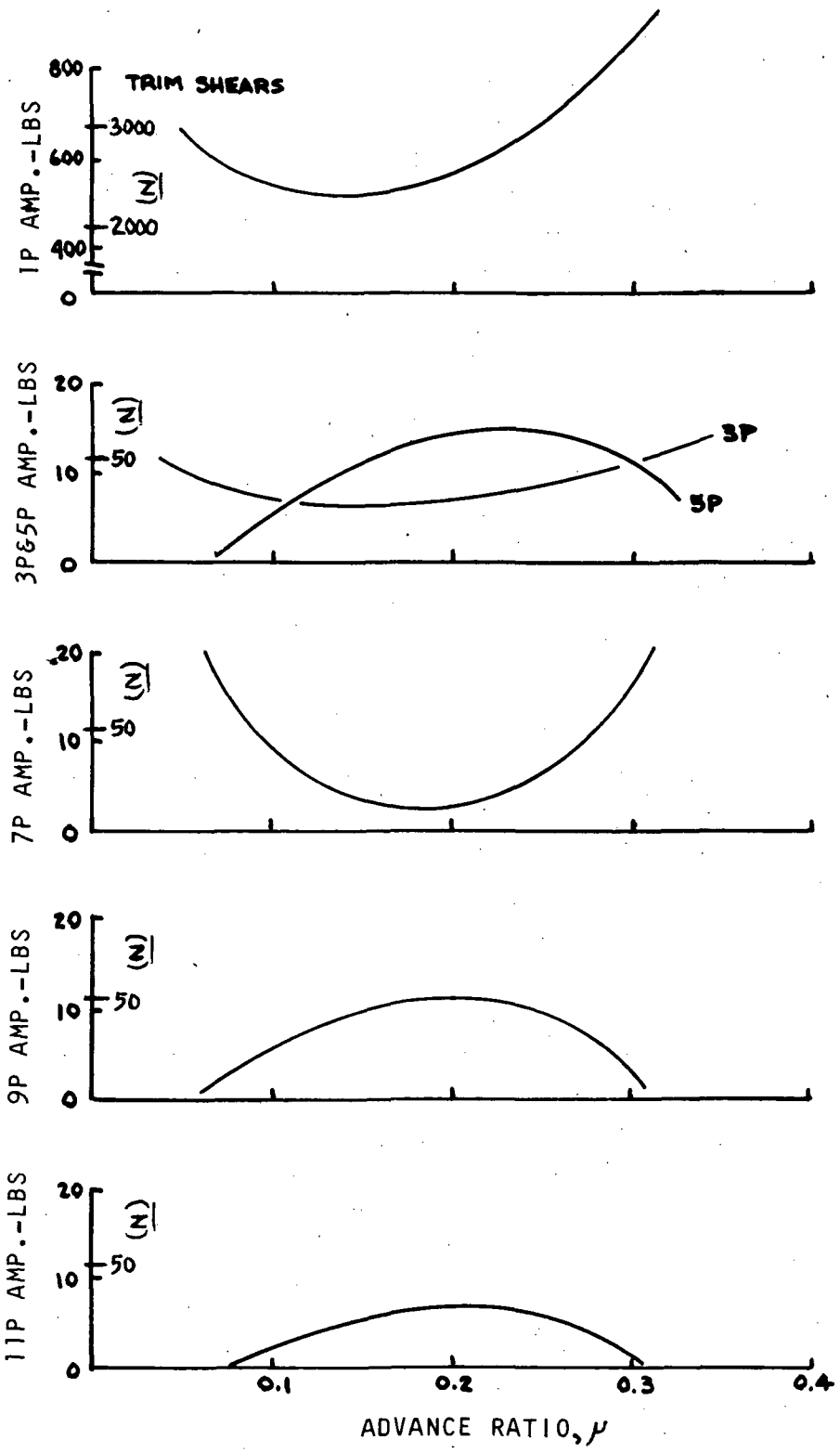

Figure 28. AMPLITUDE OF TRIM & TRANSMITTED CHORDWISE SHEARS vs ADVANCE RATIO, JET-OFF.

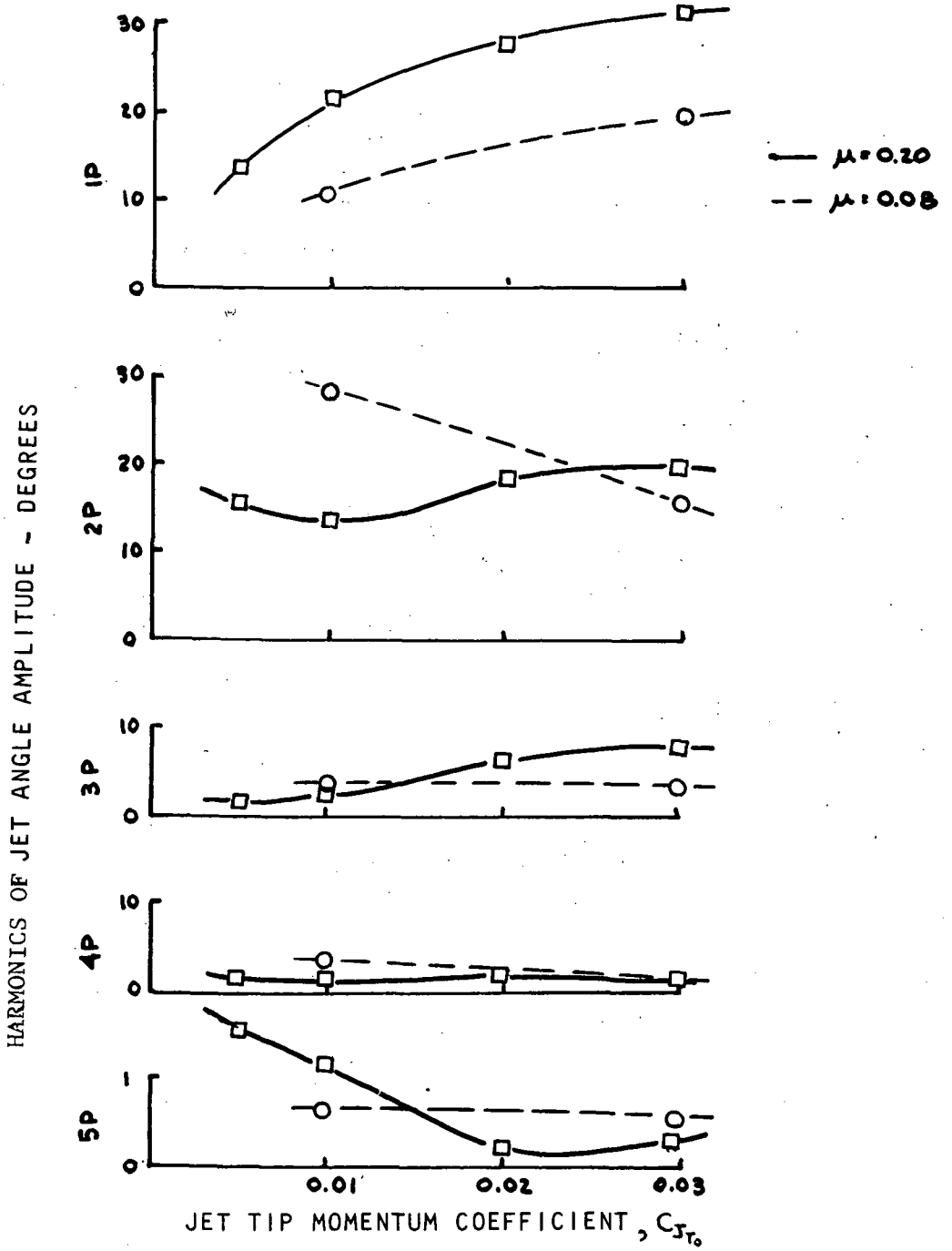

Figure 29. HARMONICS OF JET ANGLE AMPLITUDE REQUIRED TO SUPPRESS ALL TRANSMITTED SHEARS vs JET TIP MOMENTUM COEFFICIENT AT μ=0.08, 0.20.

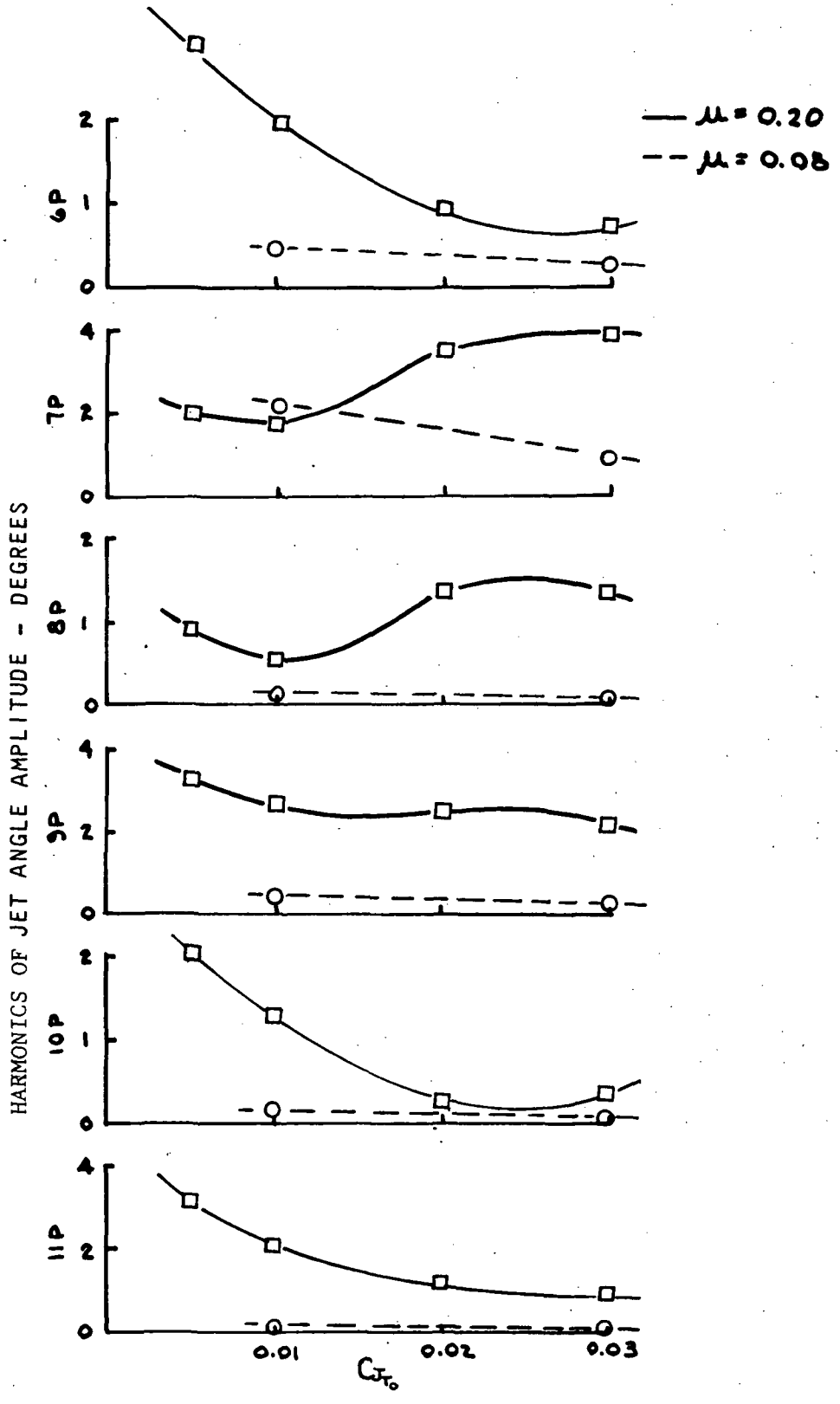

Figure 29. (CONTINUED)

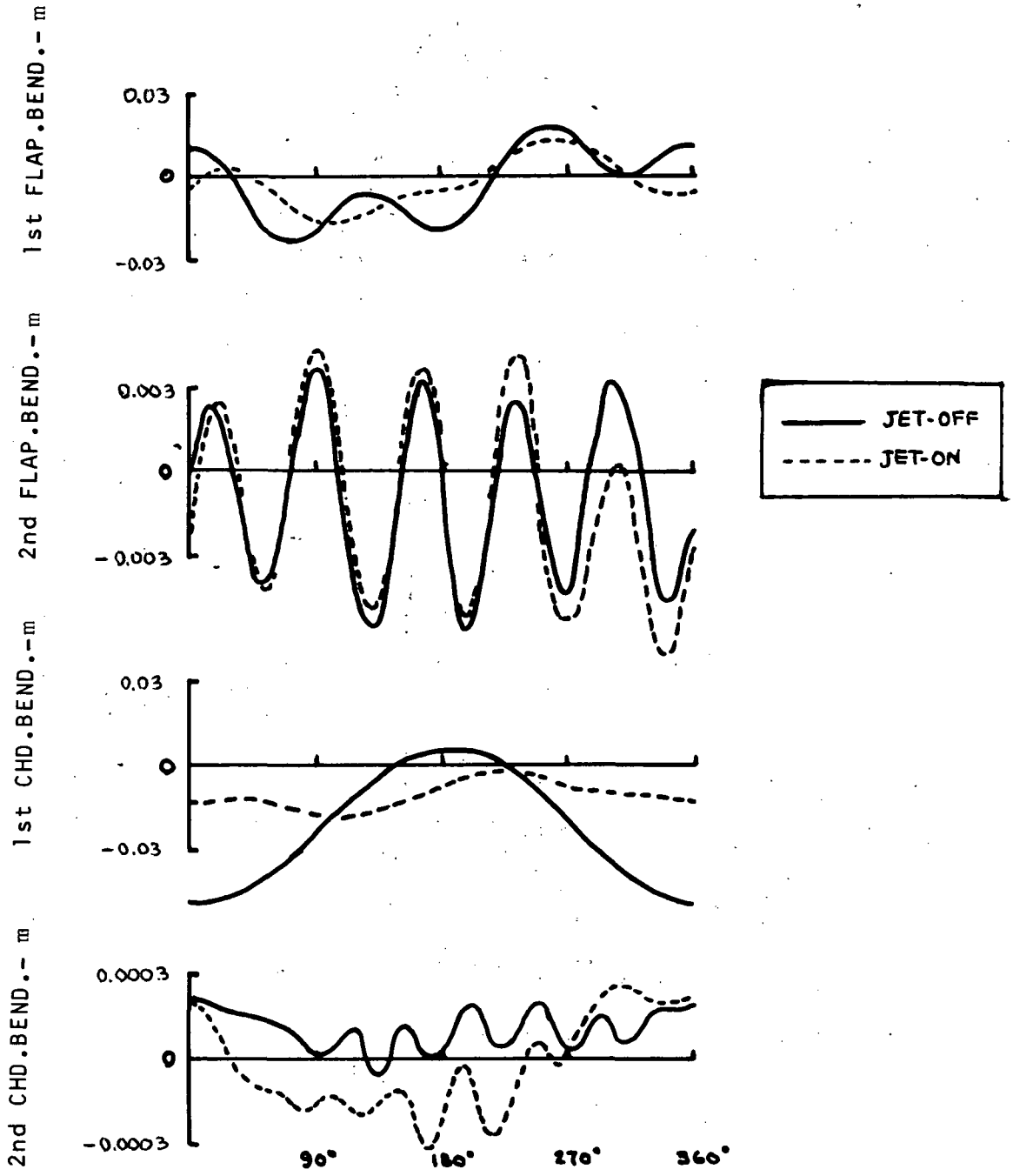

Figure 30. JET-OFF/JET-ON BLADE RESPONSES AT μ=0.20 $C_{J_{T_o}}$ =0.03.

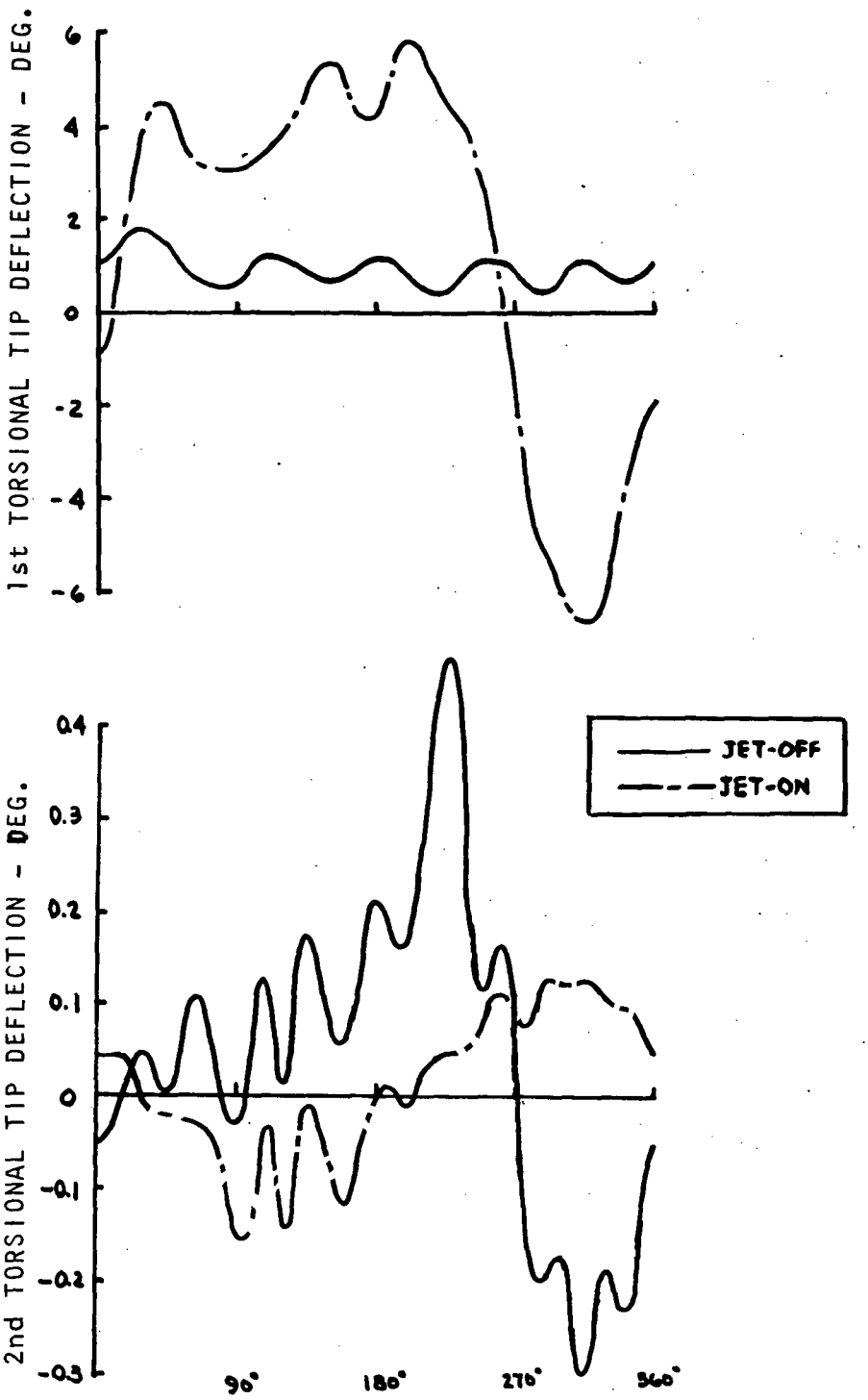

Figure 30. (CONTINUED)

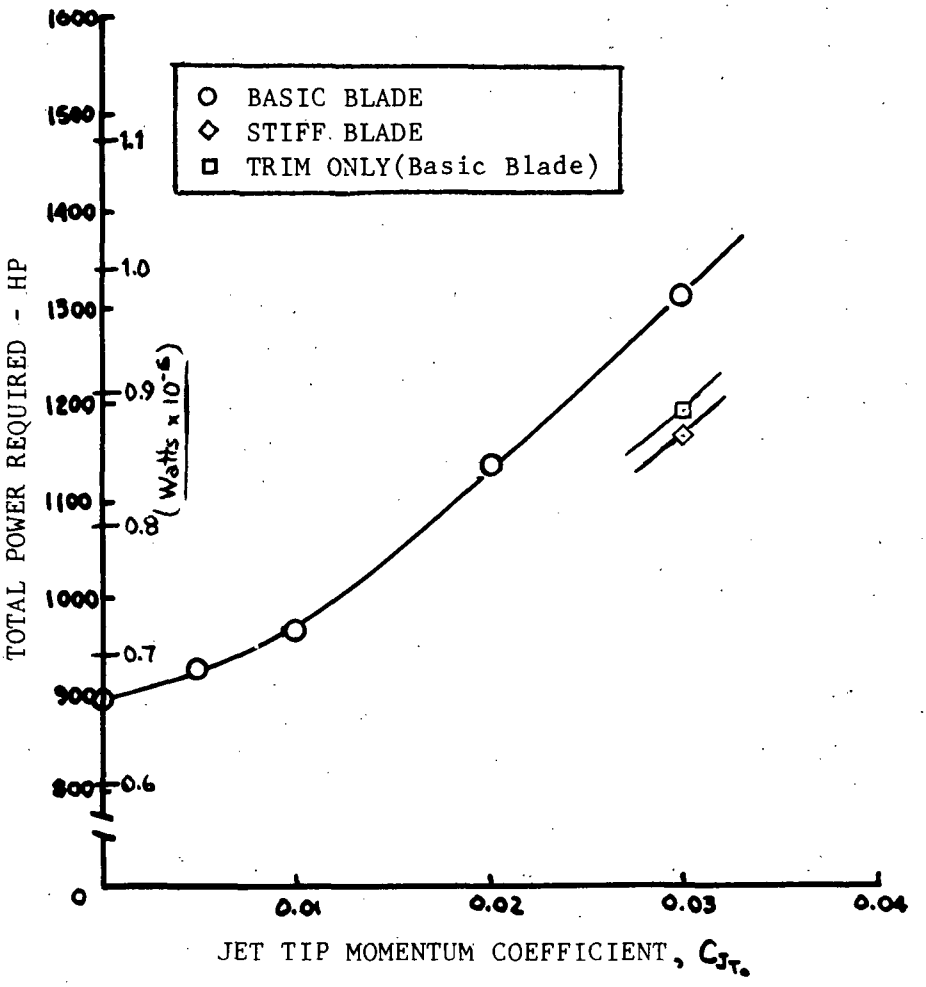

Figure 31. TOTAL POWER REQUIRED TO TRIM & SUPPRESS TRANSMITTED SHEARS vs JET TIP MOMENTUM COEFICIENT AT μ = 0.20.

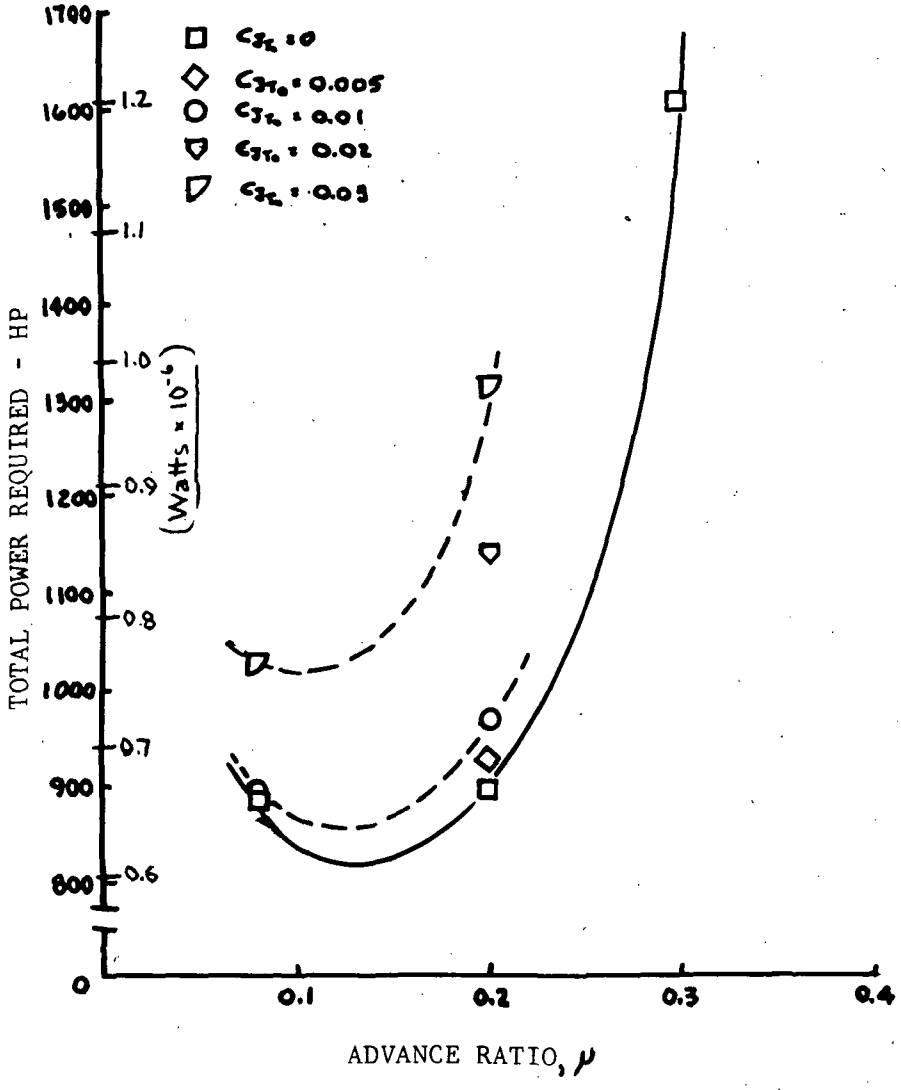

Figure 32. TOTAL POWER REQUIRED vs ADVANCE RATIO AT SEVERAL $C_{J_{T_0}}$

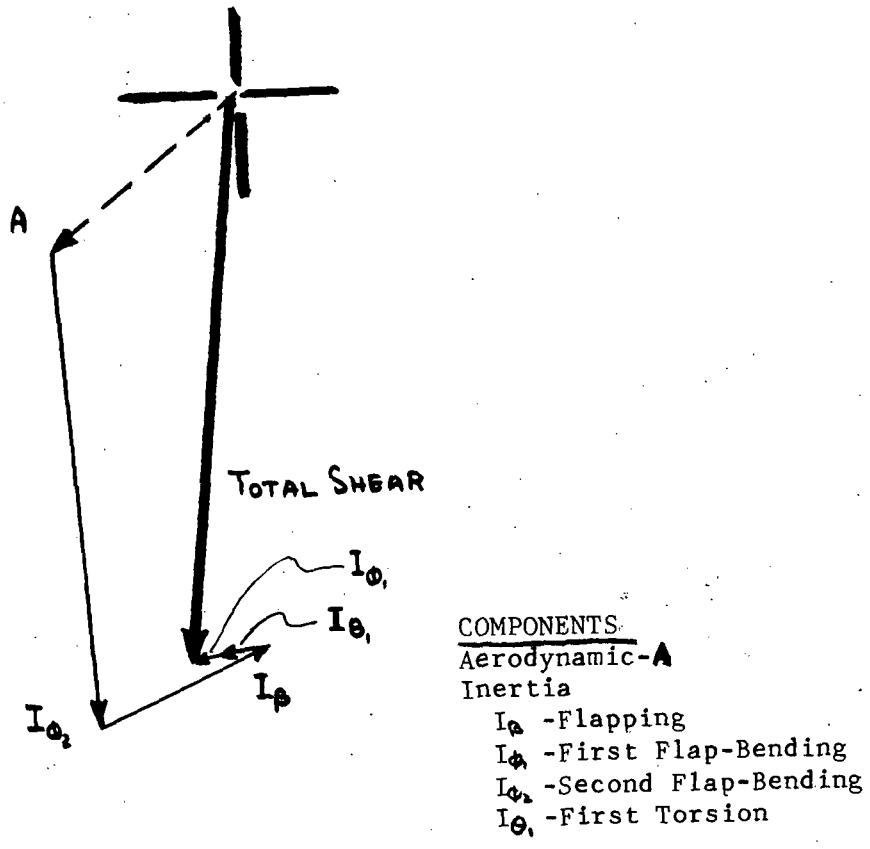

A. Jet Off - Resultant Shear

Figure 33. VECTOR COMPONENTS OF 5th HARMONIC VERTICAL BLADE ROOT SHEAR.

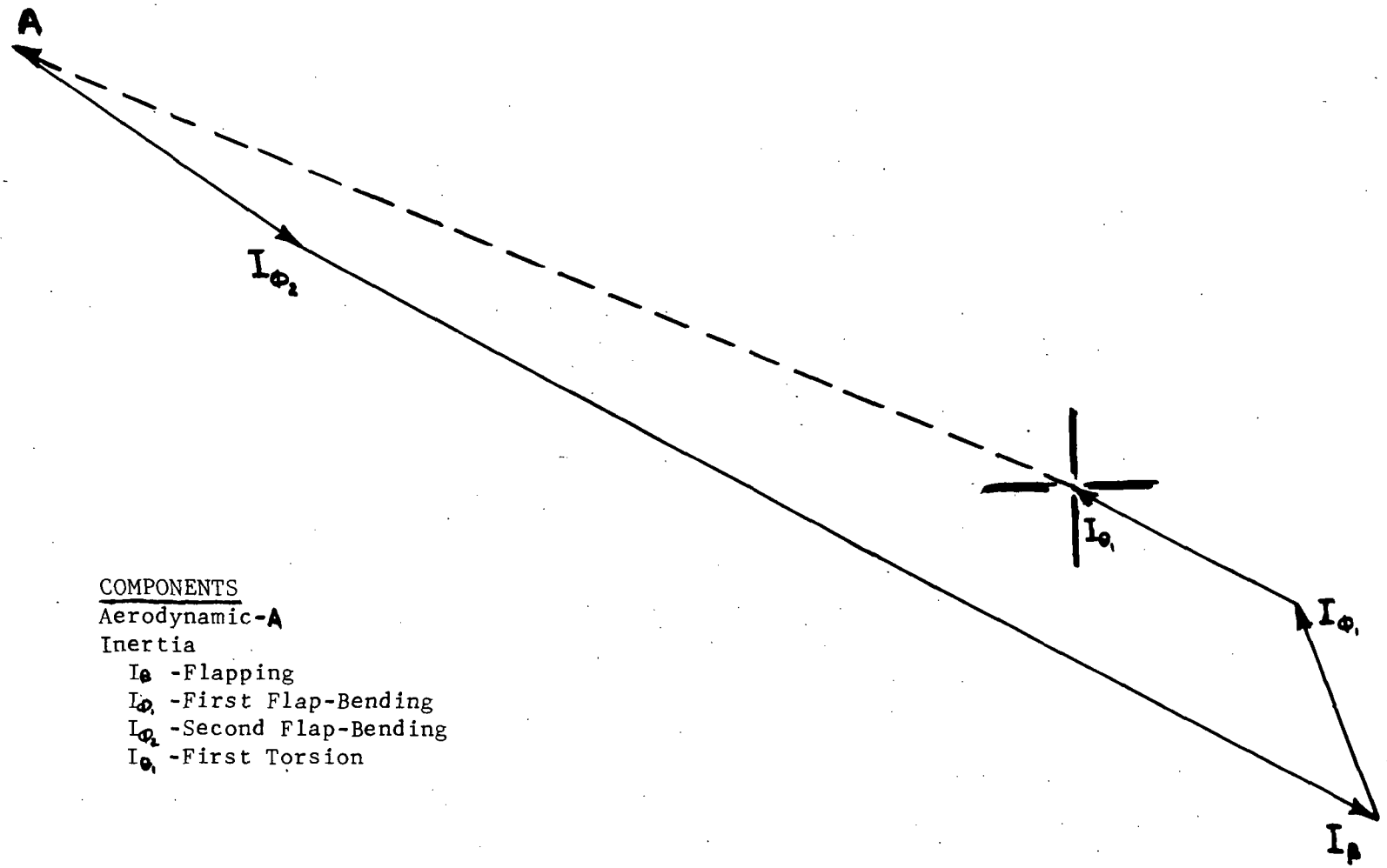

COMPONENTS
Aerodynamic-A
Inertia
- I_β -Flapping
- I_{Φ_1} -First Flap-Bending
- I_{Φ_2} -Second Flap-Bending
- I_{θ_1} -First Torsion

Figure 33. (CONTINUED) B. Jet On - Shear Suppressed

VECTOR COMPONENTS OF 5th HARMONIC VERTICAL BLADE ROOT SHEAR.

APPENDIX I

I. DETAILS OF THE AERODYNAMIC MODEL

The aerodynamic model of Reference 21 was modified to incorporate the jet flap aerodynamics for the purposes of this study. The modifications were made to include the effects of the jet on the local blade section LIFT, DRAG and MOMENTS of a rotor blade in forward flight.

The jet effects were included in the unsteady aerodynamic model of Reference 21 in a quasi-steady fashion. No jet dependent apparent mass terms were included. Similarly no explicit aerodynamic terms dependent upon the rate of change of the jet angle ($\dot{\tau}$) were included. However, the indirect effects of the unsteady jet were approximately accounted for via the wake model in that changes in the airfoil bound vorticity are reflected as changes in the wake vorticity and hence modify the impressed velocity distribution on the airfoil.

The following sections describe the heuristic approach which was employed to derive the required governing aerodynamic equations. Also presented are the expressions which resolve the airfoil section lift, drag and moment into their respective counterparts in the shaft plane for use in the trim equation and for determination of the blade root shears. Finally, the airfoil data, jet on and jet off, used in this study are presented.

I.1 Unsteady Rotor Aerodynamic Representation - No Jet

From Reference 21, the unsteady LIFT and MOMENT are given as (on a given rotor blade section with no jet)

$$\mathcal{L} = C_{L\alpha_0}\, b\rho V_1 (A_0+\tfrac{1}{2}A_1) + \pi b^2 \rho \frac{\partial}{\partial t}(3A_0+A_1+\tfrac{1}{2}A_2) \qquad \text{(I-1)}$$

$$\mathcal{M} = \pi b^2 \rho V_1 \left[(A_0+\tfrac{1}{2}A_2) - \frac{b}{2V_1}\frac{\partial}{\partial t}(A_0+\tfrac{3}{4}A_1-\tfrac{1}{4}A_3) \right] \qquad \text{(I-2)}$$

where A_0, A_1 etc. are the coefficients of the Glauert expansion for the bound vorticity, i.e.

$$\gamma(\theta,t) = 2\left[A_0(t)\cot\left(\frac{\theta}{2}\right) + \sum_{n=1}^{\infty} A_n(t)\sin n\theta \right] \qquad \text{(I-3)}$$

These coefficients are shown, via the condition for no flow through the airfoil, to be (See Figure I-1 for definitions)

$$A_{o_K} \equiv \bar{v}_{o_K} = \left(-\dot{h} + V_1 \alpha_q\right)_K + \sum_{j=1}^{NRA} S_{o_{Kj}} \Gamma_j \qquad \text{(I-4)}$$

$$A_{1_K} \equiv -\bar{v}_{1_K} = \left(b\dot{\alpha}_q\right)_K - \sum_{j=1}^{NRA} S_{1_{Kj}} \Gamma_j \qquad \text{(I-5)}$$

$$A_{n_K} \equiv -\bar{v}_{n_K} = -\sum_{j=1}^{NRA} S_{n_{Kj}} \Gamma_j \qquad n = 2,3,\ldots.. \qquad \text{(I-6)}$$

where the Σ terms are the induced velocities from the wake, the $\bar{v}_{n_K}$ are elements of the Fourier Series describing the impressed velocity distribution across the chord, and

$$\Gamma_j = \int_{-b}^{b} \gamma(x)\, dx \qquad \text{(I-7)}$$

the subscript K denotes the K^{TH} collocation point in the disk; NRA denotes total number of collocation points in the disk.

The relationship between the A's and Γ's is obtained from Equations (I-3) and (I-7) with the transformation

$$x = -b\cos\theta \qquad \text{(I-7A)}$$

introduced to yield

$$\Gamma_K = 2\pi b_K \left(A_o + \tfrac{1}{2} A_1\right)_K \quad . \qquad \text{(I-8)}$$

Since the theoretical circulation and lift curve slope are not achieved in actuality, Equation (I-8) is modified by the factor

$$C_{L\alpha_o} / 2\pi$$

where $C_{L\alpha_o}$ = actual lift curve slope for a given airfoil section,

$$\Gamma_K = C_{L\alpha_{o_K}} b_K \left(A_o + \tfrac{1}{2} A_1\right)_K \qquad \text{(I-9)}$$

Combination of Equations (I-4), (I-5) with (I-9) yields the simultaneous set of algebraic equations in the unknown Γ_K which must be solved:

$$\Gamma_K = I_K + \sum_{j=1}^{NRA} \sigma_{Kj} \Gamma_j \qquad \text{(I-10)}$$

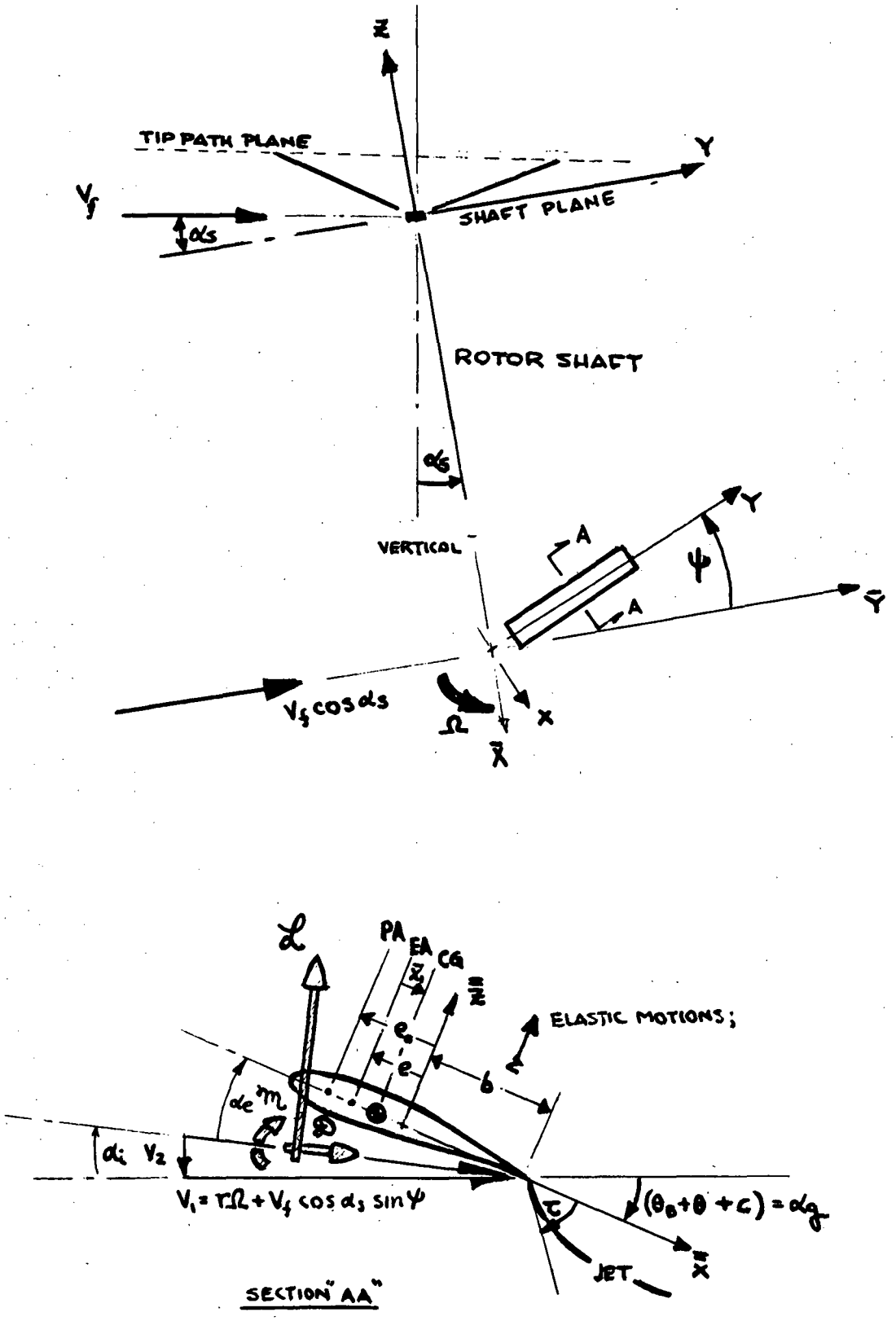

FIGURE I-1. SIGN CONVENTION USED

where

$$I_K = C_{L\alpha_{o_K}} b_K \left(-\dot{h} + V_1 \alpha_g + \frac{1}{2} b \dot{\alpha}_g\right) \qquad \text{(I-11)}$$

$$\sigma_{Kj} = C_{L\alpha_{o_K}} b_K \left(S_{o_{Kj}} - \frac{1}{2} S_{1_{Kj}}\right) \qquad \text{(I-12)}$$

I.2 Quasi-Steady Jet Flap

For steady state flow, References 25 and 26 derive the LIFT and MOMENT coefficients for a jet flap airfoil as (respectively)

$$\frac{\text{LIFT}}{\rho_o b V_1^2} = C_{L_{C_j}} = C'_{L\alpha}\alpha + C'_{L\tau}\tau + C'_{L\hat{t}}\hat{t} \qquad \text{(I-13)}$$

$$\frac{\text{MOMENT}}{2\rho_o b^2 V_1^2} = C_{M_{C_j}} = C'_{M\alpha}\alpha + C'_{M\tau}\tau + C'_{M\hat{t}}\hat{t} \qquad \text{(I-14)}$$

where $C'_{L_{\alpha,\tau,\hat{t}}}$ & $C'_{M_{\alpha,\tau,\hat{t}}}$ = lift and moment curve slopes with respect to $\alpha, \tau, \hat{t}$

α = airfoil angle of attack (2-D) (radians)

τ = jet angle relative to airfoil chordline (radians)

$\hat{t} = \bar{t}/2b$

$\bar{t}$ = maximum camber for parabolic camber (inches)

b = airfoil semichord (inches)

C_j = jet momentum coefficient

The moment of Equation (I-14) is POSITIVE LEADING EDGE DOWN and is taken about the LEADING EDGE.

The lift and moment curve slopes can be rewritten as

$$C_{L_{C_j}} = (C_{L\alpha_o} + \bar{C}_{L\alpha})\alpha + (\bar{C}_{L\tau})\tau + (C_{L\hat{t}_o} + \bar{C}_{L\hat{t}})\hat{t} \qquad \text{(I-15)}$$

$$C_{M_{C_j}} = (C_{M\alpha_o} + \bar{C}_{M\alpha})\alpha + (\bar{C}_{M\tau})\tau + (C_{M\hat{t}_o} + \bar{C}_{M\hat{t}})\hat{t} \qquad \text{(I-16)}$$

where

$C_{L\alpha_o}$, $C_{M\alpha_o}$, etc. are the airfoil lift and moment curve slopes with no jet

$\bar{C}_{L\alpha}$, $\bar{C}_{M\alpha}$, etc. are the jet on airfoil lift and moment curve slopes as functions of C_μ only

But Equation (I-16) is for a positive, leading edge down moment, and must be transferred to a positive, leading edge up moment about the airfoil midchord to be consistent with RAS (See Figure I-1). Thus,

$C'_{M_{C_\mu}}$ = MOMENT ABOUT THE MIDCHORD, LEADING EDGE UP POSITIVE

$$C'_{M_{C_\mu}} = -\left[C_{M_{C_\mu}} - \frac{1}{2} C_{L_{C_\mu}} \right] \tag{I-17}$$

Now introducing the quasi-steady approximation for the effective angle of attack

$$\alpha = \alpha_g - \frac{\dot{h}}{V_1} \tag{I-18}$$

and recognizing that, quasi-statically, a pitching rate, $\dot{\alpha}_g$, is equivalent to a parabolic camber of

$$\hat{t}_e = \frac{b\dot{\alpha}_g}{4V_1} \tag{I-19}$$

with $\dot{\alpha}_g$ positive leading edge up,

then the total effective camber is given by

$$\hat{t} = \hat{t}_o + \hat{t}_e \tag{I-20}$$

where $\hat{t}_o$ = built in parabolic camber,

and Equations (I-15) and (I-17), upon substitution of equations (I-18) and (I-20) into them, become

$$C_{L_{C_\mu}} = \left(C_{L\alpha_o} + \bar{C}_{L\alpha}\right)\left(\alpha_g - \frac{\dot{h}}{V_1}\right) + \left(\bar{C}_{L\tau}\right)(\tau) + \left(C_{L\hat{t}_o} + \bar{C}_{L\hat{t}}\right)\left(\hat{t}_o + \frac{b\dot{\alpha}_g}{4V_1}\right) \tag{I-21}$$

$$\begin{aligned} C'_{M_{C_\mu}} = -\Big[&\left(C_{M\alpha_o} - \tfrac{1}{2} C_{L\alpha_o}\right)\left(\alpha_g - \frac{\dot{h}}{V_1}\right) + \left(C_{M\hat{t}_o} - \tfrac{1}{2} C_{L\hat{t}_o}\right)\left(\hat{t}_o + \frac{b\dot{\alpha}_g}{4V_1}\right) \\ &+ \left(\bar{C}_{M\alpha} - \tfrac{1}{2}\bar{C}_{L\alpha}\right)\left(\alpha_g - \frac{\dot{h}}{V_1}\right) + \left(\bar{C}_{M\tau} - \tfrac{1}{2}\bar{C}_{L\tau}\right)(\tau) + \left(\bar{C}_{M\hat{t}} - \tfrac{1}{2}\bar{C}_{L\hat{t}}\right)\left(\hat{t}_o + \frac{b\dot{\alpha}_g}{4V_1}\right) \end{aligned} \tag{I-22}$$

I.3 Combination of Jet Flap Quasi-Steady and Rotor Unsteady Aerodynamics

If a comparison is made of the quasi-steady terms of Equation (I-1), i.e.

$$\mathcal{L}_{QS} = C_{L\alpha_o}\, b\rho V_1 \left[-\dot{h} + V_1\alpha_g + \frac{1}{2} b\dot{\alpha}_g \right]^* \tag{I-23}$$

* Assuming uncambered airfoils,

with the quasi-steady approximation for the jet flap in Equation (I-21), appropriately modified by ($b\rho_0 V_1^2$), it is recognized that the non-jet dependent terms are readily identifiable (Note that $C_{L\xi_0} = \partial C_L / \partial \xi_0 = 4\pi$ or applying same correction on the theoretical lift curve slope $C_{L\xi_0} = 2C_{L\alpha_0}$). Thus if the quasi-steady terms of Equation (I-23) have added to them the remaining jet dependent terms of Equation (I-21) the resultant equations would represent the quasi-steady aerodynamics of a jet flap rotor in a "strip" sense. The remaining wake and unsteady terms are now included to complete the aerodynamic representation for the non-jet model and also allows an approximation to the jet dependent wake effects. This occurs due to the fact that the strength of the wake vortices will be dependent upon the blade bound vorticity which is proportional to the local load which is directly dependent upon the jet via Equation (I-21).

Hence the resultant LIFT expression for the jet flap rotor becomes

$$\mathcal{L} = C_{L\alpha_0} b\rho V_1 \left(A_0 + \tfrac{1}{2}A_1\right) + \pi b^2 \rho \frac{\partial}{\partial t}\left(3A_0 + A_1 + \tfrac{1}{2}A_2\right)$$
$$+ \bar{C}_{L\alpha} b\rho V_1 (A_0) + \bar{C}_{L\tau} b\rho V_1^2 (\tau) + \bar{C}_{L\xi} b\rho V_1 \left(\tfrac{1}{4}A_1\right). \qquad \text{(I-24)}$$

A similar arguement for the moment yields

$$\mathcal{M} = \pi b^2 \rho V_1 \left[\left(A_0 + \tfrac{1}{2}A_1\right) - \frac{b}{2V_1}\frac{\partial}{\partial t}\left(A_0 + \tfrac{3}{4}A_1 - \tfrac{1}{4}A_3\right)\right]$$
$$- 2\rho b^2 V_1 \left(\bar{C}_{M\alpha} - \tfrac{1}{2}\bar{C}_{L\alpha}\right)(A_0) - 2\rho b^2 V_1^2 \left(\bar{C}_{M\tau} - \tfrac{1}{2}\bar{C}_{L\tau}\right)(\tau)$$
$$- 2\rho b^2 V_1 \left(\bar{C}_{M\xi} - \tfrac{1}{2}\bar{C}_{L\xi}\right)\left(\tfrac{1}{4}A_1\right). \qquad \text{(I-25)}$$

Since the lift must be proportional to the total bound circulation plus the noncirculatory terms in the jet flapped airfoil case as in the classical case (Reference 24), the relation may be written

$$\mathcal{L} = \rho_0 V_1 \Gamma + \pi b^2 \rho \frac{\partial}{\partial t}\left(3A_0 + A_1 + \tfrac{1}{2}A_2\right) \qquad \text{(I-26)}$$

which when compared to Equation (I-24) leads to

$$\Gamma_K = \left\{ C_{L\alpha_0} b\left(A_0 + \tfrac{1}{2}A_1\right) + \bar{C}_{L\alpha} b(A_0) \right.$$
$$\left. + \bar{C}_{L\tau} bV_1 (\tau) + \bar{C}_{L\xi} b\left(\tfrac{1}{4}A_1\right)\right\}. \qquad \text{(I-27)}$$

Equation (I-27) may be rewritten to yield a form identical to Equation (I-10)

$$\Gamma_K = I_K + \sum_{j=1}^{NRA} \sigma_{Kj}\,\Gamma_j \tag{I-28}$$

but now where

$$I_K = C_{L\alpha_{o_K}} b_K \left(-\dot{h} + V_i \alpha_g + \tfrac{1}{2} b \dot{\alpha}_g\right)_K + \bar{C}_{L\alpha_K} b_K \left(-\dot{h} + V_i \alpha_g\right) + \bar{C}_{L\tau_K} b V_{i_K} \tau_K + \bar{C}_{L\hat{q}_K} b_K \left(\tfrac{1}{4} b \dot{\alpha}_g\right)_K \tag{I-29}$$

$$\sigma_{Kj} = b_K \left(C_{L\alpha_o} + \bar{C}_{L\alpha}\right)_K (S_{\alpha_{Kj}}) - \tfrac{1}{2} b_K \left(C_{L\alpha_o} + \tfrac{1}{2}\bar{C}_{L\hat{q}}\right)(S_{i_{Kj}}) \,. \tag{I-30}$$

Thus Equations (I-24), (I-25) and (I-28) when coupled with the expression for the drag at each disk collocation point completely define the aerodynamics of the rotor for the model assumed.

I.4 Section Drag Expressions

The airfoil section drag, $\mathfrak{D}$ -as defined in Figure I-1, was described as composed of two terms. The first term represented the jet off blade profile drag and was assumed to be a function of the freestream dynamic pressure, the local mach number (M), the local effective angle of attack and the airfoil profile. It was assumed that this term was unaffected by the jet. The second term represented the direct jet momentum reaction parallel to the blade chord line and a term describing the jet momentum recovery. Thus, the drag expression was written as

$$\mathfrak{D} = \left(\frac{V_i}{|V_i|}\right) b \rho V_i^2 C_{D_p}(\alpha_e, M) - \mathfrak{D}_{c_J} \,. \tag{I-31}$$

The jet dependent term, $\mathfrak{D}_{c_J}$, is defined as

$$\mathfrak{D}_{c_J} = -\rho b V_i^2 (f_{c_J} C_{J_{T_o}}) \left[T_R + (1 - T_R)\cos(\alpha_g + \tau)\right] \left(1/\bar{r} + \mu \sin\psi\right)^2 \tag{I-32}$$

where

T_R = thrust recovery constant

α_g = total local instantaneous geometric angle of attack.

I.5 Shaft Plane Forces

Resolution of the local airfoil aerodynamic forces and moments into the forces and moments (locally) referenced to the shaft

plane in the rotating frame was accomplished via the following expressions (See Figure I-1)

$$F_x' = \mathcal{L} \sin\alpha_i + \mathcal{D} \cos\alpha_i \tag{I-33}$$

$$F_y' = \mathcal{L} \sin\left(\beta_c + \sum \frac{df_{h_i}}{dr} h_i\right) \tag{I-34}$$

$$F_z' = \mathcal{L} \cos\alpha_i - \mathcal{D} \sin\alpha_i \tag{I-35}$$

$$M_{HUB} = \mathcal{M}_{HUB} \tag{I-36}$$

Under the assumption of small angles ($\alpha_i \ll 1$), Equations (I-33) to (I-36) become

$$F_x' = \mathcal{L}(\alpha_i) + \mathcal{D} \tag{I-37}$$

$$F_y' = \mathcal{L}\left(\beta_c + \sum \frac{df_{h_i}}{dr} h_i\right) \tag{I-38}$$

$$F_z' = \mathcal{L} - \mathcal{D}(\alpha_i) \tag{I-39}$$

$$M_{HUB} = \mathcal{M}_{HUB} \tag{I-40}$$

The local induced angle α_i , was written as

$$\alpha_i = \frac{\dot{h}}{V_t} = \frac{\text{TOTAL RELATIVE AIR VELOCITY NORMAL SHAFT PLANE}}{V_t}$$

$$= \frac{1}{V_t}\left\{ V_f \sin\alpha_s + V_f \cos\alpha_s \cos\psi \left(\beta_c + \sum \frac{df_{h_i}}{dr} h_i\right) + \sum f_{h_i} \dot{h}_i - e \sum f_{\theta_\gamma} \dot{\theta}_\gamma - e_o \sum f_{c_j} \dot{c}_j + v_{w_i} \right\} \tag{I-41}$$

where

β_c - precone angle
f_{h_i} - mode shape of i^{th} flatwise mode
h_i - tip deflection of i^{th} flatwise mode
f_{θ_γ} - mode shape of γ^{th} torsional mode
θ_γ - tip deflection of γ^{th} torsional mode
f_{c_j} - mode shape of j^{th} control mode
c_j - tip deflection of j^{th} control mode
e - distance from elastic axis to midchord

e_o - distance from control axis to midchord

w_i - induced velocity.

The forces and moments given by Equations (I-37) through (I-40) were then used to determine the generalized forces and hence the blade root shears.

I.6 Airfoil Characteristics

The lift, drag and moment expressions of Equations (I-24), (I-31) and (I-25) respectively were defined in terms of jet off and jet on airfoil characteristics,

$$(C_{L_{\alpha_o}}, \bar{C}_{L_\alpha}), (\bar{C}_{L_\tau}), (C_{L_{\hat{\xi}_o}}, \bar{C}_{L_{\hat{\xi}}})$$

$$(C_{M_\alpha}, \bar{C}_{M_\alpha}), (\bar{C}_{M_\tau}), (C_{M_{\hat{\xi}_o}}, \bar{C}_{M_{\hat{\xi}}})$$

and

$$(C_{D_p})$$

These airfoil data are required as input to the RAS program; theoretical or experimental values may be used. For the jet off coefficients, $C_{L_{\alpha_o}}$, $C_{M_{\alpha_o}}$, $C_{L_{\hat{\xi}_o}}$ and $C_{M_{\hat{\xi}}}$ a radial distribution may be inputed. These values are used up to the stall angle. For the present study the following values were used as obtained for the NACA 0012 airfoil from Reference 28

$$C_{L_{\alpha_o}} = 5.73$$
$$C_{L_{\hat{\xi}}} = 2C_{L_{\alpha_o}}$$
$$C_{M_{\alpha_o}} = (C_{L_{\alpha_o}}/4)$$
$$C_{M_{\hat{\xi}_o}} = C_{L_{\alpha_o}}$$

The corresponding experimental airfoil drag data (Reference 28) required a two-variable polynomial fit. The variables were α_e & M (M = Mach no.). A third order polynomial on α_e was fit for the C_{D_p} vs α_e curve at four discrete mach numbers (0.45, 0.50, 0.60 and 0.80). The resulting set of coefficients were then cross fit as a function of M. Thus

$$C_{D_p} = a_0(M) + a_1(M)\alpha_e + a_2(M)\alpha_e^2 + a_3(M)\alpha_e^3$$

For each M, a value of α_{LIMIT} was selected at which the value of C_{D_p} was limited. For all α_e above α_{LIMIT}, $C_{D_p} = C_{D_{p\,LIMIT}}$.

This was done primarily to simplify the polynomial fits required to represent the C_{D_p} variation. A plot of the computed C_{D_p} vs α_e for several M is presented in Figure I-2.

The jet on coefficients, $\bar{C}_{L_\alpha}$, $\bar{C}_{M_\alpha}$ etc. were adapted from Hough (Reference 25) where plots of $\bar{C}_{L_\alpha}$ etc. vs C_J are presented. Polynomial fits on C_J were made for each aerodynamic coefficient. A synopsis of the polynomials used in this study along with the range of C_J applicability of each is presented in Table I-1. Also presented are the jet off values. Presented in Figure (I-3) are plots of these jet on coefficients for the range of C_J encountered in this study. Note that C_{L_τ} and C_{M_τ} are plotted as their negative values.

I.7 Treatment of Stall and Reverse Flow

The stall characteristics of the jet flap airfoil have been assumed to be substantially those of the jet off airfoil. Thus the stall angle for the no jet airfoil will remain the stall angle for the jet on airfoil. However the maximum attainable lift coefficient will be larger by an amount proportional to $C_J, \alpha_{STALL}, \tau$.

An airfoil section is defined to be stalled when

$$\alpha_e = \frac{A_0}{V_1} > \alpha_M \text{ , for } +V_1 \qquad \text{(I-42)}$$

or

$$\alpha_e = \frac{A_0}{V_1} > \alpha'_M \text{ , for } -V_1 \text{ (reversed flow)} \qquad \text{(I-43)}$$

where

$\left.\begin{matrix}\alpha_M \\ \alpha'_M\end{matrix}\right\}$ input stall angles for forward and reversed flow respectively

A_0 uniform component of chordwise distribution of impressed velocity as per (I-4).

The expressions defining the lift, drag, pitching moment, and total bound circulation of the airfoil section operating above the stall angle of attack are presented below.

For the total bound circulation, a maximum or limiting value in defined based on α_M , thereby

$$\Gamma_{M_K} = b V_{1_K} \left[(C_{L_{\alpha_0}} + \bar{C}_{L_\alpha}) \sin \alpha_M + \bar{C}_{L_\tau} \tau \right] \qquad \text{(I-44)}$$

where $\alpha_M = \alpha_M$ or α'_M depending on the sign of V_{1_K} .

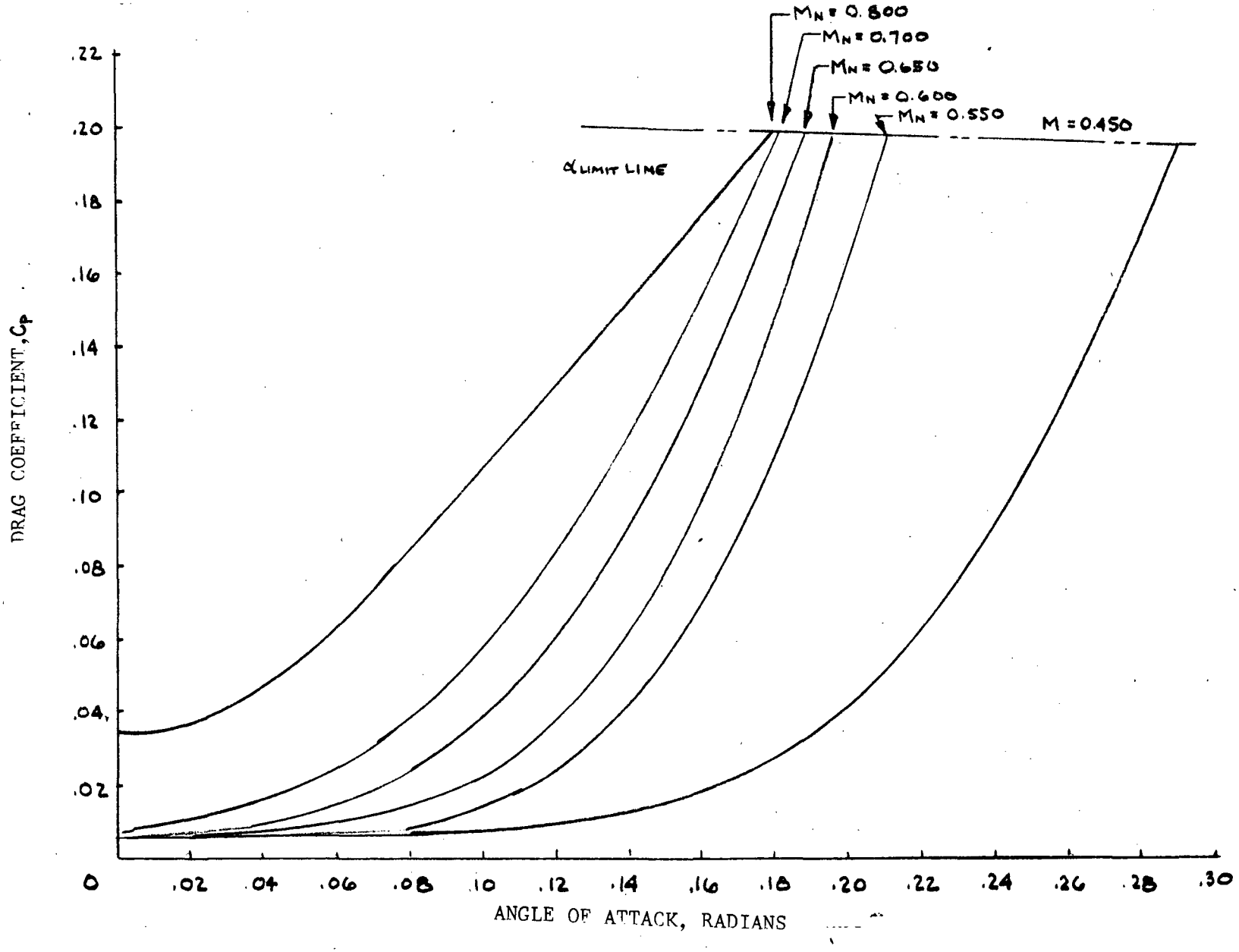

Figure I-2 PLOT OF DRAG COEFFICIENT vs ANGLE OF ATTACK

TABLE I-1

SPECIFIC EXPRESSIONS FOR AIRFOIL COEFFICIENTS
AND RANGE OF APPLICABILITY

SLOPE	JET INDEP.	JET DEPENDENT	C_J RANGE
C_{L_α}	$C_{L_{\alpha_o}}=6.73$	$C_{L_{\alpha_o}}\left(0.151\,C_J^{1/2}+0.219\,C_J\right)$	$0\leq C_J\leq 5.0$
C_{L_τ}	0	$\left(2C_{L_{\alpha_o}}C_J\right)^{1/2}\left(1+0.181\,C_J^{1/2}+0.139\,C_J\right)^{1/2}$	$0\leq C_J\leq 5.0$
C_{L_ξ}	$2C_{L_{\alpha_o}}$	$\left(2C_{L_{\alpha_o}}\right)\left(2.008\,C_J-1.772\,C_J^{1/2}-0.904\,C_J^2+0.198\,C_J^3\right)$	$0\leq C_J\leq 2.0$
C_{M_α}	$C_{L_{\alpha_o}}/4$	$\left(C_{L_{\alpha_o}}/4\right)\left(0.239\,C_J-0.0159\,C_J^2\right)$	$0\leq C_J\leq 5.0$
C_{M_τ}	0	$C_{L_{\alpha_o}}\left(0.114\,C_J+0.293\,C_J^{1/2}\right)$	$0\leq C_J\leq 5.0$
C_{M_ξ}	$C_{L_{\alpha_o}}$	$C_{L_{\alpha_o}}\left(0.305\,C_J-0.798\,C_J^{1/2}+0.070\,C_J^2-0.0161\,C_J^3\right)$	$0\leq C_J\leq 1.0$

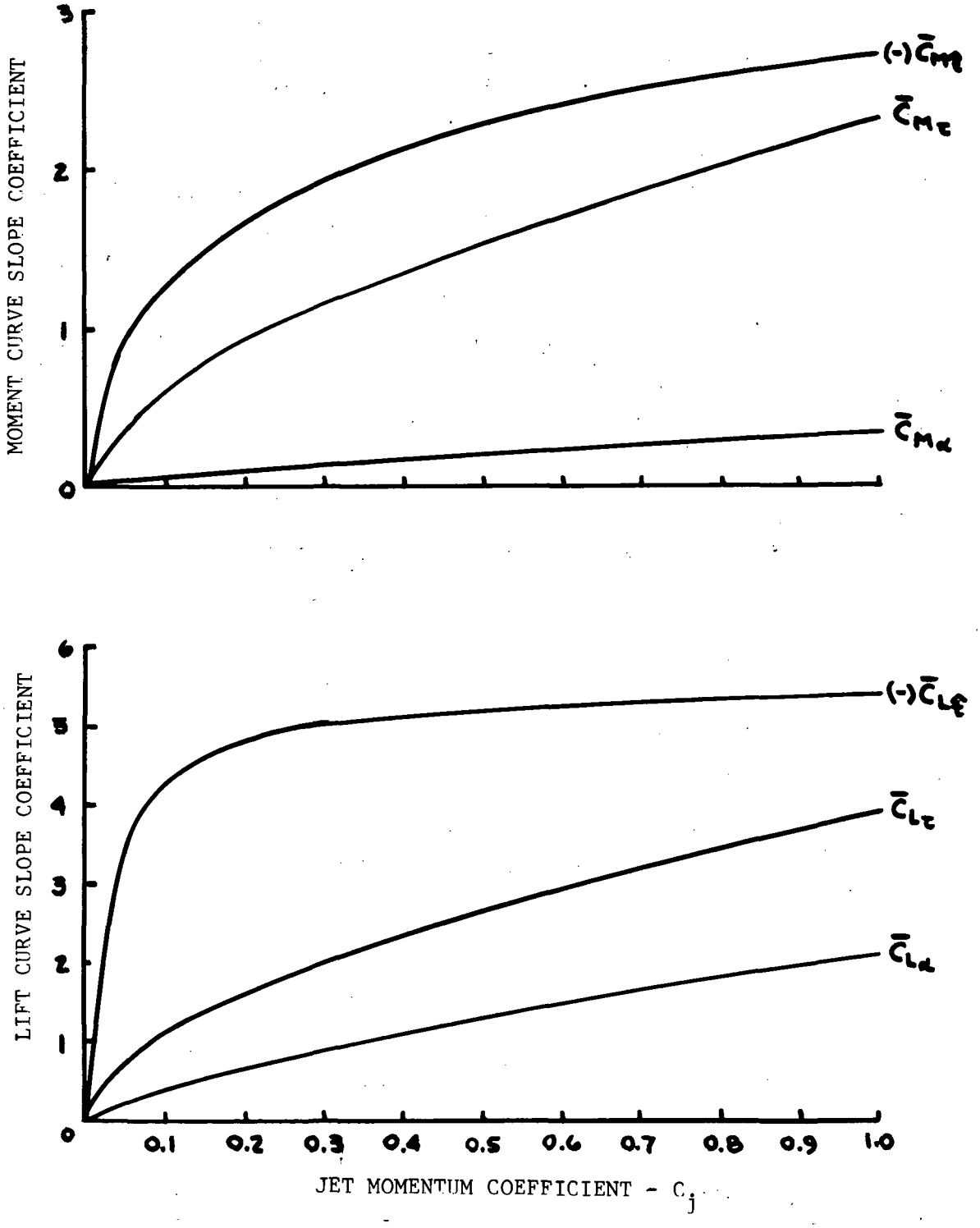

Figure I-3 LIFT AND MOMENT CURVE SLOPES vs JET MOMENTUM COEFFICIENT

For a small range of α_e from α_M to $\bar{\alpha}$, it was assumed that Γ_K remained constant and equal to Γ_{MK}; for α_e from $\bar{\alpha}$ to $\pi/2$, Γ_K was assumed to vary linearly to zero. The defining equations are

$$\bar{\alpha} = (1.25)\,\alpha_M \tag{I-45}$$

for $(\alpha_M \leq |\alpha_e| \leq \bar{\alpha})$

$$\Gamma_K = \Gamma_{MK}(SGN\,\alpha_e) \tag{I-46}$$

for $(\bar{\alpha} < |\alpha_e| < \pi/2)$

$$\Gamma_K = \left[\Gamma_M - \left(\frac{\Gamma_M}{\pi/2 - \bar{\alpha}}\right)(|\alpha_e| - \bar{\alpha})\right](SGN\,\alpha_e) \tag{I-47}$$

A pictorial description of the above is presented in Figure (I-4).

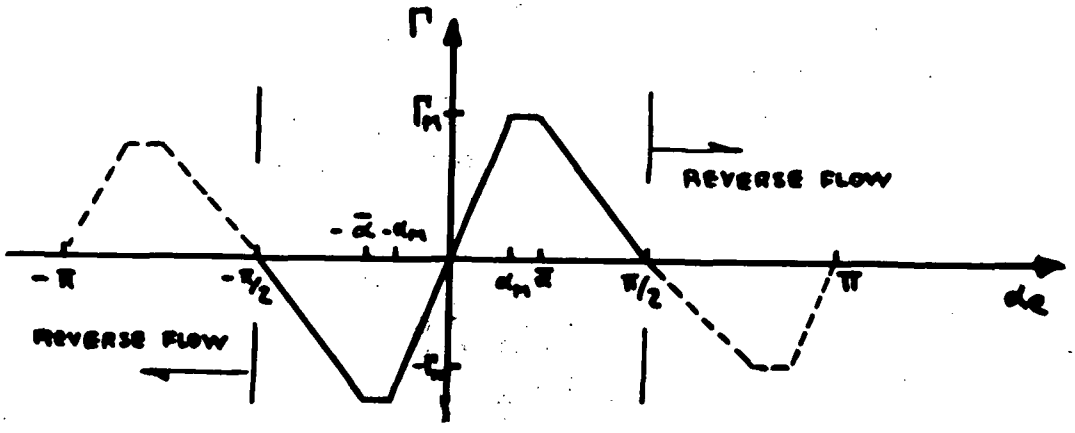

Figure I-4 STALLED GAMMA CHARACTERISTICS

Thus during the solution the magnitudes of the Γ which are shed into the wake are limited to reasonable values. This is an approximation to prevent large, unrealistic values of vorticity

from being shed into the wake from sections which are above their stalling angle of attack.

The lift and pitching moment are computed by (I-24) and (I-25) when the airfoil section is below stall. But when the section is stalled, the lift is approximated by the following:

$$\mathcal{L}_K = \rho V_{IK} \Gamma_{MK} + \Delta l_K \tag{I-48}$$

where

$$\Delta l_K = 2\rho b_K V_{TK}^2 \sin^2 \alpha_{e_K}$$

That is, the stalled lift is computed as the sum of the stalled (limited) circulatory lift and a cross-flow drag force, Δl_K .

The corresponding stalled moment is computed as

$$m_{MK} = \mathcal{L}_{MK} (\bar{CP})(S_{GN} \alpha_e) \tag{I-49}$$

where

$$\bar{CP} = \frac{b}{2}\left[1 - \frac{(|\alpha_e| - \alpha_M)}{(\pi/2 - \alpha_M)}\right]$$

Thus the stalled pitching moment about the midchord is computed as the moment due to the stalled lift, $\mathcal{L}_{MK}$ acting at a center of pressure which moves toward the midchord as α_e approaches $\pi/2$. At $\alpha_e = \pi/2$, the pitching moment goes to zero as might be expected for a flat plate normal to the direction of flow. The velocity, V_T , is the total local resultant velocity acting normal to the spanwise axis (or midchord axis) of the local blade segment and is given by

$$V_T^2 = V_1^2 + V_2^2 \tag{I-50}$$

The velocities V_1 and V_2 are the two orthogonal components of V_T in a plane normal to the local spanwise axis. Velocity V_1 lies on the intersection of this plane with a plane normal to the shaft.

In reverse flow regions, jet off, the same approach as outlined above and depicted in Figure I-4 (see reverse flow region) is employed with appropriate sign changes to define the blade sectional forces and moments.

With the jet on in reverse flow it was assumed that the effect of the jet would be to cause flow separation and hence the airfoil

was assumed to be stalled for all α_e . Thus the corresponding lift and moment were computed as

$$\mathcal{L}_K = \Delta l_{M_K} + \rho b_K V_{1K}^2 C_{J_K} \sin \tau_K \qquad \text{(I-51)}$$

(jet on, reverse flow)

$$m = -\rho b_K V_{1K}^2 C_{J_K} \sin \tau_K \qquad \text{(I-52)}$$

The expression for the drag given by Equation (I-31) includes the influence of stall through the C_{D_P} characteristics used (Figure I-2). The direct jet momentum contribution to the drag is assumed to be unchanged by stall.

APPENDIX II

II.0 ROTOR TRIM EQUATIONS

The rotor trim equations incorporated into the formulation are for the zeroth harmonic rotor forces and moments as defined in the non-rotating shaft oriented coordinate system. The equations for these trim parameters are written in terms of all six components of the blade root forces and moments. Thus these equations are explicit functions of the blade response, the aerodynamic loads, and the rotor control variables (i.e., all the other dependent variables). They are based on the development by Chang, presented in Reference 29, and were generalized to accommodate most any combination of blade root constraint. They contain non-linear terms which depend on steady-state values of parameters such as flapping and lagging displacements and, for a blade without a lag hinge, the steady dragwise root moment. Because these steady-state parameters are constants which can readily be estimated, the non-linear terms are accommodated by inputing and using the estimated values.

The different blade root constraints give rise to different terms, thus the form of the equations change with root constraint. For example, a blade without flapping hinges has a large hub moment contribution from the lift loading, $\ell(r)$ given by,

$$M_\ell = \int_0^R r\ell(r)dr$$

Whereas a blade with a flap hinge has, instead, a term given by

$$M_\ell = r_F \int_0^R \ell(r)dr$$

where r_F is the flap hinge offset from rotor shaft. Many similar situations exist for the rotor forces and moments due to blade inertia, centrifugal, and aerodynamic loadings.

In the computer program, the required change in the form of the trim equations with blade root articulation is implemented by including in the equations the terms for all the different root conditions. Each of the terms have additional coefficients which are either zero or one depending on the articulation. Thus the appropriate terms (or parts thereof) are kept and/or deleted in various combinations as required. This implementation requires only two inputs, F and L. These inputs

represent the presence or absence of flapping and lagging articulation respectively by a value of 1 or 0.

There are three rotor trim forces and three moments--all are included in the analysis. Of the forces, one component (that normal to the shaft-plane) is already represented by the sum of the zeroth harmonics of the blade root shear, so that it was only necessary to add the equations for the remaining two inplane-components of rotor trim force. Relative to the moments, because only steady trimmed flight is considered, one of the moment equations (for yawing moment) is implicitly satisfied (eliminated) by always constraining the rotor side force to be equal to the value of the rotor torque divided by the tail rotor moment arm. Thus only the equations for the remaining two rotor trim moments (pitch and roll) need be added to the analyses. Therefore of the six force/moment equations describing the rotor trim, only four had to be added to the analysis.

Each of these four trim parameters is primarily a function of the first harmonic blade responses and airloads, thus their equations are included in the first harmonic equation-set. The equations presented on the following pages are in the form as they would appear in the set of simultaneous equations at the first harmonic. In these trim equations FM1 and LM1 defined as

$$FM1 = |F-1|$$

$$LM1 = |L-1|$$

are computed internally and used in addition to F and L to include and delete terms according to the articulation.

The remaining symbols represent physical parameters of the rotor and blades, and the harmonic components of the blade responses, and airloadings as defined at the end of this Appendix. The dependent variables of the equations are underlined.

PITCHING MOMENT TRIM EQUATION:

$$\left(\frac{2}{\Omega^2}\right)\underline{M_P} =$$

$$\sum_{j=1,2,3}\left[(FM1)\,M_{rh_j} + (F)\,r_F\,M_{h_oh_j}\right](\underline{A_1h_j})$$

$$-(F)\left[(LM1)\frac{c_o'}{\Omega^2(R-r_F)} + (L)\left\{\frac{(A_oH_1)}{(R-r_F)}(T_{rH_1} - r_F M_{H_1}) + \frac{(r_L-r_F)}{\Omega^2(R-r_F)}(A_oD)\right\}\right](\underline{B_1h_1})$$

$$-\sum_{j=1,2}[J_{\theta_j}](\underline{B_1\theta_j}) - [J_{c_1}](\underline{B_1C_1})$$

$$+\sum_{j=1,2}\left[(2)(LM1)\left\{(FM1)B_c(T_{rH_j} - r_c M_{H_j}) + (F)\frac{(A_oh_1)}{(R-r_F)}(T_{rH_j} - r_F M_{H_j})\right\}\right.$$

$$\left.+(L)\left\{(FM1)B_c(r_L-r_c) + (F)(r_L-r_F)\frac{(A_oh_1)}{(R-r_F)}\right\}(T_{H_oH_j} + M_{H_oH_j})\right](\underline{B_1H_j})$$

$$+\left(\frac{1}{\Omega^2}\right)\left[(FM1)B_{1c} - (LM1)\left\{(FM1)B_c + (F)\frac{(A_oh_1)}{(R-r_F)}\right\}C_{1S}' - (B_1G_{c_1})\right.$$

$$\left.+(F)\,r_F(A_1G_{1h_o}) + (L)\left\{(FM1)B_c(r_L-r_c) + (F)(r_L-r_F)\frac{(A_oh_1)}{(R-r_F)}\right\}(B_1G_{H_o})\right]$$

ROLLING MOMENT TRIM EQUATION:

$$\left(\frac{2}{\Omega^2}\right)\underline{M_R} =$$

$$\sum_{j=1,2,3}\left[(FMI)\,M_{rh_j} + (F)\,r_F\,M_{h_oh_j}\right](\underline{B_ih_j})$$

$$-(F)\left[(LMI)\frac{C_o'}{\Omega^2(R-r_F)} + (L)\left\{\frac{(A_oH_i)}{(R-r_F)}(T_{rH_i} - r_F M_{H_i})\right.\right.$$

$$\left.\left. + \frac{(r_L-r_F)}{\Omega^2(R-r_F)}(A_oD)\right\}\right](\underline{A_ih_i})$$

$$-\sum_{j=1,2}[J_{\theta_j}](\underline{A_i\theta_j}) - [J_{c_i}](\underline{A_iC_i})$$

$$+\sum_{j=1,2}\left[(2)(LMI)\left\{(FMI)B_c(T_{rH_j} - r_c M_{H_j}) + (F)\frac{(A_oh_i)}{(R-r_F)}(T_{rH_j} - r_F M_{H_j})\right\}\right.$$

$$\left. + (L)\left\{(FMI)B_c(r_L-r_c) + (F)(r_L-r_F)\frac{(A_oh_i)}{(R-r_F)}\right\}(T_{H_oH_j} + M_{H_oH_j})\right](\underline{A_iH_j})$$

$$+\left(\frac{1}{\Omega^2}\right)\left[(FMI)B_{is} - (LMI)\left\{(FMI)B_c + (F)\frac{(A_oh_i)}{(R-r_F)}\right\}C_{ic}' - (A_iG_{c_i})\right.$$

$$\left. + (F)\,r_F(B_iG_{ih_o}) + (L)\left\{(FMI)B_c(r_L-r_c) + (F)(r_L-r_F)\frac{(A_oh_i)}{(R-r_F)}\right\}(A_iG_{H_o})\right]$$

LONGITUDINAL FORCE TRIM EQUATION:

$$\left(\frac{2}{\Omega^2}\right)(\underline{X}) =$$

$$-(F)\left[\frac{(A_0 G_{h_0})}{(R-r_F)\Omega^2}\right](\underline{A_1 h_1})$$

$$-\left\{(FM1)B_c + (F)\frac{(A_0 h_1)}{(R-r_F)}\right\}\sum_{j=1,2,3} m_{h_j}(\underline{A_1 h_j})$$

$$-\sum_{j=1,2}(T_{H_0 H_j} + M_{H_0 H_j})(\underline{B_1 H_j})$$

$$-\left(\frac{1}{\Omega^2}\right)\left[(B_1 G_{H_0}) + \left\{(FM1)\beta_c + (F)\frac{(A_0 h_1)}{(R-r_F)}\right\}(A_1 G_{h_0})\right]$$

LATERAL FORCE TRIM EQUATION:

$$\left(\frac{2}{\Omega^2}\right)(\underline{Y}) =$$

$$-(F)\left[\frac{(A_0 G_{h_0})}{(R-r_F)\Omega^2}\right](\underline{B_1 h_1})$$

$$-\left\{(FM1)B_c + (F)\frac{(A_0 h_1)}{(R-r_F)}\right\}\sum_{j=1,2,3} m_{h_j}(\underline{B_1 h_j})$$

$$-\sum_{j=1,2}(T_{H_0 H_j} + M_{H_0 H_j})(\underline{A_1 H_j})$$

$$-\left(\frac{1}{\Omega^2}\right)\left[(A_1 G_{H_0}) + \left\{(FM1)\beta_c + (F)\frac{(A_0 h_1)}{(R-r_F)}\right\}(B_1 G_{h_0})\right]$$

Nomenclature for Trim Equations

β_c - Built in precone

r_L, r_F, r_e - Offset from rotor shaft of flap, lag, and equivalent precone hinges

$$M_{H_0H_j} = \int_0^R m f_{H_0} f_{H_j} dr$$

$$M_{h_0h_j} = \int_0^R m f_{h_0} f_{h_j} dr$$

$$M_{rh_j} = \int_0^R m r f_{h_j} dr$$

$$M_{H_j} = \int_0^R m f_{H_j} dr$$

$$M_{h_j} = \int_0^R m f_{h_j} dr$$

$$T_{rH_j} = \int_0^R m r f_{H_j} dr$$

$$J_{\theta_j} = \int_0^R \left[\frac{dI_x}{dr} + \frac{dI_z}{dr}\right] f_{\theta_j} dr$$

$$J_{c_i} = \int_0^R \left[\frac{dI_x}{dr} + \frac{dI_z}{dr}\right] f_{c_i} dr$$

where m - spanwise mass distribution

f_{h_j} - flapwise mode shapes

f_{H_j} - edgewise mode shapes

f_{θ_j}, f_{c_i} - torsion and pitch mode shapes

$\left[\frac{dI_x}{dr} + \frac{dI_z}{dr}\right]$ - torsion or pitch mass moment of inertia distribution

The following are harmonic components of the dependent variables (blade response)

β_{1c}, β_{1s} - 1st harmonic flapping, cosine and sine components

(A,h_j)
(A,H_j)
(A,θ_j)
(A,C_1)
} - 1st harmonic cosine components flapwise, edgewise, torsion, and rigid body pitch

(B,h_j)
(B,H_j)
(B,θ_j)
(B,C_1)
} - 1st harmonic sine components of the above

C_0', C_{1c}', C_{1s}' - zeroth, and the 1st harmonic cosine and sine components of

$$\int_{r_F}^{R} (r - r_F)\, \mathfrak{D}(r,\psi)\, dr$$

where $\mathfrak{D}(r,\psi)$ is the aerodynamic drag distribution

The following are generalized aerodynamic forces:

(A,G_{h_0})
(A,G_{H_0})
(A,G_{C_1})
} - 1st harmonic cosine components of $\int_0^R F(r)\, dr$ where the $F(r)$ is $\mathfrak{I}(r), \mathfrak{D}(r), \mathfrak{M}(r)$ respectively for h_0, H_0, C_1.

(B,G_{h_0})
(B,G_{H_0})
(B,G_{C_1})
} - 1st harmonic sine components of the above

APPENDIX III

III.0 JET COMPRESSOR POWER REQUIRED

The total power required for the jet flap rotors studied herein may be written as

$$P_T = P_R + P_c \qquad \text{(III-1)}$$

where

P_R = shaft power required by the Rotor, HP,

P_c = compressor power required to supply the jet, HP.

The rotor shaft power required, P_R, is computed directly as an integral part of RAS program as

$$P_R = \frac{N\Omega}{2\pi(550)} \int_0^{2\pi} \int_0^R r\, F_x'\, dr\, d\psi \qquad \text{(III-2)}$$

where

N = number of blades

$F_x' = \mathcal{L}(\alpha_i) + \mathcal{D}$ (see Eq. I-37 of Appendix I).

To determine the compressor power, P_c, a simplified analysis for a one-dimensional, compressible channel flow was employed. It can be shown that for isentropic flow

$$P_c = \frac{\dot{M}_{J_T}\, g\, \bar{R}\, \gamma\, T_{ATM} \left[(\bar{p}_o / p_{ATM})^{\frac{\gamma-1}{\gamma}} - 1 \right]}{550(\gamma-1)\,\eta_c} \qquad \text{(III-3)}$$

where $\dot{M}_{J_T}$ - total Rotor mass flow rate (i.e., for all blades

$\bar{p}_o$ - total pressure at compressor outlet

p_{ATM} - atmospheric pressure

T_{ATM} - atmospheric temperature

$\bar{R}$ - gas constant

γ - ratio of specific heats, (1.4 for air)

η_c - compressor efficiency (assumed at 0.8)

g - gravitational acceleration, (32.2 ft/sec^2).

There are two unknown parameters in Equation (III-3); they are the total Rotor mass flow rate for all blades, $\dot{M}_{J_T}$ and the pressure ratio ($\bar{P}_o / P_{ATM}$).

The mass flow rate, $\dot{M}_{J_T}$, may be determined as a function of the pressure ratio by considering the mass flow rate per unit span from a converging tube or orifice for an adiabatic frictionless flow (see Figure III-1).

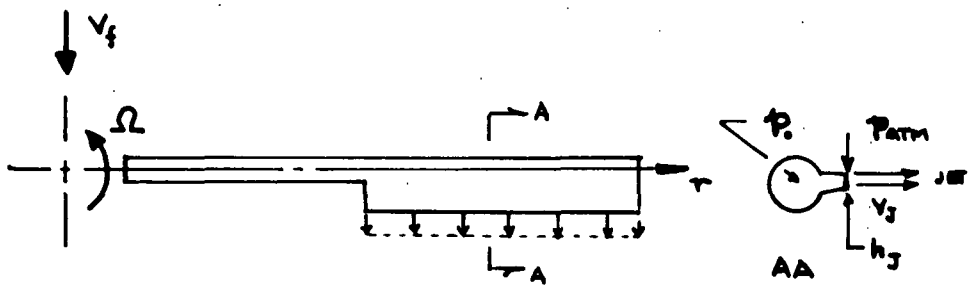

Figure III-1 ASSUMED JET DUCT CONFIGURATION

The mass flow per unit span is thus given by

$$\dot{m}_J = \frac{d\dot{m}_J}{dr} = \frac{h_J}{g}\left[\left(\frac{\gamma}{\gamma-1}\right)\left(2g\frac{P_{ATM}^2}{RT_{ATM}}\right)\left\{\left(\frac{P_{ATM}}{P_o}\right)^{\frac{2}{\gamma}} - \left(\frac{P_{ATM}}{P_o}\right)^{\frac{1+\gamma}{\gamma}}\right\}\right]^{1/2} \quad \text{(III-4)}$$

where h_J = height of the jet slot, ft

g = 32.2 FT/SEC^2

$P_o = \bar{P}_o$ - (duct losses).

The total mass flow rate required of the compressor for N blades is then given by

$$\dot{M}_{J_T} = N\int_{r_J}^{R}\left(\frac{d\dot{m}_J}{dr}\right)dr \quad \text{(III-5)}$$

where r_J = inboard radial extent of the jet.

If the radial distribution of the jet slot height, h_J , is given by

$$h_J = f_{c_J} h_{J_{TIP}} \tag{III-6}$$

then the expression for the total rotor mass flow rate as a function of the pressure ratio is obtained from Equation III-5 upon substitution of (III-4) and (III-6),

$$\dot{M}_{J_T} = \frac{N h_{J_{TIP}}}{g} \int_{r_J}^{R} f_{c_J} \left[\quad \right]^{1/2} dr \tag{III-7}$$

An expression for the pressure ratio, (p_o / p_{ATM}), can be obtained by considering the jet velocity, V_J , at the exit of the nozzle of Figure III-1,

$$V_J = \left\{ 2 \left(\frac{\gamma}{\gamma-1} \right) \left(\frac{p}{\rho} \right)_{ATM} \left\{ 1 - \left(\frac{p_{ATM}}{p_o} \right)^{\frac{\gamma-1}{\gamma}} \right\} \right\}^{1/2}. \tag{III-8}$$

If the jet velocity is required to be directly proportional to the local freestream velocity, it can be written as

$$V_J = k_o (R\Omega)(\bar{r} + \mu \sin\psi) \tag{III-9}$$

where k_o is the proportionality constant.

Then using Equation (III-9) in Equation (III-8) and solving for (p_o / p_{ATM}) an approximate expression for the pressure ratio is obtained as

$$\left(\frac{p_o}{p_{ATM}} \right) \approx \left\{ \left\{ 1 + k_o^2 (R\Omega)^2 C_o \bar{r}^2 \right\} + 2k_o^2 (R\Omega)^2 C_o \bar{r} \mu \sin\psi + k_o^2 (R\Omega)^2 C_o (\mu \sin\psi)^2 \right\}^{\frac{\gamma}{\gamma-1}} \tag{III-10}$$

where $C_o = 2g\bar{R}T_{ATM}(\gamma/\gamma-1)$. (III-10A)

Thus from Equation (III-10), (III-7) and (III-3), the compressor power may be determined as a function of ambient air condition, advance ratio, the slot height distribution and duct pressure losses.

For the cases analyzed, the following simplifing assumptions were made:

(i) the azimuthal and spanwise distributions of the jet velocity are constant and equal to the maximum rotor tip velocity, i.e.

$$V_J = k_\bullet (R\Omega)(1+\mu) \qquad \text{(III-11)}$$

(ii) centrifugal pumping action was just sufficient to balance duct pressure losses and hence (III-11A)

$$P_\bullet = \bar{P}_\bullet$$

(iii) the atmospheric condition to which the jet exhausted were those of the ambient air-stream at infinity.

The assumption of Equation (III-11) yields for Equation (III-10)

$$\left(\frac{P_\bullet}{P_{ATM}}\right) \approx \left[1 + k_\bullet^2 (R\Omega)^2 C_\bullet + 2k_\bullet^2 (R\Omega)^2 C_\bullet \mu + k_\bullet^2 (R\Omega)^2 C_\bullet \mu^2 \right]^{\frac{\gamma}{\gamma-1}} \qquad \text{(III-10B)}$$

The jet slot height at the tip may be written as a function of $C_{J_{T_\bullet}}$ as

$$h_{J_{TIP}} = C_{J_{T_\bullet}} \frac{\rho g b (R\Omega)}{k_\bullet (1+\mu)} \left[\mu^2 \right]^{-1/2} \qquad \text{(III-12)}$$

which when substituted in the Equation (III-7) yields

$$\dot{M}_{J_T} = C_{J_{T_\bullet}} \frac{N(b\rho R\Omega)}{k_\bullet (1+\mu)} \int_{r_J}^{R} f_{c_J}\, dr \,. \qquad \text{(III-13)}$$

Presented in Figure 13 are plots of V_J, $\dot{M}_{J_T}$, and $P_\bullet / P_{ATM}$ vs μ for various $C_{J_{T_\bullet}}$. The following are the values of the parameters employed in this study.

$N = 2$	$k_\bullet = 1.2$
$R\Omega = 760.3$ ft/sec.	$r_J = 12.1$ ft
$R = 24.2$ ft	$\rho = 0.002255$ slugs/ft
$\gamma = 1.4$	$\bar{R} = 53.3$ ft/°Rankine
$b = 0.755$ ft	

APPENDIX IV

IV.0 DETAILS OF THE PROBLEM FORMULATION

Fundamentally the overall problem is formulated in terms of more (two) dependent variables than equations. Two constraint equations are then added to this equation-set so as to make the number of equations equal to the number of variables (effectively reducing the number of variables by two).

The nature of the problem is such that the solutions are periodic on the rotor speed; thus expanding the solution in a Fourier series (Section 4.2) results in doubling the number of equations and dependent variables. That is each basic dependent variable of the problem is represented by its amplitude and phase (sine and cosine components). With the exception of the rotor trim parameters, all dependent variables are defined in the rotating shaft oriented coordinate system. The rotor trim parameters are defined in the non-rotating shaft oriented coordinate system.

The formulation is implemented such that the amplitude and phase of any two of the dependent variables may be constrained individually at each harmonic. The following paragraphs describe this overall problem formulation in more detail.

Classically the set of equations describing a system is written such that all the terms which are functions of the dependent variables are grouped on the left-hand side of the equations. The remaining terms (not functions of the dependent variables) are then grouped on the right-hand side of the equation and are commonly referred to as the forcing functions of the system. However it is not possible to formulate the aeroelastic response problem in this manner with sufficient accuracy, as explained in the following.

The rotor aeroelastic response problem can be considered as being composed of two separate but interacting aspects -- they are a structural dynamics representation and a representation of the system aerodynamics. In reality these two aspects are intimately interrelated. Because it is not possible to accurately express the aerodynamic forces experienced by the blades as explicit functions of the blade response (including the effects of the wake, etc.), the aerodynamic forces are computed by what is more properly described as a numerical simulation of the aerodynamic aspect of the problem. That is, given the rotor

operating conditions and the blade response, the simulation computes the resulting aerodynamic forces as functions of time such that they are consistent with the blade response, the wake of the individual blades, and the non-uniform inflow (as discussed in Section 4.1). These resulting aerodynamic forces are, however, the sum of the response dependent airloads and the response independent airloads (i.e., the forcing functions for the dynamic system). Thus the aerodynamic forcing functions and the response dependent aerodynamic forces are not available separately, nor is a description of the latter available as explicit functions of the dependent variables for writing the equations. That is, with a numerical simulation of the aerodynamic aspect of the problem, it is not possible to write the equations of the system in the classical form. The procedure for handling this apparent difficulty is part of the solution procedure and is described in Section 4.4.

The vertical and inplane blade root shears are functions of the blade dynamic response as well as the aerodynamic loadings and thus were treated as two additional basic dependent variables. That is, the equations for these two components of blade root shear are added to the seven equations of blade motion at each harmonic (except the first).

Because the longitudinal and lateral inplane rotor trim forces (i.e., the zeroth harmonic components in the non-rotating reference system) are determined by the first harmonic blade root shears, these shears cannot be constrained independent of the rotor trim forces. Thus, at the first harmonic, the rotor trim equations (forces and moments) were added to the seven blade equations of motion, instead of the blade root shear equations, because these trim parameters depend on the blade dynamic response and aerodynamic loadings, at the first harmonic. At the zeroth harmonic the vertical blade root shears are the rotor force normal to the shaft plane so no modification was required to include this trim parameter.

Included in each of the resulting nine equations at each harmonic are terms which explicitly depend on each of two control parameters. They are the rigid blade pitch angle (collective and cyclic) and the jet flap deflection angle. Associated with the rigid blade pitch variable are mass, elastic, centrifugal, gyroscopic, and aerodynamic coupling terms in each of the nine equations. The jet flap variable has no mass/elastic characteristics and therefore has only aerodynamic coupling terms in each of the nine equations. These two control variables are not considered as "degrees-of-freedom", i.e., there are no equations of motion representing them. However, they are treated as

dependent variables in the equation set. Thus there are eleven basic dependent variables but only nine equations.

Two "constraint" equations are, therefore, added to the equation set (resulting in a set of eleven equations) which in effect reduces the number of basic dependent variables to nine so that the number of equations and variables are equal. As explained below, these two constraint equations are used to select which and to what value two of the eleven basic dependent variables are to be constrained.

All of the coefficients in each of the constraint equations are zero except for a "one" at the "column-position" of the variable to be constrained. The right hand side of each constraint equation is set equal to the desired constraint value for the constrained variable. Thus, for example, if equations seven and eight of the eleven equations (presented here in matrix notation),

$$F\bar{x}_j = \bar{y}_j \quad ; \; j = 1,2,\cdots,11 \tag{4.3.-1}$$

are the constraint equations and it is desired to constrain, say, x_4 and x_9 respectively to the values A and B, then the "one" would be put in column positions 4 and 9 of Equations 7 and 8 respectively and y_7 set equal to A and $y_8 = B$. Thus Equations 7 and 8 of (4.3-1) would be

$$0\cdot x_1 + 0\cdot x_2 + 0\cdot x_3 + 1\cdot x_4 + 0\cdot x_5 + \cdots + 0\cdot x_{11} = y_7 = A$$

$$0\cdot x_1 + 0\cdot x_2 + \cdots + 0\cdot x_8 + 1\cdot x_9 + 0\cdot x_{10} + 0\cdot x_{11} = y_8 = B$$

which reduce to

$$x_4 = A$$

$$x_9 = B.$$

The variables selected to be constrained (i.e., the positions of the "one" in each constraint equation) and the constraint values are controlled by program inputs.

Because the problem is periodic and the number of equations is twice the number of basic dependent variables (as explained at the beginning), there are actually 22 simultaneous equations at each harmonic for the 11 dependent variables. This quite general formulation of the aeroelastic response problem thus allows the amplitude and phase of any two of the eleven dependent variables

at each harmonic to be constrained to any desired value and the resulting solution obtained. It can be used to perform the direct rotor aeroelastic solution by constraining the pitch control at 1P, i.e., given the operating condition and control setting, compute the resulting unsteady airloads, blade responses, rotor loads and moments, and performance. It can also be used to determine the pitch control required to attain trim by constraining the rotor trim forces and moments at 1P. Or it can be used to perform either one of the above solutions with constraints impressed at the higher harmonics on any of the variables. Thus the method has great versatility and power.